SOME ASPECTS OF QUANTUM THEORY OF CHANNELING

A Thesis Submitted
In Partial Fulfilment of the Requirements
for the Degree of
DOCTOR OF PHILOSOPHY

By
ANAND PRAKASH PATHAK

to the

DEPARTMENT OF PHYSICS

INDIAN INSTITUTE OF TECHNOLOGY KANPUR

MARCH, 1971

DEDICATED

TO

MY PARENTS

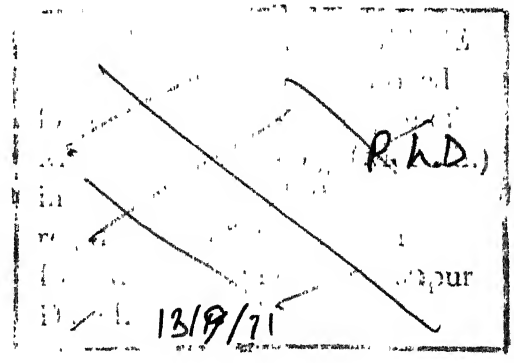

13.9.71

CERTIFICATE

Certified that the work presented in this thesis has been carried out by Mr. Anand Prakash Pathak under my supervision and has not been submitted elsewhere for a degree.

(M. Yussouff)
Lecturer
Physics Department
Indian Institute of Technology
Kanpur, (UP), India

March 11, 1971.

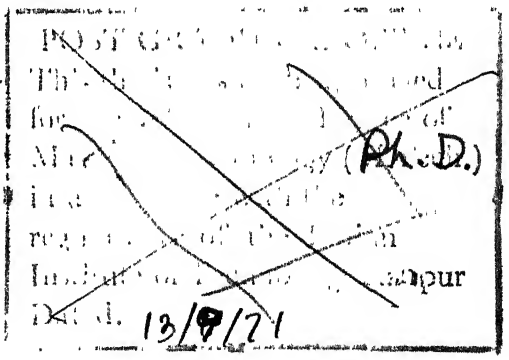

ACKNOWLEDGEMENTS

The author is indebted to Dr. M. Yussouff for suggesting the problem and for his guidance and continuous encouragement throughout the course of the present work. The author is also thankful to Professor J. Mahanty for his keen interest in this work and for many helpful and illuminating discussions at various stages of its progress.

The author is thankful to Dr. J.U. Andersen, University of Aarhus, Denmark, for some discussions. Thanks are also due to Drs. T.V. Ramakrishnan and K.C. Sharma and other members of the Solid State Theory group for many helpful discussions.

The author is thankful to his friends M/S A.K. Kapoor and V.V.Bhokare for their cooperation and for a pleasant and memorable association with them. Thanks are also due to the colleagues M/S V.M. Raval, K.P. Singh, G.L. Dwivedi and Drs. M.V. Krishnan and P. Singh for a nice company.

Financial assistance from the Council of Scientific and Industrial Research, New Delhi and Indian Institute of Technology Kanpur, is gratefully acknowledged. Finally the author wishes to thank Mr. J. K. Misra for typing the manuscript patiently, and to Mr. Lallu Singh for cyclostyling.

A. P. Pathak

TABLE OF CONTENTS

LIST OF TABLES

LIST OF FIGURES

SYNOPSIS

SOME ASPECTS OF QUANTUM THEORY OF CHANNELING

Anand Prakash Pathak
Ph.D.
Department of Physics
Indian Institute of Technology Kanpur
March 1971

In the present work, the quantum mechanical approach to the theory of channeling and blocking of particles in crystals has been investigated using Debye model for lattice vibrations and one phonon approximation for inelastic processes taking place in the crystal when the particles propagate through it. The channeling and emission of charged particles in crystals and anomalous penetration of neutrons have been considered to illustrate the various aspects of the quantum theory of channeling. The rate of energy loss of charged particles due to conduction electrons is important under channeling conditions and has been calculated using a dielectric formulation.

After a review of the classical theory of Lindhard in the Chapter I, the need for a quantum theory has been briefly discussed. In the Chapter II, a general formulation for channeling of particles into crystals has been developed and an expression for the renormalization of the initial state wave function due to inelastic processes has been obtained using a general interaction potential. The approximation involved here is that the crystal is initially in a very low lying state and only the states

close to the initial state of the crystal are excited by the incident particle under channeling conditions. The general formula has been simplified using first Born approximation and Debye model for lattice vibrations to calculate the imaginary part of the renormalization matrix which governs the attenuation of the particles.

In Chapter III, different potential models have been employe to illustrate the details of the calculation. Using a potential for neutrons which goes over to Fermi pseudo-potential as its width vanishes, it has been shown that for anomalous penetration, the interaction potential should be weak compared to the particle energ and should be localized around the lattice sites. It is shown that the more localized and weak is the interaction potential, the more pronounced is the channeling effect. For charged particles, two potential models have been employed, the screened Coulomb and Born-Mayer. The channeling behaviour is again determined by the range of the potential. When the width of screened Coulomb potential is equal to the width of Born-Mayer potential, the screened Coulomb potential is more favourable for channeling. The temperature dependence of the process due to lattice vibrations, comes primarily through the Debye-Waller factor and tends to reduce the anomalous effect. The energy dependence of the expressions supports the experimentally established fact that $X_{1/2}$, the thickness into the crystal at which one half of the initially channeled particles have escaped, is proportional to the particle energy.

The problem of emission of particles from the source embedde in the crystal has been studied quantum mechanically in Chapter IV. The real part of the renormalization matrix adds a correction term to the Fourier transform of the potential, which determines the width of the emission pattern. The magnitude of this correction term is extremely small at high particle energies but starts increa ing as $1/E_p$ for low energies. Unlike the previous quantum mechanical treatment of this problem, the attempt here has been to calculate the attenuation due to inelastic processes using renormalization matrix and is found to be small compared to phenomenologically chosen value. The attenuation depends upon the particle mass m_o and energy E_p as $(m_o/E_p)^{1/2}$. An interesting feature of the present formalism is qualitative indication of difference in widths of electron and positron emission patterns even in the two beam theory.

The energy loss of the particles moving in channels is mainly through the excitation of the conduction electrons as colle tive oscillations. The corresponding contribution has been calculated numerically in Chapter IV using a dielectric formulation with different models for dielectric function. The stopping power dE/dx is found to be very nearly inversely proportional to velocit for particle velocities less than about ten times the Fermi velocity. For higher velocities, the usual velocity dependence ($dE/dx \propto 1/V^2$) is obtained. Finally the conclusions have been summarized in the last chapter.

CHAPTER I

INTRODUCTION

1.1 Discovery and Applications of Channeling:

The study of channeling and blocking phenomena in crystals is a new and developing branch of Solid State Physics. When energetic particles incident on a crystal move along directions close to the principal crystallographic axes or planes, they penetrate anomalously long distances and are said to be channeled. The importance and applications of channeling technique in Solid State Physics is attracting many workers to look into the details of the phenomena and to search for new applications of the technique. A substantial amount of experimental work has been done during the last five years; mostly at the Chalk River Nuclear Laboratories, Canada and the University of Aarhus, Denmark. The technique is finding extensive use and has proved to be very useful in Nuclear Physics too, as for example in nuclear lifetime measurements.

Historically, the directional effects were anticipated as early as 1912 by Stark and Wendt[1] but the detailed theoretical and experimental investigation of the problem was delayed until the last decade. In 1963, Robinson and Oen[2] made a computer simulation of the heavy ion motion in crystals. They investigated

the slowing down of 1-10 keV heavy ions in a lattice model which included realistic repulsive interaction and obtained very large penetrations for particles with initial velocities nearly parallel to close-packed directions. Experimentally this effect was first observed in studies on the penetration of keV ion in crystals by Piercy et al.[3] and by Lutz and Sizemann[4]. They found by measuring the distribution of penetration distances, that a significant fraction of ions incident along low index directions had anomalously long range. At about the same time, Nelson and Thompson[5] observed anomalously high transmission of 50-75 keV protons and helium ions in low index directions of thin gold single crystals. The effect was further confirmed by the experiments of Dearnaley and others[6] who reported that in the transmission experiments, using thin single crystals of Si, 1 - 10 MeV protons and alpha particles lose energy more slowly, if injected parallel to a close-packed axis or plane. Similar reductions in energy loss were observed[7] for bromine and iodine ion beams at energies upto 100 MeV. These experiments and the detailed range measurements of Kornelson et al.[8] on heavy ion beams in single crystals fully confirmed the channeling concept and established that in an aligned crystal, more than 50% of the beam becomes channeled and penetrates much further than the observed range for an irregular array of target atoms (i.e. amorphous target).

The first accurate and comprehensive theoretical treatment of these directional effects was given by Lindhard[9] in 1965.

This treatment is based on the classical orbital picture of the actual steering mechanism for the motion of the particle in a crystal. The experimental development was extremely rapid following this classical theory of Lindhard. A good amount of experimental work has been done on heavy ion ranges in tungsten single crystal[10], wide angle Rutherford scattering in tungsten and silicon[11], and other diamond-type lattices[12] (such as diamond, Si, Ge, GaP, GaAs, GaSb), x-ray production in Al and Cu[13] by proton bombardment and neutron production by nuclear reaction of protons in copper[14] (Cu^{65} (p, n) Zn^{65}). A more detailed account of experimental work has been reported at the International Conference on Electromagnetic Isotope Separators and related ion Accelerators and their Application to Physics[15a] and at the International Conference on Atomic Collisions and Penetration Studies with energetic (keV) ion beams held at Chalk River, Ontario[15b].

The phenomenon of 'channeling' has proved to be a very useful tool for making some very important experimental studies. It can be used to find out whether a doped impurity has occupied a substitutional site or an interstitial site[16,17] in the crystal. Further, one can study the lattice disorders[18] and surface effects[19] using this technique. It has been applied to the study of nuclear-life times[20] also, in a very interesting way. One particularly useful application of the channeling technique has been the study of ion implantation in semiconductors[21,22,23] in which the location of the implanted ions and a determination of

damage produced is studied by means of the channeling behaviour of MeV projectiles. The technique has also been used in finding out the location of inert gas atoms in some crystals[24] (such as KCl, CaF_2 and UO_2). Another related phenomenon, which on one hand, gave rise to the feeling of the existence of the directional effects in crystals[25,26] and initiated its discovery and now, on the other hand, uses channeling as a technique for its own detailed investigation and development[27], is the phenomenon of 'sputtering' where the yield of the atoms from the target due to bombardment of high energy ions and protons depends upon the crystallographic directions. A simple theory of 'sputtering' has been given by Lehman[28]. A more detailed information regarding the discovery and applications of channeling and blocking phenomena are discussed in the review articles by Datz et al.[29], Erginsoy, and Davies[30].

The following section contains a brief review of the classical theory proposed by Lindhard. The underlying basic assumptions which lead to a consistent approximation method for treating the channeling phenomena, have been given and the conditions of their validity are derived briefly. The applicability of this theory and the cases,where a quantum mechanical theory has to be used in view of the fact that the former cannot give any thing beyond the gross features of the phenomena, are indicated in the last section of the present chapter.

1.2 Review of the Classical Theory:

The classical theory of directional effects in perfect crystals proposed by Lindhard[9] is based on the 'orbital picture' of fast moving particles and their steering by the densely packed strings or planes of atoms existing in the crystal. The theory has been constructed on the basis of four main assumptions which lead to a consistent approximation procedure for the treatment of motion of the particle in channels.

First, the angles of scattering of the particle may be assumed to be small. This assumption is valid for fast heavy ions moving close to the crystallographic directions and obviously, scattering by large angles would imply that the original direction is completely lost. The deflections can then be computed classically as if the atoms are infinitely heavy i.e. as if the particles were moving in an external fixed potential.

The second assumption is that the strongest correlation occurs for a collision with a row of atoms. The other atoms in the crystal have a negligible influence on the correlations occuring in one particular row of atoms. This assumption holds because a collision demands that the particle comes close to the atom and collisions are strongly correlated if the particle moves at a small angle with a row of atoms (as a consequence of the first assumption). However, if it passes close to one atom in the row, it must also pass close to the neighbouring atoms in the same row. This leads to the concept of a string of atoms,

characterized merely by the constant distance of separation 'd' of atoms, placed on a straight line. In first approximation, it can be said that the collisions occur with one string at a time, the string collisions being independent and uncorrelated. The physical importance of the string is emphasized by the fact that practically all the physical processes caused by the particle or influencing its path, demand that it comes close to the string. One exception is the resonance excitation of the atomic electrons which may take place far away from the particle, if it has a high velocity. The simplicity of the string approximation is due to the fact that the lattice structure does not enter into the problem, the only lattice parameter coming into picture being the distance d between atoms in the string. The strings belonging to low index directions have a small value of d, and are the most pronounced ones. Correlations weaker than those of strings are expected for crystal planes, atomic pairs etc.

The third assumption is regarding the adequacy of the classical orbital picture. Since the individual collisions of the particles with charge z_1e and velocity v with the crystal-atoms of charge z_2e, need quantal corrections either when the quantity $\chi = (2z_1z_2e^2/\hbar v)$ is not large compared to unity[31] or when the impact parameter is large; the classical approximation might seem to be doubtful in several cases. However, it has been shown by Lindhard (Ref.9, Appendix B) that the classical

description of many successive collisions with atoms in a string does not become invalid at high velocities.

Lastly, the idealized case of a perfect lattice and a perfect string may be used as a first approximation. The thermal and zero point vibrations of atoms can be considered to be comparatively small and their influence on the symmetry properties of the lattice is assumed to be negligible.

With these assumptions Lindhard introduced the idea of continuum approximation to the potential of a string. Using this in conjunction with the assumption of small angle scattering leads to an expression for critical angle for channeling. The basis of the continuum approximation is to assume that many consecutive atoms in the string simultaneously influence the particle trajectory. The average potential responsible for the deflection is obtained by averaging over the whole string. Thus if we take ions as the incident particles, the average potential at a distance r from the string is given by

$$U(r) = \int_{-\infty}^{\infty} \frac{dz}{d} V\left(\sqrt{z^2 + r^2}\right) \qquad (1.1)$$

where V(R) is the ion-atom potential and d is the distance between atoms in the string which has been assumed to be along the z-axis. For R not very much larger than a, the potential V(R) is essentially of Thomas Fermi type and we may write

$$V(R) = \frac{z_1 z_2 e^2}{R} \phi_o (R/a) \qquad (1.2)$$

where a is the screening length of the particle atom interaction and is given by $a = a_o \times 0.8853 \, (z_1^{2/3} + z_2^{2/3})^{-1/2}$ and $\phi_o(R/a)$ is the Fermi function belonging to one isolated atom[32]. Equation (1.1) shows that, the variation of U with 1/r is by one power less than the variation of V with 1/r. From the equations (1.1) and (1.2), we may write

$$U(r) = \frac{z_1 z_2 e^2}{d} \xi (r/a) \qquad (1.3)$$

with $$\xi (r/a) = \int_{-\infty}^{\infty} \frac{dz}{\sqrt{z^2+r^2}} \phi_o(\sqrt{z^2+r^2}/a) \qquad (1.4)$$

A detailed and more accurate estimate of $\xi (r/a)$ is given elsewhere[33]. For the present purpose, we may use some what simpler estimates. In order to get qualitative insight in the behaviour of ξ, i.e. of U, we note that $\phi_o \approx 1$ for $R/a \ll 1$ so that from (1.4), (r/a) should increase logarithmically for small r. Thus,

$$\xi (r/a) \approx 2 \log \frac{Ca}{r} \quad \text{for } r < Ca \qquad (1.5)$$

where the constant of integration 2 log C is determined by the screening. A better estimate valid for all r has been taken to be be

$$\xi (r/a) \approx \log \left[\left(\frac{Ca}{r}\right)^2 + 1 \right] \qquad (1.6)$$

so that $\xi (r/a) \approx (Ca/r)^2$ for $r > Ca$. The constant C has been chosen to be $\sqrt{3}$ which gives fairly good overall fit. The expressions for the density of electrons $\rho(R)$ and atomic potential

V(R) corresponding to formula (2.6) for $\xi(r/a)$ are given by

$$\rho(R) = \frac{3}{4\pi} z_2 \frac{(Ca)^2}{[R^2+(Ca)^2]^{5/2}} \qquad (1.6a)$$

$$V(R) = z_1 z_2 e^2 \left[\frac{1}{R} - \frac{1}{(R^2+C^2a^2)^{1/2}}\right] \qquad (1.6b)$$

The condition for validity of continuum approximation for the potential due to the string is obtained by demanding that the distance d between successive atoms in a string is small compared to $\Delta t.\ v_{||}$ where $v_{||} = v \cos\psi$ is the velocity component parallel to the string and can be taken approximately equal to v for small ψ, and collision time $\Delta t \simeq r_{min}(l)/(v \sin\psi)$, l being the impact parameter with the string and $r_{min}(l)$, the corresponding minimum distance of approach. The condition for validity of the continuum approximation thus becomes

$$\Delta t.\ v \cos\psi \simeq \frac{r_{min}(l)}{\psi} > d \qquad (1.7)$$

Let us apply the condition (1.7) in its most restrictive form so that we demand its fulfilment for l = 0 and determine $r_{min}(l=0,\psi)$ (hereafter written simply as r_{min}) by

$$U(r_{min}) = \frac{1}{2} M_1 v^2 \sin^2\psi \simeq E_p \psi^2 \qquad (1.8)$$

so that the condition (1.7) becomes

$$\frac{Ca}{\psi d} \exp\left(-\frac{\psi^2 d}{2b}\right) > 1 \qquad (1.9)$$

with $b = z_1 z_2 e^2/E_p$ and E_p is particle energy. For ψ increasing

from zero, the inequality is violated first by the rapid decrease of the exponential, provided $(Ca/\psi d)$ can remain large. Thus the condition (1.9) requires that

$$\psi < \psi_1 = \sqrt{2b/E_p} = \sqrt{E_1/E_p}, \quad E_1 = 2z_1 z_2 e^2/d \qquad (1.10)$$

provided $Ca/\psi_1 d > 1$ i.e. $\psi_1 < a/d$ or $E_p > E' = 2z_1 z_2 e^2 d/a^2$ (1.11)

At low energies where (1.10) is not valid, one uses (1.6) in (1.7) and (1.8), getting the condition

$$\psi < \psi_2 = (Ca\psi_1/d\sqrt{2})^{1/2} \qquad (1.12)$$

and since $C/\sqrt{2} \simeq \sqrt{3}/\sqrt{2} \simeq 1$, the critical angle ψ_2 applies when

$$\psi_1 > a/d \quad \text{or} \quad E < E' \qquad (1.13)$$

From the above expressions (1.8)-(1.13), we note that the potential energy barrier $E_p \psi_1^2$ (for $E_p > E'$) is independent of energy but for $E_p < E'$, the corresponding barrier $E_p \psi_2^2$ varies as $E_p^{1/2}$ and decreases as the particle energy decreases. In contrast to ψ_1 in (1.10), ψ_2 in (1.12) depends upon the atomic radius and on the behaviour of screened atomic potential. As a consequence, (1.12) cannot be expected to hold accurately at very low energies.

The behaviour of a beam of particles moving through a lattice is qualitatively discussed by equations (1.10) and (1.12). If the initial angle ψ is less than ψ_1, the continuum picture of the string applies and the beam obeying this condition is said to be aligned beam (the condition for aligned beam being $\psi < C'\psi_1 = \psi_c$, C' of order 1-2) when $\psi > C'\psi$, one gets the random beam. Thus

the yield of a reaction requiring the incident particle to come close to the lattice atoms (within about 0.2 Å) such as Rutherford scattering, nuclear reactions etc., will depend upon the angle of incidence. It starts decreasing when the angle of incidence with respect to a prominent crystallographic direction is less than ψ_c and it reaches minimum value for $\psi = 0$, corresponding to a completely aligned beam. This minimum yield has been estimated to be[34]

$$\chi_{min} = Nd\pi (\rho_\perp^2 + a^2)$$

where $\rho_\perp^2$ is the mean square amplitude of lattice vibrations perpendicular to the string and a is the Thomas Fermi screening distance.

Another important case of channeling is the case of planar channeling which occurs when the particle moves parallel to a crystallographic plane. The correlations here are weaker and less effective than for the string case. Using continuum approximation, the average potential in this case can be written as

$$Y(y) = Nd_p \int_0^\infty 2\pi r \, dr \, V(\sqrt{y^2+r^2}) \qquad (1.14)$$

where y is the distance from the plane and Nd_p represents the average number of atoms per unit area of the plane, d_p being the distance between the consecutive planes. The ion-atom potential V(R) is given by (1.2). Using the standard atomic potential (1.6b), one gets

$$Y(y) = 2\pi z_1 z_2 e^2 \, Nd_p \left[(y^2 + C^2a^2)^{1/2} - y \right] \qquad (1.15)$$

which corresponds to the expression (1.6) for ξ (r/a) for the string case.

The criteria for the use of continuum potential for planar case is much more involved than for a string. The approximate condition for this case, as found by Lindhard[9], is

$$\zeta^2(1+\zeta^2)^2 \left[(\zeta^2+1)^{1/2} - \zeta \right] > \alpha \qquad (1.16)$$

with $\alpha = E_p'/E_p$, $\zeta = y_{min}/Ca$, $E_p' = \dfrac{z_1 z_2 e^2}{2\pi C^3 a^3 Nd_p} \sim z_1 z_2^2 \times 30$ eV.

and y_{min} is the minimum distance of approach to the plane.

Another consequence of directional effects is observed when the particles, emitted from sources (such as radioactive nuclei) embedded in a crystal propagate through it. The intensity of the emission pattern is found to depend strongly on the direction of observation with respect to a prominent crystallographic direction or plane. For positrons, the emission pattern has a dip along the directions along which maximum channeling occurs (when the emitter is at a lattice site). On the other hand, one gets a strong peak along these directions, for the case of electron emission. This phenomenon is called blocking and has also been treated by the classical theory of Lindhard. Supposing that the emitting nucleus is in the neighbourhood of an atomic position in the perfect string, one takes the probability distribution dP(r) of this nucleus, in space to be of the

Gaussian type

$$dP = e^{-r^2/\rho^2} \; 2rdr. \; \alpha/\rho^2 \qquad (1.17)$$

where ρ^2 is the mean square displacement due to the thermal vibrations and $\alpha = (1 - e^{-r_o^2/\rho^2})^{-1}$ is normalization constant and r_o is defined as $\pi r_o^2 = (Nd)^{-1}$. Then the probability distribution of transverse energy of particles is found to be (assuming $\rho << r_o$ i.e. $\alpha \approx 1$)

$$\Pi_{out}(E_\perp)dE_\perp = \exp\left[-\frac{C^2a^2}{\rho^2}\left(e^{2E_\perp/E_p\psi_1^2}-1\right)^{-1}\right]-\exp\left[-\frac{r_o^2}{\rho^2}\right] \qquad (1.18)$$

and the integrated dip in the emitted intensity is given by

$$\Omega \simeq \frac{\pi\psi_1^2}{2} \log \frac{\gamma C^2a^2 + \rho^2}{\rho^2}, \quad \gamma = 1.78 \qquad (1.19)$$

This expression shows that as the thermal vibrations tend to increase the mean square displacement ρ^2, the dip becomes less pronounced. For the ideal case of no thermal vibrations, one gets maximum dip.

Equation (1.19) can be used to calculate Ω if ρ is known. On the other hand if Ω is experimentally measured then the calculated value of ρ from eqn. (1.19) can be compared with its value determined otherwise. Apart from such estimates, it is seen that Ω is proportional to $\psi_1^2 = 2z_1z_2e^2/dE$. Thus the particles emitted with less energy will show a more pronounced dip than that exhibited by particles emitted with higher energy.

1.3 Need for Quantum Theory

The classical theory reviewed in the last section as proposed by Lindhard has been found to be in good agreement with experiments on heavy ion and alpha particle channeling. The magnitude of critical angle, ranges of ions, yields of Rutherford scattering and nuclear reactions etc. have been measured and results compared with the classical predictions are found to be in satisfactory agreement[10-23]. However, for light particles, such as the electrons and positrons, the classical theory cannot be used if one needs anything beyond the gross features, mainly because of two reasons: Firstly, the phenomena must be closely coupled to the Bragg reflections and other related interference effects which are observed in electron micrographs. Actually the phenomena observed in the electron microscope is described in terms of wave interference; Bragg angles and resonance widths dominate the intensity patterns even when the electron wave-length is very much smaller than the lattice spacing of the target crystal. Secondly, according to classical mechanics, the trajectory of a particle with a definite energy, moving through a fixed potential field V(r) remains the same if the mass of the particle is changed. In the corresponding quantum mechanical treatment, there is a direct dependence on the mass which vanishes only when the particle mass becomes arbitrarily large. It has been demonstrated by Lervig et al.[35] that electrons and positrons definitely exhibit many of the non classical features.

Actually, it has been established by DeWames et al.[36,37] that in the phenomena of channeling, the particle mass and the strength of the interaction potential simultaneously play an important role in determining the extent to which the classical theory may be used. They have shown explicitly that when, either the particle mass or the strength of the interaction potential becomes small, one should use quantum mechanical treatment. This criteria indicates clearly as to why neutrons and protons, inspite of their equal mass, are to be treated differently. Because of the weak strength of interaction for neutron case, it has to be treated quantum mechanically where as the protons, which interact via strong Coulomb (or screened Coulomb) field may be treated classically. Similarly, the electrons and positrons are expected to exhibit pronounced quantum effects in the emmission experiments[38,39] because of their small mass. Even in the case of protons, where the classical treatment should be applied and the wave mechanical treatment has been shown[40] to yield classical results in the limit of proton channeling conditions; there are some experimental observations[41,42] which can be explained only on the basis of wave mechanical theory. This point has been emphasized by Chadderton[43] by considering the proton channeling experiments of Gibbson et al.[41]. The presence of anomalously high energy loss and anomalously low energy loss components in the transmitted energy spectra is a definite indication of the

importance of interference effects due to wave nature of protons. Another evidence for existence of proton waves, is observation of star patterns[42]. Apart from these reasons, a purely quantum mechanical description of the atomic processes leading to directional effects in crystals is very much desirable from the standpoint of solid state theory.

The wave interference in electron channeling has been treated by many authors[44-47] and the problem has been essentially that of electron diffraction. On the other hand, for the case of neutrons, the effects of crystal periodicity have been neglected till the pioneering work of DeWames et al.[49] in this direction, published in 1966. They used quantum mechanics to explore the possibility of anomalous transmission of particles in the crystals. This has been further investigated in detail by the author[50].

In the present work, a general quantum mechanical formalism has been developed in Chapter II which has been applied to the channeling of electrons, positrons and neutrons in Chapter III. The problem of emission of charged particles (such as electrons and positrons) has been treated in Chapter IV and the corresponding blocking effects investigated. The energy lost to conduction electrons by the charged particles during the phenomena of channeling and blocking has been calculated using a dielectric formulation in Chapter V. The conclusions have been briefly summarized in the last Chapter.

CHAPTER II

QUANTUM THEORY OF CHANNELING

2.1 General Formulation:

The basic concept in the theory of directional effects in propagation of particles through crystals is to realize the crucial role of the crystal symmetry and its effects on the particle wave function. It has been customary in the theory of anomalous transmission for particles to draw analogies from the corresponding effects for x-rays which is known experimentally as Borrmann effect[51]. This effect is known theoretically[52] to be a consequence of the crystal periodicity which leads to the formation of standing waves in the crystal when the Bragg condition is satisfied. Those waves which have their antinodes at atomic sites are attenuated at an enhanced rate, while those having nodes at the atomic sites are negligibly attenuated and hence anomalously transmitted. The similar physical picture regarding the crystal periodicity is also true for the anomalous transmission of particles in the two beam theory. Therefore every attempt to understand the effect theoretically, must necessarily assume the existence of the crystal periodicity and any deviations from it must be treated in perturbation approximation. This feature is present in the Lindhard's classical theory[9] (discussed in Sec. 1.2) in which as a first approximation, regular chains of

close-packed atoms, called strings are assumed to exist in the crystal and also in the quantum formalism of DeWames et al.[45] where the crystal is assumed to be in ground state having exact periodicity of lattice.

In the present work, we assume that the crystal is initially in a very low lying state $|n\rangle$, so that the approximate crystal periodicity still exists. This effectively means that the crystal is at very low temperature and as far as the crystal symmetry is concerned, the lattice vibrations do not destroy it to any considerable extent. Therefore, as soon as the particles which outside the crystal were described in terms of plane waves, enter into the crystal, they are influenced by the periodic interaction potential of the crystal. It is known from the band theory of electrons in solids that as a consequence of Bloch theorem, the wave function of a particle in a periodic potential should be a Bloch wave. Consequently, the incident plane waves must go over to Bloch waves inside the crystal whose wave vectors should be determined by using the boundary condition at the crystal surface.

Another approximation that we make, is that only a few states which are close to the initial state of the system, are excited due to the incoming particles. This may not be obvious due to the fact that channeling takes place with fairly energetic particles. However, if we realize that the particles moving

close to the channeling conditions,do not come very close to the lattice atoms,as assumed by Lindhard to illustrate the steering mechanism and hence they have only gentle collisions with the lattice atoms. Consequently the approximation is quite reasonable under the conditions that exist in a channeling experiment. Under this approximation, the matrix element of the potential V_{nm} between the crystal eigen states $|n>$ and $|m>$ has approximate symmetry possessed by V when $|m>$ is closed to the initial state $|n>$ and can be expanded in lattice Fourier series. In particular, we will consider only one phonon inelastic processes implying thereby $|m> = |n \pm 1>$.

Now we consider a perfect crystal described by the Schrodinger eqn.

$$H_o|n> = E_n |n> \qquad (2.1)$$

where H_o is the second quantized Hamiltonian and E_n is the energy of the crystal when it is in the n-th eigen state, assumed to be the initial state which is very low lying at some low temperature. A beam of particles each of mass m_o, energy E_p is incident upon it. The total Hamiltonian of the system consisting of the crystal and the particle can be written as

$$H = H_o + H_p + V \qquad (2.2)$$

where H_p is the free particle Hamiltonian $-\hbar^2 \nabla^2/2m_o$ and V represents the interaction between the particle and the crystal.

Thus the total system is described by the Schrodinger eqn.

$$H\Psi = E\Psi \tag{2.3}$$

The total wave function Ψ may be expanded as

$$\Psi(\underline{r}, \{\underline{R}_\sigma\}) = \sum_m \phi_m(\underline{r}) \; |m\rangle \tag{2.4}$$

where $\underline{r}$ is the position of the particle, $\underline{R}_\sigma$ is the actual position of σ-th nucleus i.e. $\underline{R}_\sigma = \underline{\sigma} + \underline{u}_\sigma$, $\underline{\sigma}$ and $\underline{u}_\sigma$ being the normal position and the displacement of σ-th atom, respectively. Using eqns.(2.1)-(2.4), we get the eqn. for $\phi_n(\mathbf{r})$ as

$$\left[\frac{\hbar^2}{2m_o} \nabla^2 + (E - E_n)\right] \phi_n(\underline{r}) = \sum_m V_{nm}(\underline{r}) \; \phi_m(\underline{r}) \tag{2.5}$$

Eqn. (2.5) is similar to the corresponding equation obtained in scattering theory, with right hand side including a non-local term in n space i.e. both the elastic ($m = n$) and inelastic ($m \neq n$) processes being included. We will see that the inelastic part is responsible for both, attenuation and anomalous transmission.

As discussed earlier, the particle wave function $\phi_n(r)$ should be a Bloch wave and can be written as

$$\phi_n(\underline{r}) = e^{i\underline{k}_M \cdot \underline{r}} \; u_n(\underline{r}) \tag{2.6}$$

where the periodic function $u_n(\underline{r})$ has crystal periodicity such that $u_n(\underline{r}) = u_n(\underline{r} + \underline{\sigma})$, $\underline{\sigma}$ being a lattice vector and $\underline{k}_M$ is the wave vector of the particle inside the crystal which may be determined by using the boundary conditions at the crystal surface. The periodic function $u_n(\underline{r})$ can be expanded as

$$u_n(\underline{r}) = \sum_h u_h(n)\, e^{i\underline{K}_h \cdot \underline{r}}$$

so that $$\phi_n(\underline{r}) = \sum_h u_h(n)\, e^{i(\underline{K}_h + \underline{k}_M)\cdot \underline{r}} \qquad (2.7)$$

where $\underline{K}_h$ is a reciprocal lattice vector. Now, as indicated in the beginning of this section, assuming approximate symmetry for $|m>$ close to $|n>$, we expand $V_{nm}(\underline{r})$ as

$$V_{nm}(\underline{r}) = \sum_h V_h(n, m)\, e^{i\underline{K}_h \cdot \underline{r}} \qquad (2.8)$$

Using equations (2.7) and (2.8) in (2.5), we get

$$\frac{\hbar^2}{2m_o}\left[(\underline{K}_h + \underline{k}_M)^2 - k_n^2\right] u_h(n) + \sum_{g,m} V_{h-g}(n,m)\, u_g(m) = 0 \qquad (2.9)$$

where $k_n^2 = 2m_o (E-E_n)/\hbar^2 = 2m_o E_p/\hbar^2$, E_p being the particle energy.

Eqn. (2.9) is to be solved for the coefficients $u_g(m)$. To do this we note that it can be written in matrix form as

$$\hat{A}\, \underline{U} = -\hat{V}\, \underline{U} \qquad (2.10)$$

Here $\underline{U}$ is a column matrix, each element being specified by the crystal eigen state n and the Fourier index h. Thus, a particular element $U^{hn} = u_h(n)$ is h-th Fourier coefficient in the expansion of $u_n(\underline{r})$, the periodic part of the Bloch wave $\phi_n(\underline{r})$. Similarly the elements of the matrices $\hat{A}$ and $\hat{V}$ are specified, $\hat{A}$ being a diagonal matrix. The particular matrix elements may be written as

$$A_{gm}^{hn} = \frac{\hbar^2}{2m_o}\left[(\underline{K}_h + \underline{k}_M)^2 - k_n^2\right] \delta_{h,g}\, \delta_{n,m} \qquad (2.11a)$$

and $$V_{gm}^{hn} = V_{h-g}(n,m) = \frac{1}{V'} \int V_{nm}(\underline{r})\, e^{-i(\underline{K}_h - \underline{K}_g).\underline{r}}\, d\underline{r} \qquad (2.11b)$$

V' being the volume of the crystal.

The matrix equation (2.10) is in general, quite complicated and difficult to solve. The high dimensionality results from the product of the number of phonon states excited and the number of Fourier coefficients to be retained in the expansions of $u_n(\underline{r})$ and $V_{nm}(\underline{r})$. A formal solution of equation (2.10) can be written as

$$\underline{U} = \underline{U}_i - \hat{G}\,\hat{V}\,\underline{U} \qquad (2.12)$$

where $\hat{G} = (\hat{A} - i\epsilon)^{-1}_{\epsilon \to 0}$ is a diagonal matrix and U_i is a solution of equation (2.10) in the limit of vanishingly weak potential, namely when the particle has not interacted with the crystal and the crystal is in its initial state $|n>$, so that a particular element of this column matrix can be written as

$$U_i^{hm} = u_h(n)\ \delta_{m,n} \,. \qquad (2.13)$$

The dimensionality of the matrix eqn. (2.12) can be reduced to a large extent by using the partitioning technique. This technique has been successfully used in investigations of defect problem[53,54]. The idea is to partition the perturbation matrices such that only submatrix is significant and to keep the rest of the elements which are negligible, as null submatrices. Thus if we take only one phonon processes, the corresponding submatrix being represented as $\hat{v}$, we can write

$$\hat{V} = \begin{pmatrix} \hat{v} & 0 \\ 0 & 0 \end{pmatrix} \qquad (2.14)$$

Here, the matrix elements corresponding to higher phonon processes have been assumed to be negligible compared to one phonon elements contained in $\hat{v}$. Partitioning other matrices accordingly,

$$\hat{G} = \begin{pmatrix} \hat{g} & 0 \\ 0 & \hat{G}' \end{pmatrix}, \quad \underline{U} = \begin{pmatrix} \underline{u} \\ \underline{U}' \end{pmatrix} \text{ and } \quad \underline{U}_i = \begin{pmatrix} \underline{u}_i \\ \underline{U}_i' \end{pmatrix} \tag{2.15}$$

where $\hat{g}$, $\underline{u}$ and $\underline{u}_i$ have the same dimensionality as $\hat{v}$ and correspond to the same space of n and h as $\hat{v}$. Using these partitioned matrices in (2.12), we get

$$\underline{u} = \underline{u}_i - \hat{g}\,\hat{v}\,\underline{u} \tag{2.16a}$$

and

$$\underline{U}' = \underline{U}_i' \tag{2.16b}$$

Now writing $\hat{v}\underline{u} = \underline{s}$ and $\hat{v}\,\underline{u}_i = \underline{s}_i$ in (2.16a), we get

$$\underline{u} = \underline{u}_i - \hat{g}\,\underline{s} \tag{2.17a}$$

which yields, $\underline{s} = \hat{M}\underline{u}_i$ with $\hat{M} = (\hat{I} + \hat{v}\hat{g})^{-1}\,\hat{v}$ (2.17b)

so that a particular matrix element can be written as

$$u^{h'm} = u_{h'}(m) = u_i^{hm} - \frac{2m_o}{\hbar^2} \sum_{g,m'} \frac{M_{gm'}^{h'm}\, u_i^{gm'}}{(\underline{K}_{h'} + \underline{k}_M)^2 - k_m^2 - i\epsilon}$$

and using eqn. (2.13), we get for $m \neq n$

$$u_{h'}(m) = -\frac{2m_o}{\hbar^2} \sum_{g} \frac{M_{gn}^{h'm}\, u_g(n)}{(\underline{K}_{h'} + \underline{k}_M)^2 - k_m^2 - i\epsilon} \tag{2.18}$$

The Bloch states $\phi_m(\underline{r})$ excited due to propagation of particles, are obtained by using (2.18) and multiplying it with $e^{i(\underline{K}_{h'} + \underline{k}_M)\cdot\underline{r}}$ and summing over h', as

$$\phi_m(\underline{r}) = -\frac{2m_o}{\hbar^2} \sum_{h',g} \frac{M_{gn}^{h'm}\, u_g(n)\, e^{i(\underline{K}_{h'} + \underline{k}_M)\cdot\underline{r}}}{(\underline{K}_{h'} + \underline{k}_M)^2 - k_m^2 - i\epsilon} \tag{2.19}$$

Now writing eqn. (2.9) as

$$\frac{\hbar^2}{2m_o}\left[(\underline{K}_h+\underline{k}_M)^2 - k_n^2\right] u_h(n) + \sum_g V_{h-g}(n,n)\, u_g(n) + \sum_{h',m\neq n} V_{h-h'}(n,m) u_{h'}(m) = 0 \qquad (2.20)$$

and substituting for $u_{h'}(m)$ from (2.18), we get

$$\frac{\hbar^2}{2m_o}\left[(\underline{K}_h+\underline{k}_M)^2 - k_n^2\right] u_h(n) + \sum_g \left[V_{h-g}(n,n)+C_{hg}(n)\right] u_g(n) = 0 \quad (2$$

where

$$C_{hg}(n) = -\frac{2m_o}{\hbar^2} \sum_{m\neq n} \sum_{h'} \frac{V^{hn}_{h'm}\, M^{h'm}_{gn}}{(\underline{K}_{h'}+\underline{k}_M)^2 - k_m^2 - i\epsilon} \qquad (2.22)$$

We now examine the conditions under which only a few waves are needed in the periodic expansion of $\phi_n(\underline{r})$. For the ideal case, in which the crystal is assumed to be exactly in the ground state, the conditions have been examined[49] for ϕ_o. We shall follow a similar procedure. If in the expansion of $\phi_n(\underline{r})$, only first term $u_o(n)$ is to be significant then the solution for $u_h(n)$ must be small compared to $u_o(n)$. Thus

$$u_h(n) = -\frac{V_h(n) + C_{ho}(n)}{\frac{\hbar^2}{2m_o}\left[(\underline{K}_h+\underline{k}_M)^2 - k_n^2\right] + V_o(n) + C_{hh}(n)} \ll 1 \qquad (2.23)$$

where $u_h(n)$ has been written in units of $u_o(n)$. Clearly, except at a Bragg condition, one is dividing a Fourier coefficient of the interaction potential (since $C_{hg}(n) \ll V_h(n)$) by an energy of the order of

$$E_h \simeq \left(\frac{\hbar^2}{2m_o}\right)\left[\underline{K}_h^2 + 2\underline{K}_h\cdot\underline{k}_n\right]$$

since $k_M \simeq k_n$ as discussed below. For reciprocal lattice vectors perpendicular to k_n, this is about 50 eV for electrons and about 0.025 eV for protons and neutrons. Away from the perpendicular, but still not satisfying a Bragg condition, for $k_n >> K_h$, the second term dominates, tending towards $E_p(K_h/k_n)$. Thus at sufficiently large energy, only the planes parallel to k_n (so that $\underline{K}_h \cdot \underline{k}_n = 0$) contribute appreciably to ϕ_n. To justify the one wave picture, when such planes exist, it is necessary that the Fourier coefficients of the potential V_h be small compared to $V_o + \hbar^2 K_h^2/2m_o$. For sufficiently high order reflection V_h will in any case be small compared to V_o, limiting thereby the number of waves which must be taken into account.

When the inequality (2.23) is violated for a single reflection - e.g. when a Bragg condition ($|\underline{K}_h + \underline{k}_n| = k_n$) is fulfilled, the first term in the denominator of (2.23) becomes negligible and the corresponding coefficient $u_h(n)$ becomes significant. This is the well known two wave picture. There will exist two solutions for ϕ_n having $\underline{k}_M$ essentially parallel to $\underline{k}_n$. When such conditions are satisfied, we can write from eqn. (2.21), the two equations for $u_o(n)$ and $u_h(n)$ as

$$\left.\begin{aligned} &\left[V_h(n)+C_{ho}(n)\right] u_o(n) + \left[\frac{\hbar^2}{2m_o}\left((\underline{K}_h+\underline{k}_M)^2-k_n^2\right)\right. \\ &\qquad \left. + V_o(n)+C_{hh}(n)\right] u_h(n) = 0 \\ &\left[\frac{\hbar^2}{2m_o}(k_M^2-k_n^2)+V_o(n)+C_{oo}(n)\right] u_o(n)+\left[V_{-h}(n)+C_{oh}(n)\right] u_h(n)=0 \end{aligned}\right\} \quad (2$$

Writing $\underline{k}_M = \underline{k}_n + \underline{\eta}$ where η is small and its squares and higher powers will be neglected, we get from eqn. (2.24),(using the Bragg condition $|\underline{K}_h+\underline{k}_n| = k_n$ and the symmetry properties[44] of the renormalization matrix),

$$\begin{aligned}
&\left[V_h(n)+C_{ho}(n)\right]u_o(n)+\left[2\eta\gamma_n k_n+V_o(n)+C_{oo}(n)\right]u_h(n) = 0 \\
&\left[2\eta\gamma_n k_n+V_o(n)+C_{oo}(n)\right]u_o(n)+\left[V_h(n)+C_{ho}(n)\right]u_h(n) = 0
\end{aligned} \tag{2.25}$$

where $\gamma_n = \hat{k}_n.\hat{n}$, $\hat{n}$ being the unit normal to the entrance surface and $\hat{k}_n$ is unit vector along $\underline{k}_n$. For nonvanishing values of $u_o(n)$ and $u_h(n)$, the determinant of the equations (2.25) should vanish. This gives, on simplification, two values of η as

$$\eta_{\pm} = (k_n/2\gamma_n E_p)\left[\pm(V_h(n)+C_{ho}(n))-(V_o(n)+C_{oo}(n))\right] \tag{2.26}$$

Thus the two waves have wave vectors $(\underline{k}_n+\underline{\eta}_+)$ and $(\underline{k}_n+\underline{\eta}_-)$. The decay (attenuation) of these two solutions with penetration distance is determined by the imaginary part of $\eta_{\pm}$,

$$\text{Im } \eta_{\pm} = (k_n/2\gamma_n E_p)\left[\pm \text{ Im } C_{ho}(n)-\text{Im } C_{oo}(n)\right] \tag{2.27}$$

We notice that for Im $C_{ho}(n) \simeq$ Im $C_{oo}(n)$, the solution corresponding to η_+ will propagate almost without attenuation while other is attenuated at twice the rate of one wave solution. These solutions are,

$$\begin{aligned}
\phi_n(\underline{r}) &= \phi_n^+(\underline{r}) + \phi_n^-(\underline{r}) \\
\phi_n^+(\underline{r}) &\simeq \left[\exp i(\underline{k}_n+\eta_+\hat{n}).\underline{r}\right]\ (1-e^{i\underline{K}_h\cdot\underline{r}}) \\
\phi_n^-(\underline{r}) &\simeq \left[\exp i(\underline{k}_n+\eta_-\hat{n}).\underline{r}\right]\ (1+e^{i\underline{K}_h\cdot\underline{r}})
\end{aligned} \tag{2.28}$$

Here $\phi_n^+(\underline{r})$ which corresponds to η_+, has nodes at the atomic sites where the scattering out of the beam occurs, so that the attenuation is minimized, while the other wave $\phi_n^-(\underline{r})$ has anti-notes at these sites and the attenuation is enhanced because of scattering. This picture is analogous to that applied in the theory of anomalous transmission of x-rays[52]. It should be noted that even when several orders of reflection from the same plane contribute appreciably to $\phi_n(\underline{r})$, these two solutions ϕ_n^+ and ϕ_n^- dominate and one still gets anomalous transmission. In many interesting cases, this two beam theory is sufficient to give the essential features of the phenomena. A detailed account of the many beam solution in electron microscopy has been given elsewhere[55].

From the discussion following eqn. (2.22) upto this point, it is clear that calculations of penetration depths and the conditions for anomalous transmission need a detailed knowledge of the renormalization matrix. However, one must get into numerical computations regarding inversion, diagonalization and multiplication of matrices to obtain further results. This expression (2.22) may be seen to be similar to that obtained in the corresponding exact approach to scattering theory using T-matrix[56] where the problem ends up with numerical inversion and diagonalization of complicated T-matrix. Consequently, we shall now use first Born approximation to illustrate the analytical results.

2.2 First Born-Approximation:

Let us consider the matrix $\hat{M} = (\hat{I} + \hat{v}\hat{g})^{-1}\,\hat{v}$. If the interaction potential is weak so that the elements of the matrix $\hat{v}$ are small and the particle energy is sufficient to make sure that the elements of the diagonal matrix $\hat{g}$ are small such that the product $\hat{v}\hat{g}$ may be taken to be small compared with the unit matrix $\hat{I}$, then we can make a binomial expansion, to get

$$\hat{M} = \hat{v} - \hat{v}\,\hat{g}\,\hat{v} + \hat{v}\,\hat{g}\,\hat{v}\,\hat{g}\,\hat{v} - \ldots . \qquad (2.29)$$

This expression admits of successive approximations. The use of the first term $\hat{v}$ yields the first Born approximation result. Similarly, the second term corresponds to second Born approximation and so on.

Thus the first Born approximation in (2.22) yields

$$C_{hg}(n) = -\frac{2m_o}{\hbar^2} \sum_{m\neq n} \sum_{h'} \frac{V^{hn}_{h'm}\, V^{h'm}_{gn}}{(\underline{K}_{h'}+\underline{k}_M)^2 - k_m^2 - i\epsilon}$$

$$= -\frac{2m_o}{\hbar^2}\,\frac{1}{V}\int d\underline{r}\int d\underline{r}'\, e^{-i(\underline{K}_h+\underline{k}_M).\underline{r}+i(\underline{K}_g+\underline{k}_M).\underline{r}'}$$

$$\times \sum_{m\neq n}\left(\frac{1}{V}\sum_{h'}\frac{e^{i(\underline{K}_{h'}+\underline{k}_M).(\underline{r}-\underline{r}')}}{(\underline{K}_{h'}+\underline{k}_M)^2 - k_m^2 - i\epsilon}\right) V_{nm}(\underline{r})\,V_{mn}(\underline{r}') \qquad (2.30)$$

where in writing the last step, we have used the expressions for $V^{hn}_{h'm}$ etc. from eqn. (2.11) and $\underline{k}_M.(\underline{r}-\underline{r}')$ has been suitably added and subtracted in the exponential.

If one retains the second term in the expansion of $\hat{M}$, one gets the next order correction to $C_{hg}(n)$ as

$$C_{hg}^{(1)} = \left(\frac{2m_o}{\hbar^2}\right)^2 \frac{1}{V'} \int d\underline{r} \int d\underline{r}' \int d\underline{r}'' \, e^{-i(\underline{K}_h+\underline{k}_M).\underline{r}+i(\underline{K}_g+\underline{k}_M).\underline{r}''}$$

$$\times \sum_{m'} \sum_{m\neq n} V_{nm}(\underline{r}) \, V_{mm'}(\underline{r}') \, V_{m'n}(\underline{r}'')$$

$$\times \left(\frac{1}{V'} \sum_{h'} \frac{e^{i(\underline{K}_{h'}+\underline{k}_M).(\underline{r}-\underline{r}')}}{(\underline{K}_{h'}+\underline{k}_M)^2-k_m^2-i\epsilon}\right)\left(\frac{1}{V'} \sum_{h''} \frac{e^{i(\underline{K}_{h''}+\underline{k}_M).(\underline{r}'-\underline{r}'')}}{(\underline{K}_{h''}+\underline{k}_M)^2-k_{m'}^2-i\epsilon}\right)$$

and in this fashion, the successive approximations may be evaluated. While the analytical calculation becomes increasingly difficult for higher correction terms, the essential features may be illustrated by first Born approximation.

As we have seen, the attenuation of the two waves in the two beam theory, is determined by $\mathrm{Im}\, \eta_{\pm}$ which in turn needs the detailed calculation of imaginary part of the renormalization matrix elements. From eqn. (2.30) we write

$$\mathrm{Im}\, C_{hg}(n) = -\frac{2m_o}{\hbar^2} \frac{\pi}{V'} \int d\underline{r} \int d\underline{r}' \, e^{-i(\underline{K}_h+\underline{k}_M).\underline{r}+i(\underline{K}_g+\underline{k}_M).\underline{r}'}$$

$$\sum_{m\neq n} \left(\frac{1}{V'} \sum_{h'} e^{i(\underline{K}_{h'}+\underline{k}_M).(\underline{r}-\underline{r}')} \delta\left[(\underline{K}_{h'}+\underline{k}_M)^2-k_m^2\right]\right) V_{nm}(\underline{r}) V_{mn}(\underline{r}') \tag{2.31}$$

Noting that the imaginary part of $\underline{k}_M.\underline{r}$ is small over many unit cells, we put $\underline{k}_M \sim \underline{k}_n$ in the expression (2.31). Further, since the summation over h' in eqn. (2.31) extends over whole of the reciprocal space, we can replace it by a sum over $\underline{k} = \underline{K}_{h'}+\underline{k}_M$ to write

$$\frac{1}{V'} \sum_{h'} e^{i(\underline{K}_{h'}+\underline{k}_M).(\underline{r}-\underline{r}')} \delta\left[(\underline{K}_{h'}+\underline{k}_M)^2-k_m^2\right]$$

$$= \frac{1}{V'} \sum_{\underline{k}} e^{i\underline{k}.(\underline{r}-\underline{r}')} \delta(k^2-k_m^2) \tag{2.32}$$

Since the wave vector $\underline{k}_M$ may have any value depending upon the incident particle energy, the variable $\underline{k}$ is continuous like the usual wave vector in the reciprocal space, and one can replace the summation over $\underline{k}$ by an integration to obtain,

$$\text{Im } C_{hg}(n) = -\frac{2m_o\pi}{V'\hbar^2(2\pi)^3} \int d\underline{k} \int d\underline{r} \int d\underline{r}' e^{i(\underline{k}-\underline{k}_n-\underline{K}_h)\cdot\underline{r} - i(\underline{k}-\underline{k}_n-\underline{K}_g)\cdot\underline{r}'} \times \sum_{n'\neq n} V_{nn'}(\underline{r})\, V_{n'n}(\underline{r}')\, \delta(k^2-k_{n'}^2) \quad (2.33)$$

which is exactly the same result as has been obtained[50] by starting with the first Born approximation solution to $\phi_m(\underline{r})$

$$\phi_m(\underline{r}) = -\frac{2m_o}{\hbar^2} \int dr' \, \frac{e^{ik_m|\underline{r}-\underline{r}'|}}{4\pi|\underline{r}-\underline{r}'|} V_{mn}(r')\, \phi_n(\underline{r}')$$

in eqn. (2.5) and then using the appropriate expansions of $V_{nn}(\underline{r})$ and $\phi_n(\underline{r})$.

Now let us choose a general interaction potential, which interms of the atomic potentials, may be written as $V(\underline{r}) = \sum_{\underline{\sigma}} V_\sigma(\underline{r}-\underline{R}_\sigma)$, $V_\sigma(\underline{r}-\underline{R}_\sigma)$ representing the interaction potential between the incident particle and the atom (or ion) at position $\underline{\sigma}$. The actual position of the σ-th atom $\underline{R}_\sigma$ may be written as $\underline{R}_\sigma = \underline{\sigma} + \underline{u}_\sigma$, where $\underline{u}_\sigma$ is the displacement from the equilibrium position of the lattice site σ, due to thermal vibrations. Thus from (2.33), we get

$$\text{Im } C_{hg}(n) = -\frac{2m_o\pi}{V'\hbar^2(2\pi)^3} \int d\underline{k} \sum_{n'\neq n} \sum_{\underline{\sigma},\underline{\sigma}'} V_\sigma(\underline{k}-\underline{k}_n-\underline{K}_h) e^{i(\underline{k}-\underline{k}_n-\underline{K}_h)\cdot\underline{\sigma}} V_{\sigma'}(\underline{k}-\underline{k}_n-\underline{K}_g) e^{-i(\underline{k}-\underline{k}_n-\underline{K}_g)\cdot\underline{\sigma}'} \delta(k^2-k_{n'}^2) \langle n| e^{i(\underline{k}-\underline{k}_n-\underline{K}_h)\cdot\underline{u}_\sigma} |n'\rangle \times \langle n'| e^{-i(\underline{k}-\underline{k}_n-\underline{K}_g)\cdot\underline{u}_{\sigma'}} |n\rangle \quad (2.34)$$

where $V_\sigma(\underline{K}) = \int V_\sigma(\underline{r})\, e^{i\underline{K}\cdot\underline{r}}\, d\underline{r}$

The matrix elements $\langle n | e^{i\underline{K}\cdot\underline{u}_\sigma} | n' \rangle$ for $n' \neq n$, as they are involved in the expression (2.34), correspond to exchange of phonons i.e. inelastic processes. The procedure to evaluate these, is to expand $\underline{u}_\sigma$ as,

$$\underline{u}_\sigma = \left(\frac{\hbar^2}{2MN}\right)^{1/2} \sum_{j,s} \frac{\underline{\epsilon}_s}{\xi_j^{1/2}} \left[a_j\, e^{i\underline{f}_j\cdot\underline{\sigma}} + a_j^\dagger\, e^{-i\underline{f}_j\cdot\underline{\sigma}}\right] \quad (2.35)$$

where ξ_j and $\underline{f}_j$ are energy and wave vector of j-th phonon, respectively, and $\underline{\epsilon}_s$ ($s = 1,2,3$) are their polarization vectors. The lattice is supposed to be monoatomic, M denoting the mass of each atom. There are N atoms in the crystal. Here a_j and $a_j^\dagger$ are the well known phonon creation and annihilation operators for j-th phonon.

The phonon state $|n\rangle$ is written as $|n_1, n_2, \ldots\rangle$, $n_1, n_2, \ldots$ representing occupation numbers corresponding to different normal modes so that the matrix element to be evaluated may be written as,

$$\langle n' | e^{i\underline{K}\cdot\underline{u}_\sigma} | n \rangle = \langle n_1', n_2', \ldots | e^{i(Q_{j\sigma} a_j + Q_{j\sigma}^* a_j^\dagger)} | \ldots n_2, n_1 \rangle$$

$$= \prod_{j=1}^{N} \langle n_j' | e^{i(Q_{j\sigma} a_j + Q_{j\sigma}^* a_j^\dagger)} | n_j \rangle \quad (2.36)$$

where

$$Q_{j\sigma} = \left(\frac{\hbar^2}{2MN\xi_j}\right)^{1/2} \sum_s (\underline{K}\cdot\underline{\epsilon}_s) e^{i\underline{f}_j\cdot\underline{\sigma}} \quad (2.37)$$

For an inelastic process involving multiphonon exchange, it has been shown by Kothari and Singwi[57] that the probability of any two phonons to have same wave vector (i.e. exchange of any two

phonons corresponding to the same mode of vibration) is negligibly small compared to the process in which all the phonons being exchanged, have different wave vectors. Therefore, for an 1 phonon exchange process, eqn. (2.36) may be written as

$$\langle n'|e^{i\underline{K}.\underline{u}_\sigma}|n\rangle = \prod_{j=1}^{l} \langle n_j \pm 1|e^{i(Q_{j\sigma}a_j + Q^*_{j\sigma}a_j^\dagger)}|n_j\rangle \prod_{j=l+1}^{N} \langle n_j|e^{i(Q_{j\sigma}a_j + Q^*_{j\sigma}a_j^\dagger)}|n_j\rangle \quad (2.38)$$

However, at any finite temperature T, since the exact n_j corresponding to a given initial state $|n\rangle$ is never known, we should take an average over initial state so that the required matrix element becomes

$$\langle n'|e^{i\underline{K}.\underline{u}_\sigma}|n\rangle = \sum_{n_1=0}^{\infty}\sum_{n_2=0}^{\infty}\cdots\sum_{n_N=0}^{\infty}\left(\prod_{j=1}^{N}\omega(n_j)\right) \prod_{j=1}^{l}\langle n_j\pm1|e^{i(Q_{j\sigma}a_j+Q^*_{j\sigma}a_j^\dagger)}|n_j\rangle \prod_{j=l+1}^{N}\langle n_j|e^{i(Q_{j\sigma}a_j+Q^*_{j\sigma}a_j^\dagger)}|n_j\rangle \quad (2$$

where $\omega(n_j)$ is the probability of n_j phonons of wave vector $\underline{f}_j$ being present in the field when the lattice is at a temperature T and is given by

$$\omega(n_j) = (1-e^{-\xi_j/k_BT})\, e^{-n_j\xi_j/k_BT} \quad (2.40)$$

For an 1 phonon process this averaging has been shown[58] to be equivalent to replacing the operator of the form exp (U) by $(U^l/l!)\exp(\frac{1}{2}\langle U^2\rangle_T)$. Thus for emission of 1 phononswe get

$$\langle n'|\exp(i\underline{K}.\underline{u}_\sigma)|n\rangle = \prod_{j=1}^{l}\frac{[iQ^*_{j\sigma}(n_j+1)^{1/2}]^l}{l!}\, e^{-W} \quad (2.41)$$

where the Debye-Waller factor 2W is given by[57],

$$2W = 2DK^2$$
$$\text{with} \quad 2D = (\hbar^2/2MN) \sum_j \frac{1}{\xi_j} \coth(\xi_j/2k_BT) \tag{2.42}$$

We note that eqn. (2.41) gives the matrix element for exchange of l phonons each having different frequency. But, since it has been shown[59] that exchange of two phonons of same type is N^{-1} times less probable compared to one phonon process, eqn. (2.41) gives the matrix element for a general l-phonon process within the approximation of neglecting terms of order N^{-1} compared to unity.

We also see from eqn. (2.41) that an l-phonon process involves the l-th power of $Q_{j\sigma} \simeq (\text{energy transfer}/N\,\xi_j)^{1/2}$, which is a small quantity, so that the corresponding matrix element decreases rapidly as l increases. Moreover, the multi-phonon processes do not permit even the approximate symmetry, which is so crucial for anomalous transmission. Therefore as a first approximation, we take only the one phonon contributions in eqn. (2.41) so that we can write

$$\langle n'|\exp(-i\underline{K}.\underline{u}_{\sigma'})|n\rangle = -iQ^*_{\sigma'}(n_1+1)^{1/2} \exp(-DK^2) \tag{2.43}$$

where the subscript j = 1 has been dropped from $Q^*_{1\sigma}$, $\underline{f}_1$ and ξ_1.

The corresponding matrix element for absorption of l-phonons is obtained similarly and one gets

$$\langle n|\exp(i\underline{K}.\underline{u}_{\sigma})|n'\rangle = \prod_{j=1}^{l} \frac{\left[iQ_{j\sigma}n_j^{1/2}\right]^l}{l!} e^{-W} \tag{2.44}$$

so that in one phonon approximation, we have

$$\langle n|\ \exp\ (i\underline{K}.\underline{u}_\sigma)|n'\rangle = iQ_\sigma\, n_1^{1/2}\ \exp\ (-DK^2) \qquad (2.45)$$

After substituting such matrix elements in eqn. (2.34) one should average the expression over initial state. This is because the crystal is at some finite temperature T and due to thermal vibrations, n_1, corresponding to a given initial state $|n\rangle$, is never exactly known. Therefore we replace n_1 and (n_1+1) by the corresponding averages

$$\langle n_1\rangle = (e^{\xi/k_BT}-1)^{-1}$$
$$\text{and} \qquad \langle n_1+1\rangle = (1-e^{-\xi/k_BT})^{-1} \qquad (2.46)$$

where k_B is the Boltzman constant. Thus finally we get from eqn. (2.34),

$$\text{Im}\ C_{hg}(n) = -\frac{2m_o\pi}{V'\hbar^2(2\pi)^3}\int d\underline{k}\ \sum_{\underline{\sigma},\underline{\sigma}'} V_\sigma(\underline{k}-\underline{k}_n-\underline{K}_h)V_{\sigma'}(\underline{k}-\underline{k}_n-\underline{K}_g)$$
$$\times\ \frac{1}{N}\sum_{\underline{f}}\left(\frac{\hbar^2}{2MN\xi}\right)\left[\frac{\delta(k^2-k_{n+1}^2)}{(1-e^{-\xi/k_BT})}\ e^{i\underline{f}.(\underline{\sigma}-\underline{\sigma}')} + \frac{\delta(k^2-k_{n-1}^2)}{(e^{\xi/k_BT}-1)}\ e^{-i\underline{f}.(\underline{\sigma}-\underline{\sigma}'}\right.$$
$$\times\ \exp\left[i(\underline{k}-\underline{k}_n).(\underline{\sigma}-\underline{\sigma}')\right](\underline{k}-\underline{k}_n-\underline{K}_h).(\underline{k}-\underline{k}_n-\underline{K}_g)$$
$$\times\ \exp(-D\left[(\underline{k}-\underline{k}_n-\underline{K}_h)^2+(\underline{k}-\underline{k}_n-\underline{K}_g)^2\right]) \qquad (2.47)$$

since $\exp\ (\pm\ i\underline{K}_h.\underline{\sigma}) = 1$.

Since any of the phonon modes could be excited due to the propagation of particle through the crystal, we have summed over all possible values of $\underline{f}$ and divided by N, the total number of possible phonon modes. The probability factors for the

phonon to have corresponding energy ξ are supplied by $(1-e^{-\xi/k_BT})^{-1}$ and $(e^{\xi/k_BT}-1)^{-1}$. Thus eqn. (2.47) gives the expression for Im $C_{hg}(n)$ in one phonon approximation, for a general interaction potential between the particle and the crystal lattice atoms and for a general dispersion for the lattice vibrations.

In order to proceed a little further with eqn. (2.47), we assume the crystal to have no isotopes present and that the nuclear spin of lattice ions may be neglected. Under this assumption, the Fourier transform of the potential, $V_\sigma(\underline{K})$ becomes independent of σ so that writing $V_\sigma(\underline{K}) = V(\underline{K})$ in eqn. (2.47), we get

$$\text{Im } C_{hg}(n) = -\frac{2m_o\pi}{V'\hbar^2(2\pi)^3}\int d\underline{k} V(\underline{k}-\underline{k}_n-\underline{K}_h)V(\underline{k}-\underline{k}_n-\underline{K}_g)(\underline{k}-\underline{k}_n-\underline{K}_h).(\underline{k}-\underline{k}_n-$$

$$\times\ e^{-D\left[(\underline{k}-\underline{k}_n-\underline{K}_h)^2+(\underline{k}-\underline{k}_n-\underline{K}_g)^2\right]}\sum_{\underline{\sigma},\underline{\sigma}'} e^{i(\underline{k}-\underline{k}_n).(\underline{\sigma}-\underline{\sigma}')}\ \frac{1}{N}\sum_{\underline{f}}\left(\frac{\hbar^2}{2MN\xi}\right.$$

$$\times\left[\frac{\delta(k^2-k_n^2+\frac{2m_o\xi}{\hbar^2})}{(1-e^{-\xi/k_BT})}e^{i\underline{f}.(\underline{\sigma}-\underline{\sigma}')}+\frac{\delta(k^2-k_n^2-\frac{2m_o\xi}{\hbar^2})}{(e^{\xi/k_BT}-1)}e^{-i\underline{f}.(\underline{\sigma}-\underline{\sigma}')}\right](2.$$

If there are isotopes, however, additional terms will appear in eqn. (2.48). For example, an isotope sitting at the origin, whose interaction potential is δV in addition to that of a normal atom, will contribute terms involving integrations over the products of V and δV in eqn.(2.48).

Now the summation over $\underline{\sigma}$ and $\underline{\sigma}'$ in eqn. (2.48) can be written in the form $\left|\sum_{\underline{\sigma}} e^{i(\underline{k}-\underline{k}_n+\underline{f}).\underline{\sigma}}\right|^2$. This type of summations frequently occur in the neutron scattering cross section calculations and

can be performed easily[57,60] to yield $\frac{(2\pi)^3 N}{v_c} \sum_{h'} \delta(\underline{k}-\underline{k}_n \pm \underline{f}+\underline{K}_{h'})$ where v_c is volume of the unit cell. Using these simplifications, eqn. (2.48) can be written as,

$$\text{Im } C_{hg}(n) = -\frac{2m_o\pi}{V'\hbar^2(2\pi)^3} \int d\underline{k}\, V(\underline{k}-\underline{k}_n-\underline{K}_h)V(\underline{k}-\underline{k}_n-\underline{K}_g)(\underline{k}-\underline{k}_n-\underline{K}_h).(\underline{k}-\underline{k}_n-\underline{K}_g$$

$$\times e^{-D[(\underline{k}-\underline{k}_n-\underline{K}_h)^2+(\underline{k}-\underline{k}_n-\underline{K}_g)^2]} \frac{(2\pi)^3}{v_c} \sum_{\underline{f}} [G_1(\underline{f}) \sum_{h'} \delta(\underline{k}-\underline{k}_n+\underline{f}+\underline{K}_{h'})$$

$$+G_2(\underline{f}) \sum_{h''} \delta(\underline{k}-\underline{k}_n-\underline{f}+\underline{K}_{h''})] \qquad (2.49)$$

$$\text{where} \quad G_1(\underline{f}) = \frac{\hbar^2}{2MN\xi} \frac{\delta(k^2-k_n^2+2m_o\xi/\hbar^2)}{(1-e^{-\xi/k_BT})} \qquad (2.50)$$

$$\text{and} \quad G_2(\underline{f}) = \frac{\hbar^2}{2MN\xi} \frac{\delta(k^2-k_n^2-2m_o\xi/\hbar^2)}{(e^{\xi/k_BT}-1)} .$$

Since energy $\xi(\underline{f})$ is periodic in the reciprocal space, $\xi(\underline{f})=\xi(\underline{f}+\underline{K}_h)$ and the $\underline{f}$-dependence of $G_1(\underline{f})$ and $G_2(\underline{f})$ is only through $\xi(\underline{f})$, we have $G_1(\underline{f}) = G_1(\underline{f} \pm \underline{K}_{h'})$ for all $\underline{K}_{h'}$ and $G_2(\underline{f}) = G_2(\underline{f} \pm \underline{K}_{h''})$ for all $\underline{K}_{h''}$. Therefore the terms in the square brackets in eqn. (2.49), which are being summed over $\underline{f}$, can be written as

$$\sum_{\underline{f}} \left[\sum_{h'} G_1(\underline{f}+\underline{K}_{h'})\delta(\underline{k}-\underline{k}_n+\underline{f}+\underline{K}_{h'})+ \sum_{h''} G_2(\underline{f}-\underline{K}_{h''})\delta(\underline{k}-\underline{k}_n-\underline{f}+\underline{K}_{h''})\right]$$

$$= \sum_{\underline{f}} \sum_{h'} \left[G_1(\underline{f}+\underline{K}_{h'})\delta(\underline{k}-\underline{k}_n+\underline{K}_{h'}+\underline{f})+G_2(\underline{f}-\underline{K}_{h'})\delta(\underline{k}-\underline{k}_n-\underline{f}+\underline{K}_{h'})\right]$$

$$= \sum_{h'} \left[\sum_{\underline{f}} G_1(\underline{f}+\underline{K}_{h'})\delta(\underline{k}-\underline{k}_n+\underline{f}+\underline{K}_{h'})+ \sum_{\underline{f}} G_2(\underline{f}-\underline{K}_{h'})\delta(\underline{k}-\underline{k}_n-\underline{f}+\underline{K}_{h'})\right]$$

$$= \sum_{h'} \sum_{\underline{f}'} \left[G_1(\underline{f}')\delta(\underline{k}-\underline{k}_n+\underline{f}') +G_2(\underline{f}')\delta(\underline{k}-\underline{k}_n-\underline{f}')\right]$$

$$= N \sum_{\underline{f}} \left[G_1(f)\delta(\underline{k}-\underline{k}_n+\underline{f})+G_2(\underline{f})\delta(\underline{k}-\underline{k}_n-\underline{f})\right] \qquad (2.51)$$

where $\underline{f}$ is restricted to the first Brillouin zone.

Now substituting (2.51) in eqn.(2.49), using δ-functions, $\delta(\underline{k}-\underline{k}_n \pm \underline{f})$ for $\underline{k}$-integration and replacing summation over $\underline{f}$ by an integration $V'/(2\pi)^3 \int d\underline{f}$, we get

$$\text{Im } C_{hg}(n) = -\frac{m_o}{2Mv_c(2\pi)^2} \int \frac{d\underline{f}}{\xi} \left[\frac{V(\underline{f}+\underline{K}_h)V(\underline{f}+\underline{K}_g)}{(1-e^{-\xi/k_BT})} (\underline{f}+\underline{K}_h).(\underline{f}+\underline{K}_g) \right.$$

$$\times e^{-D\left[(\underline{f}+\underline{K}_h)^2+(\underline{f}+\underline{K}_g)^2\right]} \delta\left(f^2-2\underline{f}.\underline{k}_n+\frac{2m_o\xi}{\hbar^2}+\frac{V(\underline{f}-\underline{K}_h)V(\underline{f}-\underline{K}_g)}{(e^{\xi/k_BT}-1)}\right.$$

$$\left.\left. \times (\underline{f}-\underline{K}_h)\cdot(\underline{f}-\underline{K}_g)\, e^{-D\left[(\underline{f}-\underline{K}_h)^2+(\underline{f}-\underline{K}_g)^2\right]} \delta\left(f^2+2\underline{f}.\underline{k}_n-\frac{2m_o\xi}{\hbar^2}\right)\right] \quad (2.\right.$$

This general expression admits the use of dispersion for any realistic model for lattice vibrations and can be used with any interaction potential by using the corresponding Fourier transform in eqn. (2.52).

2.3 Debye Model Calculations:

It is well known that the Debye model represents a reasonable approximation to the actual lattice vibrations in the crystals, particularly corresponding to the low frequency part of the actual phonon dispersion. In this model, it is assumed that[6] the lattice vibrates as if it were an elastic continuum but the frequencies of vibration cannot exceed a certain maximum value, chosen to make the total number of modes equal to the total number of classical degrees of freedom.This is specially true for the long wave length lattice vibrations which cannot see the detailed lattice structure. If the modes are classified by

their frequencies, the frequency distribution function $g(\omega)$ is proportional to ω^2 in elastic medium. We choose a maximum frequency ω_o at which this distribution is cut off so that the total number of distinct modes equals 3N. The corresponding dispersion is simply expressed as $\xi(\underline{f}) = \hbar\omega(\underline{f}) = \hbar cf$ where c is the velocity of sound in the medium. Thus the maximum value ω_o corresponds to a cut off in the frequency given by f_o. The Brillouin zone, which limits the range of allowed values of f, is replaced by a sphere of same volume with radius f_o. This sphere is called the Debye sphere. Since the Debye sphere is to contain N points at a density $V'/8\pi^3$ in f-space, we must have

$$N = \frac{V'}{8\pi^3} \frac{4\pi}{3} f_o^3$$

i.e. $$f_o = (6\pi^2/v_c)^{1/3} \qquad (2.53)$$

A more detailed review of the Debye theory has been given by Blackman[62].

In spite of the approximate nature of the Debye model, one gets quite satisfactory results in many interesting cases, when Debye model is used for lattice vibrations. Particularly, whenever the results depend upon an integration over $\underline{f}$ in reciprocal space, it is found to give very good results. The most striking example is that of neutron scattering cross-sections. The total cross-sections (elastic and inelastic, both) are found to agree with experiments quite well. An excellent review on

thermalization of neutrons and applicability of Debye model has been given by Kothari and Singwi[57].

For the present purpose we see that our expression (2.52) contains integrations over the phonon wave vector $\underline{f}$. Therefore the use of the Debye model is reasonably good and is relatively simple to yield analytical results. This is so in view of the fact that particles moving near the principal crystallographic axes, do not come much close to the lattice atoms and very high frequency modes are not excited even when the particle energy is large.

Now writing $\xi = \hbar cf$ in eqn. (2.52), we get

$$\text{Im } C_{hg}(n) = -\frac{m_o}{2M\hbar cv_c(2\pi)^2}\int\frac{df}{f}\Big[\frac{V(\underline{f}+\underline{K}_h)V(\underline{f}+\underline{K}_g)}{(1-e^{-\hbar cf/k_BT})}(\underline{f}+\underline{K}_h).(\underline{f}+\underline{K}_g)$$

$$\times\ e^{-D\left[(\underline{f}+\underline{K}_h)^2+(\underline{f}+\underline{K}_g)^2\right]}\delta(f^2-2\underline{f}.\underline{k}_n+\frac{2m_ocf}{\hbar})+\frac{V(\underline{f}-\underline{K}_h)V(\underline{f}-\underline{K}_g)}{(e^{\hbar cf/k_BT}-1)}$$

$$\times\ (\underline{f}-\underline{K}_h).(\underline{f}-\underline{K}_g)e^{-D\left[(\underline{f}-\underline{K}_h)^2+(\underline{f}-\underline{K}_g)^2\right]}\delta(f^2+2\underline{f}.\underline{k}_n-\frac{2m_ocf}{\hbar})\Big] \quad (2.54)$$

$$\text{so that}\quad \text{Im } C_{oo}(n) = -\frac{m_o}{2M\hbar cv_c(2\pi)^2}\int f\,df\,V^2(f)\,e^{-2Df^2}$$

$$\times\Big[\frac{\delta(f^2-2\underline{f}.\underline{k}_n+\frac{2m_ocf}{\hbar})}{(1-e^{-\hbar cf/k_BT})}+\frac{\delta(f^2+2\underline{f}.\underline{k}_n-\frac{2m_ocf}{\hbar})}{(e^{\hbar cf/k_BT}-1)}\Big] \quad (2.55)$$

$$\text{and}\quad \text{Im } C_{ho}(n) = -\frac{m_o}{2M\hbar cv_c(2\pi)^2}\int\frac{df}{f}\Big[\frac{V(\underline{f}+\underline{K}_h)V(\underline{f})}{(1-e^{-\hbar cf/k_BT})}\underline{f}.(\underline{f}+\underline{K}_h)$$

$$\times\ e^{-D\left[(\underline{f}+\underline{K}_h)^2+f^2\right]}\delta(f^2-2\underline{f}.\underline{k}_n+\frac{2m_ocf}{\hbar})+\frac{V(\underline{f}-\underline{K}_h)V(\underline{f})}{(e^{\hbar cf/k_BT}-1)}$$

$$\times\ \underline{f}.(\underline{f}-\underline{K}_h)e^{-D\left[(\underline{f}-\underline{K}_h)^2+f^2\right]}\delta(f^2+2\underline{f}.\underline{k}_n-\frac{2m_ocf}{\hbar})\Big] \quad (2.56)$$

Now these expressions can be used to calculate $\mathrm{Im}\eta_{\pm}$ of eqn. (2.27) for any interaction potential by using the corresponding Fourier transform in the expressions for Im C_{ho} (n) and Im C_{oo} (n). In the next chapter we give the calculations of Im C_{ho}(n) and Im C_{oo}(n) for neutrons and charged particles to find the attenuations of the two waves ϕ_n^+ and ϕ_n^- and the conditions for anomalous transmission.

CHAPTER III

CALCULATION USING DIFFERENT POTENTIAL MODELS

3.1 Fermi Pseudopotential - Neutrons:

The possibility of anomalous neutron transmission was realized shortly after this effect had been identified and understood for x-rays[51,52]. However, no theoretical investigation was made at that time and the only experiment directed toward seeing anomalous neutron transmission yielded a negative result[63], apparently due to crystal imperfections. There has been no further attempt to experimentally demonstrate anomalous neutron transmission.The main difficulty in such experiments is that neutrons have already high penetrating power because of extremely short range nuclear interaction between neutron and atomic nucleus and it becomes extremely difficult to notice directional effects in neutron transmission. However, theoretically the problem does carry some interest and recently, DeWames et al.[49] have investigated the theoretical aspects of anomalous neutron penetration in perfect crystals. Their theory is similar to that presented in this work but they assumed the crystal to be initially in the ground state at T = 0 and used the Einstein model for lattice vibrations. In what follows, we shall treat this problem using the formalism of Chapter II.

For neutrons, the two particle interaction potential is very local, the range being of the order of nuclear dimensions. For wavelengths larger than the nuclear scattering length a', one can replace the actual interaction by a potential whose width is intermediate between the scattering length and the wavelength. We shall choose a form which passes directly over to the Fermi pseudo-potential[64] as the width β^{-1} vanishes:

$$v(r) = -\frac{2\pi\hbar^2}{m_o}\frac{\beta^2}{(\pi)^{3/2}} a\, e^{-\beta^2 r^2} \tag{3.1}$$

where a is the scattering length of a bound atom in the crystal and is related to the scattering length of the individual atom a' by the relation $a = a'(M+m_o)/M$. As $\beta^{-1} \to 0$, v(r) of eqn.(3.1) goes to Fermi pseudo-potential[57,65].

Thus the total interaction potential between the neutron and the crystal can be written as

$$V(r) = -\frac{2\pi\hbar^2}{m_o}\frac{\beta^2}{\pi^{3/2}} \sum_{\sigma} a_\sigma\, e^{-\beta^2(\underline{r}-\underline{R}_\sigma)^2} \tag{3.2}$$

$$\text{so that } V_\sigma(\underline{r}-\underline{R}_\sigma) = -\frac{2\pi\hbar^2}{m_o}\frac{\beta^2}{\pi^{3/2}} a_\sigma\, e^{-\beta^2(\underline{r}-\underline{R}_\sigma)^2} \tag{3.3}$$

Here a_σ has dimension of length and becomes scattering length (of a bound atom at the lattice site σ) in the case of Fermi pseudo-potential ($\beta^{-1} \to 0$). From eqn. (3.3) we calculate $V_\sigma(\underline{K})$ a

$$\begin{aligned} V_\sigma(\underline{K}) &= \int V_\sigma(\underline{r})\, e^{i\underline{K}\cdot\underline{r}}\, d\underline{r} \\ &= -\frac{2\pi\hbar^2}{m_o}\frac{\beta^2}{\pi^{3/2}} a_\sigma \int e^{-\beta^2 r^2}\, e^{i\underline{K}\cdot\underline{r}}\, d\underline{r} \\ &= -\frac{2\pi\hbar^2}{m_o} a_\sigma\, e^{-K^2/4\beta^2} \end{aligned} \tag{3.4}$$

In the approximation of zero nuclear spin of the crystal atoms and no isotopes present, a_σ is independent of σ and we get,

$$V(\underline{K}) = - \frac{2\pi\hbar^2}{m_o} a \; e^{-K^2/4\beta^2}. \qquad (3.5)$$

Using this in eqn. (2.56) we get

$$\text{Im } C_{ho}(n) = - \frac{\hbar^3 a^2}{2Mm_o cv_c} \int \frac{d\underline{f}}{f} \left\{ \frac{(\underline{f}+\underline{K}_h).\underline{f}}{1-e^{-\hbar cf/k_BT}} \; e^{-D'\left[(\underline{K}_h+\underline{f})^2+f^2\right]} \right.$$
$$\times \delta(f^2-2\underline{f}.\underline{k}_n+\frac{2m_o cf}{\hbar}) + \frac{(\underline{f}-\underline{K}_h).\underline{f}}{(e^{\hbar cf/k_BT}-1)}$$
$$\left. \times e^{-D'\left[(\underline{K}_h-\underline{f})^2+f^2\right]} \delta(f^2+2\underline{f}.\underline{k}_n-\frac{2m_o cf}{\hbar}) \right] \Big\} \qquad (3.6)$$

where $D' = D + 1/4\beta^2$ (3.7)

In the Debye model, the maximum cut-off value of frequency f_o is always small compared to a reciprocal lattice vector K_h. In eqn. (3.7), we note that the integration over $\underline{f}$ will have this cut off f_o as the upper limit. Consequently, if we neglect $\underline{f}$ compare to the reciprocal lattice vector $\underline{K}_h$ in the Debye-Waller factor, this will not cause any significant error (because the exponent has second power of reciprocal lattice vector). This approximation is usually made in the calculations of neutron cross sections without introducing any significant error. Using this assumption in eqn. (3.6) we get,

$$\text{Im } C_{ho}(n) = - \frac{\hbar^3 a^2 e^{-D'K_h^2}}{2Mm_o cv_c} \int \frac{d\underline{f}}{f} \left[\frac{(\underline{f}+\underline{K}_h).\underline{f}}{1-e^{-\hbar cf/k_BT}} \delta(f^2-2\underline{f}.\underline{k}_n+2m_o cf/\hbar) \right.$$
$$\left. + \frac{(\underline{f}-\underline{K}_h).\underline{f}}{e^{\hbar cf/k_BT}-1} \delta(f^2+2\underline{f}.\underline{k}_n-2m_o cf/\hbar) \right] \qquad (3.8)$$

Now to do the angular integration, we choose $\underline{k}_n$ as z-axis, so that $\underline{K}_h \cdot \underline{f} = K_h f(\cos\theta \cos\alpha + \sin\theta \sin\alpha \sin\phi)$ where the phonon wave vector $\underline{f}$ has been written as (f,θ,ϕ) in polar coordinates and α is the angle between $\underline{K}_h$ and $\underline{k}_n$ (z-axis). The coordinate system has been chosen such that $\underline{K}_h$ is written as $(K_h,\alpha,0)$. Thus eqn. (3.8) may be written as,

$$\text{Im } C_{ho}(n) = -\frac{\pi\hbar^3 a^2 e^{-D'K_h^2}}{Mm_o c v_c k_n} \int_0^{f_o} f\,df \int_{-1}^{+1} dx \left[\frac{f^2+K_h f x\cos\alpha}{(1-e^{-\hbar cf/k_B T})} \frac{1}{2fk_n} \right.$$

$$\left. \delta\left(x - \frac{f+2m_o c/\hbar}{2k_n}\right) + \frac{f^2-K_h f x\cos\alpha}{(e^{\hbar cf/k_B T}-1)} \frac{1}{2fk_n} \delta\left(x + \frac{f-2m_o c/\hbar}{2k_n}\right)\right] \quad (3.$$

where we have put $\cos\theta = x$ and used $\int_0^{2\pi} \sin\phi\, d\phi = 0$. Now since, for high particle energies, f_o is always small compared to $(2k_n \pm 2m_o c/\hbar)$ we can use the δ-function in angular integration to get,

$$\text{Im } C_{ho}(n) = -\frac{\pi\hbar^3 a^2 e^{-D'K_h^2}}{2Mm_o c v_c k_n} \left[\left(1 + \frac{K_h \cos\alpha}{2k_n}\right) \int_0^{f_o} f^2 \coth\left(\frac{\hbar cf}{2k_B T}\right) df \right.$$

$$\left. + \frac{m_o c\, K_h \cos\alpha}{2\hbar k_n} f_o^2 \right] \quad (3.10)$$

The calculation of Im $C_{oo}(n)$ is relatively simple. Actually Im $C_{oo}(n)$ is related to the total inelastic cross section[66] by,

$$\text{Im } C_{oo}(n) \sim -\frac{\hbar^2 k_n}{2m_o V'} \sigma_T^{(i)} \quad (3.11)$$

where $\sigma_T^{(i)}$ is the total inelastic cross section. We may calculate it directly from eqn. (2.54) without making approximation of neglecting f compared to K_h in Debye-Waller exponentials. The angular integration of eqn. (2.55) yields,

$$\text{Im } C_{oo}(n) = -\frac{\pi\hbar^3 a^2}{2Mm_o c v_c k_n}\int_0^{f_o} f^2 e^{-2D'f^2} \coth\left(\frac{\hbar cf}{2k_B T}\right)df \quad (3.12)$$

This expression is more accurate than the corresponding expression (3.10) for Im $C_{ho}(n)$ because it does not use the approximation of neglecting f compared to K_h. Such accuracy is needed in calculating the attenuation of the other wave ϕ_n^- when ϕ_n^+ is anomalously transmitted.

In the low temperature limit, the f-integration can also be done easily, using the replacement $\coth(\hbar cf/2k_BT) \simeq 1+2e^{-\hbar cf/k_BT}$. In this limit, the Debye-Waller exponent D becomes,

$$D_1 = \frac{3\hbar^2}{8k_B\theta_D M}\left[1+4(T/\theta_D)^2\right] \quad (3.13)$$

and from eqn. (3.10) we get,

$$\text{Im } C_{ho}(n) = -\frac{\pi\hbar^3 a^2 e^{-D_1' K_h^2}}{2Mm_o c v_c k_n}\left[\frac{m_o c K_h \cos\alpha}{2\hbar k_n} f_o^2 + \frac{1}{3} f_o^3 \left(1+\frac{K_h\cos\alpha}{2k_n}\right)\left(1+\frac{6T^3}{\theta_D^3}\right)\right] \quad (3.14)$$

with $D_1' = D_1 + 1/4\beta^2$. Here θ_D is the Debye temperature defined as $\hbar cf_o = k_B\theta_D$ and we have neglected the terms of order higher than $(T/\theta_D)^3$. From eqn. (3.14), we can write

$$\text{Im } C_{ho}(n) = \text{Im } C_{oo}(n)\, e^{-D_1' K_h^2}\left[1+\frac{K_h\cos\alpha}{2k_n} + \frac{3m_o c K_h \cos\alpha}{2\hbar k_n f_o(1+6T^3/\theta_D^3)}\right](\quad$$

Im $C_{oo}(n)$ appearing in eqn. (3.15) is that obtained from eqn. (3.14) by putting $K_h = 0$ so that Im $C_{ho}(n)$ and Im $C_{oo}(n)$ occuring in eqn. (3.15) contain the same degree of approximation.

Now the wave ϕ_n^+ will experience no attenuation and will be anomalously transmitted when Im $n_+ = 0$ i.e. when Im $C_{ho}(n) =$ Im $C_{oo}(n)$. This leads to a condition for anomalous transmission as,

$$\frac{K_h \cos \alpha}{2k_n} \left[1 + \frac{3m_o c}{\pi f_o (1+6T^3/\theta_D^3)}\right] = \left[\exp (D_1' K_h^2) - 1\right] \quad (3.16)$$

The condition (3.16) must be exactly satisfied for complete anomalous penetration of ϕ_n^+ and when this is so, the attenuation of the other wave ϕ_n^- is determined by 2 Im $C_{oo}(n)$ and may be calculated using more accurate expression (3.12). Since L.H.S. of eqn. (3.16) is very small for high energy particles, it will be satisfied only for lowest possible values of K_h. (Of course $K_h = 0$ is ideal case in which it is exactly satisfied but physically, $K_h = 0$ does not correspond to any plane or axis in the crystal). As the magnitude of K_h increases, R.H.S. of eqn. (3.16) increases exponentially with exponent K_h^2 where as L.H.S. increases linearly with K_h. Thus only low index (principal) crystallographic planes and directions may produce anomalous transmission. Moreover, since $D_1' = D_1 + 1/4\beta^2$, the width of the interaction potential β^{-1} must be small compared to the mean square displacement so that $1/4\beta^2$ may be neglected compared with D_1, to write $D_1' = D_1$. Thus the condition (3.16) requires that the interaction potential must be localized in the vicinity of lattice sites.

When the condition (3.16) is not exactly satisfied, the attenuation of the beam ϕ_n^+ is governed by,

$$|\phi_n^+|^2 \simeq \exp\left[-\frac{\pi\hbar^3 a^2 f_o^3}{4Mm_o c v_c \gamma_n E_p}\ \frac{1}{3}\left(1+\frac{6T^3}{\theta_D^3}\right)(1-\epsilon)\hat{n}.\underline{r}\right] \quad (3.17)$$

where

$$\epsilon = e^{-D_1' K_h^2}\left[1+\frac{K_h \cos\alpha}{2k_n}+\frac{3m_o c K_h \cos\alpha}{2\hbar k_n f_o(1+6T^3/\theta_D^3)}\right] \quad (3.18)$$

and the condition (3.16) corresponds to $\epsilon = 1$. As discussed above, shorter is the range of the potential (β^{-1} small) i.e. more localized is the interaction potential, more accurately the condition (3.16) is satisfied. In the limiting case when $1/4\beta^2$ may be neglected compared to the mean square displacement $2D_1$, the attenuation, at short wavelength is independent of the potential width (β^{-1}) and is determined only by the mean square displacement.

The attenuation of the other wave ϕ_n^- near the anomalous transmission condition (3.16) is determined by 2 Im $C_{oo}(n)$. This quantity may be calculated more accurately than Im C_{ho} (n) from eqn. (3.12). In the low temperature limit, replacing coth ($\hbar cf/2k_B$ in (3.12), by $1+2e^{-\hbar cf/k_BT}$ and integrating over f, we get,

$$\text{Im } C_{oo}(n) = -\frac{\pi\hbar^3 a^2}{2Mm_o c v_c k_n}\left[\frac{\hbar c}{8k_B T D_1'^2}\left(e^{-\frac{\theta_D}{T}}-2D_1' f_o^2-1\right)\right.$$

$$-f_o\frac{e^{-2D_1' f_o^2}}{4D_1'}(1+2e^{-\theta D/T})+\frac{1}{4D_1'}\left(\frac{\pi}{8D_1'}\right)^{1/2}\left\{\text{erf}\left[f_o(2D_1')^{1/2}\right]\right.$$

$$+(2+\hbar^2c^2/2k_B^2T^2D_1')\exp(\hbar^2c^2/8k_B^2T^2D_1')$$

$$\left.\left.x\left(\text{erf}\left[f_o(2D_1')^{1/2}+\frac{\hbar c}{2k_BT(2D_1')^{1/2}}\right]-\text{erf}\left[\frac{\hbar c}{2k_BT(2D_1')^{1/2}}\right]\right)\right\}\right] \quad (3.19$$

where $\text{erf}(z) = (2/\sqrt{\pi})\int_0^z \exp(-t^2)\,dt$.

In all the above expressions, the limit of contact Fermi pseudo-potential is obtained by replacing D_1' by D_1. This limit corresponds to maximum possibility for anomalous transmission condition (3.16) to be satisfied for low index planes or axes so that the wave ϕ_n^+ is anomalously transmitted with minimum attenuation. On the other hand, the limit of a broad interaction potential (β^{-1} large) is obtained by replacing D_1' by $1/4\ \beta^2$. But in this limit, the condition (3.16) can not be satisfied. This is because the L.H.S. of eqn. (3.16) being less than 10^{-2} for typical values of k_n and K_h of interest, the R.H.S. cannot be any where close to that if $1/4\ \beta^2$ is so large compared to D_1 that $D_1' \simeq 1/4\beta^2$. This is more clearly seen from Table I where $(1-\epsilon)$ becomes about 10^{-1} for $1/4\beta^2 = 100\ D_1$. Thus the condition for anomalous penetration requires the interaction potential to be short range and the attenuation under the channeling conditions is determined by the mean square displacement. The expression for ϵ and the condition (3.16) for anomalous transmission indicate that maximum penetration occurs for low index crystallographic planes and directions.

3.2 Screened Coulomb Potential-Charged Particles:

When the charged particles (electrons, positrons, protons etc.) propagate through the crystal, three types of transitions in the crystal become important: excitation of nonlocalized electrons, excitation of electron cloud surrounding the lattice

Table I: Variation of $(1-\epsilon)$ with width of the Potential β^{-1} and temperature when K_h corresponds to {100} planes in Cu(fcc)

β^{-1} (in units of $D_1^{1/2}$)	$(1-\epsilon)$ in units of 10^{-2}			
	$T = 5^{\circ}K$	$T = 15^{\circ}K$	$T = 25^{\circ}K$	$T = 35^{\circ}K$
0.0	0.8081	0.8145	0.8271	0.8461
0.1	0.8101	0.8165	0.8292	0.8482
1.0	1.0091	1.0170	1.0328	1.0564
2.0	1.6097	1.6223	1.6474	1.6850
3.0	2.6026	2.6228	2.6631	2.7236
4.0	3.9759	4.0065	4.0676	4.1593
5.0	5.7131	5.7566	5.8437	5.9741
6.0	7.7937	7.8525	7.9698	8.1456
7.0	10.1935	10.2693	10.4207	10.6474
8.0	12.8850	12.9793	13.1677	13.4494
9.0	15.8380	15.9519	16.1795	16.5191
10.0	19.0201	19.1541	19.4214	19.8212

ion and the vibrational transitions of the lattice ion. The first effect has nothing to do with the particular direction of motion of particle and contributes a large, directionally independent background to the total attenuation which is treated in Chapter V of the present work. The latter two effects, because of their localization, will show anomalous behaviour at Bragg angles. In the present work, we illustrate the effect of localization by considering purely vibrational transitions, choosing screened Coulomb potential as the interaction between particle and crystal, in this section and Born-Mayer potential in the next section.

The ions of the crystal are sitting at various lattice sites Their interaction with any external charged particle is expected to be a Coulomb potential. But because of the collective oscillations of the conduction electron sea, this potential is screened. Thus the interaction between the lattice ions and the incident charged particle is no more a long range Coulomb interaction but is a screened Coulomb potential, the strength of the screening being determined by the density of conduction electrons. Thus the interaction potential between the incident charged particle and the crystal ions may be written as,

$$V(r) = z_1 z_2 e^2 \sum_{\sigma} \frac{e^{-\Lambda|\underline{r}-\underline{R}_\sigma|}}{|\underline{r}-\underline{R}_\sigma|} \tag{3.20}$$

so that $$V_\sigma(\underline{r}-\underline{R}_\sigma) = z_1 z_2 e^2 \frac{e^{-\Lambda|\underline{r}-\underline{R}_\sigma|}}{|\underline{r}-\underline{R}_\sigma|} \tag{3.21}$$

and $$V_\sigma(K) = V(K) = 4\pi z_1 z_2 e^2/(\Lambda^2+K^2) \tag{3.22}$$

Using (3.22) in eqn. (2.56), we get,

$$\text{Im } C_{ho}(n) = -\frac{2m_o(z_1z_2\,e^2)^2}{M\hbar cv_c}\int\frac{d\underline{f}}{f}\left\{\frac{(\underline{f}+\underline{K}_h)\cdot\underline{f}}{1-e^{-\hbar cf/k_BT}}\,\delta(f^2-2\underline{f}.\underline{k}_n+\frac{2m_ocf}{\hbar})\right.$$
$$\times\frac{e^{-D[(\underline{f}+\underline{K}_h)^2+f^2]}}{[\Lambda^2+(\underline{f}+\underline{K}_h)^2](\Lambda^2+f^2)}+\frac{(\underline{f}-\underline{K}_h)\cdot\underline{f}}{e^{\hbar cf/k_BT}-1}$$
$$\left.\times\,\delta(f^2+2\underline{f}.\underline{k}_n-\frac{2m_ocf}{\hbar})\,\frac{e^{-D[(\underline{f}-\underline{K}_h)^2+f^2]}}{[\Lambda^2+(\underline{f}-\underline{K}_h)^2](\Lambda^2+f^2)}\right\}\quad(3.23)$$

The integration involved here is difficult compared to that involved in eqn. (3.7) for the neutron case. Again we neglect $\underline{f}$ compared to the reciprocal lattice vector $\underline{K}_h$ in the Debye-Waller exponent and also in the denominators so that the integrations are simplified to some extent. Again choosing k_n as z-axis and system axes rotated such that $\underline{f} = (f, \theta, \phi)$ and $\underline{K}_h = (K_h, \alpha, 0)$. Then the angular integration may be done in a similar way as in the neutron case, to get finally,

$$\text{Im } C_{ho}(n) = -\left(\frac{2\pi m_o(z_1z_2e^2)^2\,e^{-DK_h^2}}{M\hbar cv_c\,k_n\,(\Lambda^2+K_h^2)}\right)\left[\frac{m_ocK_h\cos\alpha}{2\hbar\,k_n}\ln\left(1+\frac{f_o^2}{\Lambda^2}\right)\right.$$
$$\left.+\left(1+\frac{K_h\cos\alpha}{2k_n}\right)\int_0^{f_o}\frac{f^2\coth(\hbar cf/2k_BT)}{(\Lambda^2+f^2)}\,df\right]\quad(3.24)$$

In the low temperature limit, $\coth(\hbar cf/2k_BT) \simeq 1+2e^{-\hbar cf/k_BT}$ and f-integration may be done, to get

$$\text{Im } C_{ho}(n) = -\left(\frac{2\pi m_o(z_1z_2e^2)^2e^{-D_1K_h^2}}{M\hbar cv_c\,k_n(\Lambda^2+K_h^2)}\right)\left[\frac{m_oc\,K_h\cos\alpha}{2\hbar\,k_n}\ln\left(1+\frac{f_o^2}{\Lambda^2}\right)\right.$$
$$\left.+\left(1+\frac{K_h\cos\alpha}{2k_n}\right)F_o^{SC}(\Lambda,T)\right]\quad(3.25)$$

with $$F_o^{SC}(\Lambda, T) = f_o + 2f_o(T/\theta_D)(1-e^{-\theta_D/T}) - \Lambda\left[\tan^{-1}\left(\frac{f_o}{\Lambda}\right) + ci\left(\frac{\Lambda\hbar c}{k_B T}\right)\sin\left(\frac{\Lambda\hbar c}{k_B T}\right) - si\left(\frac{\Lambda\hbar c}{k_B T}\right)\cos\left(\frac{\Lambda\hbar c}{k_B T}\right)\right] \quad (3.26)$$

where, $si(x) = -\int_x^\infty \frac{\sin t}{t}\,dt$ and $ci(x) = -\int_x^\infty \frac{\cos t}{t}\,dt$ are the well known tabulated functions[67]. In obtaining the last two terms of eqn. (3.26), we have extended the upper limit of f-integration to ∞ because the contribution from f greater than f_o is small, for the integrals involved there, at low temperatures.

Now from eqn. (3.25) we can write,

$$\text{Im } C_{ho}(n) = \text{Im } C_{oo}(n)\,\frac{e^{-D_1 K_h^2}}{(1+K_h^2/\Lambda^2)}\left[1 + \frac{K_h \cos\alpha}{2k_n} + \left(m_o c K_h \cos\alpha/2\hbar k_n F_o^{SC}(\Lambda,T)\right)\ln\left(1+\frac{f_o^2}{\Lambda^2}\right)\right] \quad (3.27)$$

so that the condition for complete anomalous transmission is,

$$\frac{K_h \cos\alpha}{2k_n}\left[1+\frac{m_o c}{\hbar F_o^{SC}(\Lambda,T)}\ln\left(1+\frac{f_o^2}{\Lambda^2}\right)\right] = \left[\left(1+\frac{K_h^2}{\Lambda^2}\right)e^{D_1 K_h^2} - 1\right] \quad (3.28)$$

The attenuation for the wave ϕ_n^+, which penetrates anomalously at the condition (3.28), is governed by,

$$|\phi_n^+|^2 \simeq \exp\left[-\frac{\pi m_o (z_1 z_2 e^2)^2 F_o^{SC}(\Lambda,T)}{M\hbar c v_c \gamma_n E_p \Lambda^2}\left(1-\epsilon_p^{SC}\right)\hat{n}.\underline{r}\right] \quad (3.29)$$

where $$\epsilon_p^{SC} = \frac{e^{-D_1 K_h^2}}{1+K_h^2/\Lambda^2}\left[1+\frac{K_h\cos\alpha}{2k_n} + \frac{m_o c K_h \cos\alpha}{2\hbar k_n F_o^{SC}(\Lambda,T)}\ln\left(1+\frac{f_o^2}{\Lambda^2}\right)\right] \quad (3.30)$$

The effect of the screening parameter Λ on the attenuation can be examined using eqn. (3.25). Thus for Λ^2 large compared to D_1^{-1}, so that $\Lambda^2 \gg K_h^2$ and $\Lambda^2 \gg f_o^2$, one gets,

$$\text{Im } C_{ho}(n) - \text{Im } C_{oo}(n) = -\text{Im } C_{oo}(n)\left[1-e^{-D_1 K_h^2}\left(1+\frac{K_h \cos\alpha}{2k_n}\right)\right] \quad (3.31)$$

and $$\epsilon_p^{SC} = (1 + K_h \cos\alpha/2k_n)\exp(-D_1 K_h^2) \quad (3.32)$$

which is independent of Λ. Thus when the screening is very strong, implying thereby that the potential is highly localized, the condition for anomalous transmission is independent of the screening parameter. On the other hand if Λ is small compared to D_1^{-1} and can be taken to be of the order of f_o, then,

$$\text{Im } C_{ho}(n) - \text{Im } C_{oo}(n) = -\text{Im } C_{oo}(n)\left\{1 - \frac{e^{-D_1 K_h^2}}{1+K_h^2/\Lambda^2}\left[\left(1+\frac{K_h \cos\alpha}{2k_n}\right) + \frac{m_o c K_h \cos\alpha \ln 2}{2\pi k_n f_o\left(1-\frac{\Lambda}{f_o}\tan^{-1}\frac{f_o}{\Lambda}\right)}\right]\right\} \quad (3.33)$$

so that $$\epsilon_p^{SC} = \frac{e^{-D_1 K_h^2}}{1+K_h^2/\Lambda^2}\left[\left(1+\frac{K_h \cos\alpha}{2k_n}\right) + \frac{m_o c K_h \cos\alpha \ln 2}{2\pi k_n f_o\left(1-\frac{\Lambda}{f_o}\tan^{-1}\frac{f_o}{\Lambda}\right)}\right] \quad (3.34)$$

showing that weak screening cannot lead to an anomalous effect because for small values of Λ, ϵ_p^{SC} of eqn.(3.34) cannot be close to unity and hence the condition for anomalous transmission cannot be satisfied.

3.3 Born-Mayer Potential -Charged Particles:

Another model potential for the interaction between the incident charged particle and the crystal ions which has been frequently used[68-71] as for example in calculation of energy loss of charged particles during their propagation through channels, is

the Born-Mayer potential,

$$V(r) = A \sum_{\sigma} e^{-\beta_c |\underline{r}-\underline{R}_\sigma|} \tag{3.35}$$

where β_c^{-1} represents the range of interaction. Here, both the constants A and β_c depend upon the charge numbers of the incident particle and lattice atoms. For this interaction we have,

$$V_\sigma(\underline{r}-\underline{R}_\sigma) = Ae^{-\beta_c|\underline{r}-\underline{R}_\sigma|}$$

so that $V_\sigma(K) = V(K) = 8\pi A\ \beta_c/(\beta_c^2 + K^2)^2$ (3.36)

Substituting this in eqn. (2.56), we get,

$$\text{Im } C_{ho}(m) = -\frac{8A^2\beta_c^2 m_o}{M\hbar c v_c} \int \frac{d\underline{f}}{f} \left\{ \frac{e^{-D[(\underline{f}+\underline{K}_h)^2+f^2]}}{[\beta_c^2+(\underline{f}+\underline{K}_h)^2]^2(\beta_c^2+f^2)^2} \right.$$

$$\times \frac{(\underline{f}+\underline{K}_h).\underline{f}}{(1-e^{-\xi/k_BT})} \delta(f^2-2\underline{f}.\underline{k}_n+\frac{2m_o cf}{\hbar}) + \frac{(\underline{f}-\underline{K}_h).\underline{f}}{(e^{\xi/k_BT}-1)}$$

$$\left. \times \frac{e^{-D[(\underline{f}-\underline{K}_h)^2+f^2]}}{[\beta_c^2+(\underline{f}-\underline{K}_h)^2]^2(\beta_c^2+f^2)^2} \delta(f^2+2\underline{f}.\underline{k}_n-\frac{2m_o cf}{\hbar}) \right\} \tag{3.37}$$

Again we neglect $\underline{f}$ compared to reciprocal lattice vector $\underline{K}_h$ in the Debye-Waller exponentials and in the denominators, as in the case of screened Coulomb potential. Performing the angular integration by choosing k_n as z-axis, we get,

$$\text{Im } C_{ho}(n) = -\frac{8\pi A^2\beta_c^2 m_o e^{-DK_h^2}}{M\hbar c v_c k_n(\beta_c^2+K_h^2)^2} \left[\frac{m_o c\ K_h \cos\alpha\ f_o^2}{2\hbar\ k_n\ \beta_c^2\ (\beta_c^2+f_o^2)} \right.$$

$$\left. + \left(1+\frac{K_h\cos\alpha}{2k_n}\right) \int_0^{f_o} f^2 df \frac{\coth(\hbar cf/2k_BT)}{(\beta_c^2+f^2)^2} \right] \tag{3.38}$$

In the low temperature limit, $\coth(\hbar cf/2k_BT) \simeq 1+e^{-\hbar cf/k_BT}$ so that

f-integration may be performed to yield

$$\text{Im } C_{ho}(n) = -\frac{8\pi A^2\beta_c^2 m_o e^{-D_1K_h^2}}{M\hbar cv_c k_n(\beta_c^2+K_h^2)^2}\left[\frac{m_o c K_h \cos\alpha f_o^2}{2\hbar k_n \beta_c^2(\beta_c^2+f_o^2)}\right.$$

$$\left. + (1+\frac{K_h\cos\alpha}{2k_n}) F_o^{BM}(\beta_c,T)\right] \qquad (3.39)$$

with $$F_o^{BM}(\beta_c,T) = \frac{1}{\beta_c}\left\{\tan^{-1}\left(\frac{f_o/\beta_c+\sqrt{1+f_o^2/\beta_c^2}-1}{f_o/\beta_c+\sqrt{1+f_o^2/\beta_c^2}+1}\right) - \frac{f_o}{2\beta_c(1+f_o^2/\beta_c^2)}\right.$$

$$+ ci(\frac{\beta_c\hbar c}{k_BT})\sin(\frac{\beta_c\hbar c}{k_BT}) - si(\frac{\beta_c\hbar c}{k_BT})\cos(\frac{\beta_c\hbar c}{k_BT})$$

$$\left. + \frac{\beta_c\hbar c}{k_BT}\left[ci(\frac{\beta_c\hbar c}{k_BT})\cos(\frac{\beta_c\hbar c}{k_BT})+si(\frac{\beta_c\hbar c}{k_BT})\sin(\frac{\beta_c\hbar c}{k_BT})\right]\right\} \qquad (3.40)$$

Thus, $$\text{Im } C_{oo}(n) = -\frac{8A^2m_o\pi}{M\hbar cv_c k_n \beta_c^2} F_o^{BM}(\beta_c,T) \qquad (3.41)$$

and from eqn.(3.39) we can write,

$$\text{Im } C_{ho}(n) = \text{Im } C_{oo}(n)\frac{e^{-D_1K_h^2}}{(1+K_h^2/\beta_c^2)^2}\left[1+\frac{K_h\cos\alpha}{2k_n}\right.$$

$$\left. + \frac{m_o c K_h \cos\alpha f_o^2}{2\hbar k_n F_o^{BM}(\beta_c,T)\beta_c^2(\beta_c^2+f_o^2)}\right] \qquad (3.42)$$

The attenuation of the penetrating component ϕ_n^+ is given by,

$$|\phi_n^+|^2 \simeq \exp\left[-\frac{4\pi A^2 m_o F_o^{BM}(\beta_c,T)}{M\hbar cv_c \gamma_n E_p \alpha_c^2}(1-\epsilon_p^{BM})\hat{n}.\underline{r}\right] \qquad (3.43)$$

where $$\epsilon_p^{BM} = \frac{e^{-D_1K_h^2}}{(1+K_h^2/\beta_c^2)^2}\left[(1+\frac{K_h\cos\alpha}{2k_n})\right.$$

$$\left. + \frac{m_o c K_h \cos\alpha f_o^2}{2\hbar k_n F_o^{BM}(\beta_c,T)\beta_c^2(\beta_c^2+f_o^2)}\right] \qquad (3.44)$$

The condition for channeling which requires Im $C_{ho}(n)$ = Im $C_{oo}(n)$ or $\epsilon_p^{BM} = 1$, is given by

$$\frac{K_h \cos\alpha}{2k_n}\left[1+\frac{m_o c\, f_o^2}{\pi\beta_c^2(\beta_c^2+f_o^2)F_o^{BM}(\beta_c,T)}\right] = \left[\left(1+\frac{K_h^2}{\beta_c^2}\right)^2 e^{D_1 K_h^2} - 1\right] \quad (3.45$$

Now we note from eqn. (3.44), that for higher particle energies, the second and third term may be neglected and variation of the channeling parameter $(1-\epsilon_p^{BM})$ with the range of the interaction β_c^{-1} is essentially given by,

$$(1-\epsilon_p^{BM}) = 1-e^{-D_1 K_h^2}/(1+K_h^2/\beta_c^2)^2 \quad (3.46)$$

The corresponding expression (using similar approximation) for the case of screened Coulomb potential is obtained from eqn.(3.30) and is given by,

$$(1-\epsilon_p^{SC}) = 1 - e^{-D_1 K_h^2}/(1+ K_h^2/\Lambda^2) \quad (3.47)$$

The variation of $(1-\epsilon_p^{BM})$ with β_c^{-1} and that of $(1-\epsilon_p^{SC})$ with Λ^{-1} at low temperatures has been given in Tables II and III respectively.

3.4 Discussion:

If we closely examine the expressions for $(1-\epsilon_p^{SC})$ and $(1-\epsilon_p^{BM})$ and the corresponding channeling conditions (3.28) and (3.45), we notice that the range of the interaction (β_c^{-1} and Λ^{-1}) must be small for channeling conditions to be satisfied. Appearance of K_h^2 in exponential as well as multiplicative factor, at R.H.S. of eqn. (3.28) and (3.45) requires that the magnitude of K_h should be small i.e. the particles should be incident along principal

Table II: Variation of $(1-\epsilon_p^{SC})$ with width of the Screened Coulomb potential Λ^{-1} and temperature when K_h corresponds to {100} planes in Cu (fcc).

Λ^{-1} in units of $(2D_1)^{1/2}$	$(1 - \epsilon_p^{SC})$ in units of 10^{-2}			
	T = 5°K	T = 15°K	T = 25°K	T = 35°K
0.1	0.8242	0.8307	0.8436	0.8629
0.2	0.8725	0.8793	0.8929	0.9134
0.3	0.9528	0.9602	0.9751	0.9975
0.4	1.065	1.073	1.090	1.115
0.5	1.209	1.218	1.237	1.266
0.6	1.384	1.395	1.417	1.449
0.7	1.591	1.603	1.628	1.665
0.8	1.828	1.842	1.870	1.913
0.9	2.095	2.111	2.144	2.192
1.0	2.392	2.411	2.448	2.503
2.0	6.855	6.905	7.006	7.157
3.0	13.449	13.541	13.725	13.999
4.0	21.255	21.387	21.650	22.042
5.0	29.436	29.601	29.927	30.410
6.0	37.388	37.572	37.939	38.481
7.0	44.746	44.941	45.327	45.896
8.0	51.344	51.541	51.930	52.503
9.0	57.143	57.336	57.717	58.276
10.0	62.182	62.367	62.632	63.267

Table III: Variation of $(1-\epsilon_p^{BM})$ with the width of Born Mayer Potential (β_c^{-1}), corresponding to {100} planes in Cu(fcc)

β_c^{-1} (in units of $(2D_1)^{1/2}$	$(1 - \epsilon_p^{BM})$ in units of 10^{-2}			
	T = 5°K	T = 15°K	T = 25°K	T = 35°K
0.1	0.8403	0.8469	0.8600	0.8797
0.2	0.9368	0.9441	0.9588	0.9807
0.3	1.097	1.106	1.123	1.149
0.4	1.321	1.332	1.352	1.383
0.5	1.608	1.621	1.646	1.683
0.6	1.957	1.972	2.003	2.048
0.7	2.367	2.385	2.422	2.477
0.8	2.837	2.869	2.903	2.968
0.9	3.365	3.391	3.443	3.520
1.0	3.951	3.981	4.042	4.132
2.0	12.532	12.622	12.799	13.066
3.0	24.480	24.635	24.945	25.407
4.0	37.487	37.693	38.101	38.707
5.0	49.802	50.032	50.488	51.159
6.0	60.478	60.708	61.163	61.831
7.0	69.221	69.436	69.859	70.478
8.0	76.133	76.324	76.699	77.247
9.0	81.483	81.649	81.973	82.443
10.0	85.581	85.721	85.995	86.392

crystallographic planes or axes. These conclusions are similar to those derived in Section 3.1, from consideration of anomalous neutron transmission using Fermi pseudo-potential. A comparison between the results for the two potential models used for charged particles, shows that the screened Coulomb potential is more favourable for channeling than the Born-Mayer potential. This is seen clearly from Tables II and III where $(1-\epsilon_p^{SC})$ is smaller than $(1-\epsilon_p^{BM})$ for equal values of Λ^{-1} and β_c^{-1}, showing that the penetration depth in the former case is greater than in later case. Another significant difference between the two models is that the range Λ^{-1} of screened Coulomb potential depends only on the density of conduction electrons whereas the parameters of Born-Mayer interaction, A and β_c, depend upon the charge numbers of both, the incident particle and the target crystal. In particular, in the Brinkman's version[72] of the Born-Mayer potential, one has,

$$A = 2.58 \times 10^{-5} \; z_{eff}^{11/2} \quad eV$$

and $$\beta_c = z_{eff}^{1/3} / 1.5 \; a_o \qquad (3.48)$$

where $z_{eff} = (z_1 z_2)^{1/2}$, a_o is the Bohr radius and z_1, z_2 are the charge numbers of the incident particle and the crystal atom respectively. Thus as z_1 or z_2 increases, β_c^{-1} decreases, resulting in larger penetration depth. Similarly for small values of z_1 and z_2, one gets more attenuation and smaller penetration depth. But in the screened Coulomb potential, there is no such dependence on the charge number z_1 and z_2 and the penetration depth is governed only by the density of conduction electrons through the screening properties.

There are few interesting features of the channeling phenomena which may be seen to emerge as a consequence of the preceding quantum mechanical treatment of the problem. First of all, we note that the existence of anomalous effect has nothing directly to do with the wavelength of the incident particle but is rather determined by two criteria: The interaction potential must be weak compared to the particle energy as seen from the condition (2.23) for validity of two wave picture and that the interaction must be localized in the vicinity of lattice sites. The conditions for channeling corresponding to all the three potential models require that the magnitude of the reciprocal lattice vector $\underline{K}_h$, corresponding to the lattice plane or axis with which the Bragg diffraction is taking place, should be small. Thus appreciable channeling will occur only when the incident beam of particles moves in a direction close to the principal crystallographic directions or planes. The energy and temperature dependence of the expressions for the channeling parameter $(1-\epsilon)$ is only through small factors and as such the dependence shows that high particle energy and low temperature is favourable for channeling. The energy dependence (E_p^{-1}) of the factors multiplying $(1-\epsilon)$ in the exponent of $|\phi_n^+|^2$ is in agreement with the experimentally concluded[73] fact that $X_{1/2}$, the thickness into the crystal at which one half of the initially channeled particles have escaped from the channel, is proportional to the particle energy.

CHAPTER IV

EMISSION OF CHARGED PARTICLES FROM CRYSTALS

4.1 Introduction:

It was pointed out in Sec. 3.1 that Lindhard's classical treatment is applicable only to heavy ion channeling. For light particles (such as electrons, positrons etc.) the interference effects are significant, irrespective of their wavelength and then, one has to use the quantum theory developed in last two chapters. The experimental situation for light-particle channeling seems to be poor. Some attempts towards such studies have been made by Wolf et.al.,[74] who studied electron channeling in Si single crystals by scanning electron microscopy. Similar technique has been used by Joy et al.[75] to study the electron channeling in ferromagnetic crystals. Some experimental information on high energy electron transmission has been reported by Steeds and Valdre[76]. More recently, Andersen et al.[77] have investigated the positron and electron channeling by means of Rutherford scattering. Inspite of the poor experimental situation, theoretical calculations[78,79] using standard many beam dynamical theory[55], have been made. A recent communication[80] also contains such calculations for electron channeling at high energies in gold.

The lack of availability of experimental data on light charged particle channeling would have forced one to predict theoretical results without comparison. However, the charged

particle emission problems which are governed by the same physical mechanism as the channeling problems, have been interesting experimentally as well as theoretically. A detailed experimental investigation of α-particle emission from the radioactive nuclei embedded in the crystals, has been carried out by Domeij[81,82] and coworkers[83], who found dips in emitted intensity in low index directions. Gemmell and Holland[84] have reported some measurements on the charged particle (proton, Deuteron and alpha particles) emission from the crystals. These experiments have been essentially explained by the predictions of Lindhard's classical treatment. A significant work on emission of electrons and positrons from the crystals has been reported by Uggerhoj[38] and coworkers[39]. Recently Walker et al.[85] have studied the effects of Bremsstrahlung radiations on the channeling of relativistic electrons and positrons. Although, Lindhard's classical theory has been used to interpret the patterns observed by Uggerhoj and Andersen[38,39], in view of the discussion given in Sec. 1.3, it is desirable to develop a quantum-mechanical theory taking Bragg diffractions and the interference effects into account. DeWames et al.[36,37] have given a wave mechanical theory for this problem, but their treatment, in addition to assuming the crystal to be an Einstein crystal at zero temperature, starts with an approximate form (one particle approximation) of the many particle Schrodinger equation[86] and uses the periodic potential field of the classical model.This one particle Schrodinger equation conserves the particle energy

the propagation of the emitted particle through the crystal and its subsequent escape from the crystal. We shall also neglect the interactions (if any) of the emitted particle with the emitter itself and thus we are ignoring the processes that might occur in the immediate vicinity of the emitter. Under these assumptions, we are faced with the problem of propagation of particles through the periodic potential field of the crystal. The crystal is again assumed to be in a low lying state $|n\rangle$ at some low temperature, as in Chapter II. Therefore our system is again described by the Schrodinger equation (2.3). The total wave function may again be expanded as in eqn. (2.4), and the equation satisfied by the Bloch states representing the particle wave function, is

$$\left[-\frac{\hbar^2\nabla^2}{2m_o} + V_{nn}(r) - E_p \right] \phi_n(r) = - \sum_{m\neq n} V_{nm}(\underline{r})\, \phi_m(\underline{r}) \quad (4.1)$$

where $E_p = E - E_n$ is the energy with which particle has been emitted from the crystal.

Now to find out the intensity at a point $\underline{r}$ outside the crystal we make use of the reciprocity relation[36,37,86], which states that the intensity at a point $\underline{r}$ outside the crystal due to emission at a point $\underline{r}_e$ inside the crystal, is equal to the intensity at the emitter site when the emitter has been placed at the observation point $\underline{r}$. Thus

$$\phi_n\ (\underline{r}, \underline{r}_e) = \phi_n\ (\underline{r}_e, \underline{r}) \quad (4.2)$$

which holds as long as one neglects the reflections at the crystal surface. If the R.H.S. of eqn. (4.1), representing the

renormalization is neglected (because its magnitude is small, as we will see later) the relation (4.2) follows immediately from eqn. (4.1). In the general case, this relation may be derived by using time reversal invariance on the total wave function and using the eqns. (2.1) to (2.5). The reversibility rule has been experimentally demonstrated[90,91] to hold in the emission and transmission problems. Therefore, the problem has now been reduced to that of finding the intensity at the emitter site when the particles are coming from a far away point $\underline{r}$. The classical treatment given by Lindhard, also uses this reciprocity relation to relate the two problems of emission and transmission. The problem of particle penetration has been treated in detail in Chapters II and III. Here, we start by using the first Born approximation result for $\phi_m(\underline{r})$; namely,

$$\phi_m(\underline{r}) = -\frac{2m_o}{\hbar^2} \int d\underline{r}' \; \frac{e^{ik_m|\underline{r}-\underline{r}'|}}{4\pi|\underline{r}-\underline{r}'|} \; V_{mn}(\underline{r}') \; \phi_n(\underline{r}') \qquad (4.3)$$

on R.H.S. of eqn. (4.1) and use the usual expansions (2.6) to (2.8) for $\phi_n(\underline{r})$ and $V_{nn}(\underline{r})$ to get,

$$\frac{\hbar^2}{2m_o} \left[(\underline{K}_h + \underline{k}_M)^2 - k_n^2\right] u_h(n) + \sum_g \left[V_{h-g} + C_{hg}(n)\right] u_g(n) = 0 \qquad (4.4)$$

where

$$C_{hg}(n) = -\frac{2m_o}{V'\hbar^2} \int d\underline{r} \int d\underline{r}' \; e^{-i(\underline{K}_h+\underline{k}_n).\underline{r}+i(\underline{K}_g+\underline{k}_n).\underline{r}'} \times \sum_{n'\neq n} V_{nn'}(\underline{r}) \; V_{n'n}(\underline{r}') \; \frac{e^{ik_{n'}|\underline{r}-\underline{r}'|}}{4\pi|\underline{r}-\underline{r}'|} \qquad (4.5)$$

and $V_{h-g} = V_{h-g}(n,n)$. Eqn. (4.4) may be written simply, as

$$(2\delta + \zeta_h)u_h(n) + \sum_g W_{h-g}\, u_g(n) = 0 \qquad (4.6)$$

where $2\delta E_p = (\hbar^2/2m_o)\, k_M^2 - E_p$

$$(\hbar^2/2m_o)\,[K_h^2 + 2\underline{K}_h \cdot \underline{k}_M] = \zeta_h\, E_p \qquad (4.7)$$

and $W_{h-g} = [V_{h-g} + C_{hg}(n)]/E_p$

Now we use the boundary conditions at the surface, to calculate $\underline{k}_M$. If we restrict the sums in eqn.(4.6) to N terms, there will be N independent solutions for δ and hence for the Bloch-coefficients u_h; all belonging to the same energy E_p. These solutions must be superposed to obtain a wave function which matches properly on to the plane wave which is incident on the crystal surface from the direction of the point of observation. Neglecting the reflected wave, one can write the boundary condition as,

$$\phi_n(r) = \sum_j A_j\, e^{i\underline{k}_M^{(j)} \cdot \underline{r}} \sum_h u_h^{(j)}\, e^{i\underline{K}_h \cdot \underline{r}} = e^{i\underline{k}_n \cdot \underline{r}} \qquad (4.8)$$

for all $\underline{r}$ such that $\hat{n} \cdot \underline{r} = 0$ (i.e. at the surface). One satisfies these boundary conditions by choosing[92],

$$\underline{k}_M^{(j)} = \underline{k}_n + k_n^2\, \delta^{(j)}\, \hat{n} / \underline{k}_n \cdot \hat{n} \qquad (4.9)$$

and taking $A_j = \bar{u}_o^{(j)}$ where the bar over $u_o^{(j)}$ denotes complex conjugation. In fact, the second term on R.H.S. in eqn.(4.9) is just $\eta_{\pm}$ introduced in Chapter II, for the two beam case i.e. when single Bragg reflection is considered so that j has only two values.

The intensity at the emitter site can thus be written as,

$$|\phi_n(\underline{r}_e,\underline{r})|^2 = |\sum_j \bar{u}_o^{(j)}\, e^{i\underline{k}_M^{(j)}\cdot\underline{r}} \sum_h u_h^{(j)}\, e^{i\underline{K}_h\cdot\underline{r}}|^2$$

$$= \sum_j |\bar{u}_o^{(j)} \sum_h u_h^{(j)}\, e^{i\underline{K}_h\cdot\underline{r}}|^2 + 2\mathrm{Re} \sum_{j'>j} \Big[u_o^{(j')} \sum_{h'} \bar{u}_{h'}^{(j')}\, e^{-i\underline{K}_h\cdot\underline{r}}\Big] \Big[\bar{u}_o^{(j)} \sum_h u_h^{(j)} e^{i\underline{K}_h\cdot\underline{r}}\Big]\, e^{ik_n^2(\delta^{(j)}-\delta^{(j')})\hat{n}.\underline{r}/\underline{k}_n.\hat{n}} \quad \ldots(4.10)$$

In the last step, the intensity contributed by the cross terms between different eigen solutions has been written separately in order to display their dependence on the distance $\hat{n}.\underline{r}$, of the emitter from the crystal surface. Their evaluation, while straight forward, is tedious and adds nothing interesting to the basic character of the solution. Consequently, in the usual many beam calculations[37], a simple geometry for the crystal and for the incident beam is assumed which assures that these cross terms oscillate rapidly with emitter depth and a collection of emitters spread over a small thickness will yield an average intensity which is just the sum of diagonal terms in eqn. (4.10). This point becomes more clear from the two beam theory presented below.

The intensity pattern which one observes out side a crystal, due to a source placed inside, exhibits considerable structure and one should retain maximum number of terms in eqn. (4.10). However, almost all the features which appear, can be understood in terms of the behaviour of the intensity which one gets for the case of single Bragg reflection (two beam theory).

Specializing to the case of an emitter located at a lattice site (when emitter is at an interstitial site, the intensity maximum becomes minimum and vice versa), the two wave solution takes the form,

$$|\phi_n(t)|^2 = x^2 \exp\{-[1-\frac{\epsilon_h}{\sqrt{1+y^2}}]\, t/\xi_o''\} + (1-x)^2 \exp\{-[1+\frac{\epsilon_h}{\sqrt{1+y^2}}]\, t/\xi_o''\} + 2x(1-x)\, e^{-t/\xi_o''} \cos[\sqrt{1+y^2}\, t/\xi_h'] \quad (4.11)$$

where $x = \frac{1}{2}\left[1 + \frac{y-1}{\sqrt{1+y^2}}\right]$

$$y = \zeta_h/2W_h' \; ; \quad (\text{Re } W_h = W_h' = [V_h + \text{Re } C_{ho}]/E_p)$$

$$\epsilon_h = W_h''/W_o'' \; ; (\text{Im } W_h = W_h'' = \text{Im } C_{ho}/E_p) \quad (4.12)$$

$$\xi_h' = (k_n W_h')^{-1} \; ; \quad \xi_h'' = -(k_n W_h'')^{-1}$$

and t is the distance of the emitting atom from the crystal surface. In deriving eqn. (4.11), we have made the assumption that $W_h'' = \text{Im } C_{ho}/E_p$ is small compared to W_h' which is justified since Im C_{ho} is quite small compared to the Fourier coefficient of the potential V_h, as we shall see in Sec. (4.4).

Thus the calculation of $|\phi_n(t)|^2$, the intensity at the emitter site (and hence at the observation point) is essentially that of renormalization matrix and the Fourier coefficient of the potential V_h. Im C_{ho} has been calculated in Chapter III.

We calculate now, Re C_{ho} using same approximations, namely one phonon approximation for inelastic processes and Debye model for lattice vibrations.

4.3 Renormalization Matrix Elements:

From eqn. (4.5) we can write for the real part of the renormalization matrix as,

$$\text{Re } C_{hg}(n) = -\frac{2m_o}{V'\hbar^2(2\pi)^3}\int d\underline{k}\int d\underline{r}\int d\underline{r}'\ \exp\left[i(\underline{k}-\underline{k}_n-\underline{K}_h).\underline{r}\right.$$

$$\left.-i(\underline{k}-\underline{k}_n-\underline{K}_g).\underline{r}'\right]\sum_{n'\neq n} V_{nn'}(\underline{r})\ V_{n'n}(\underline{r}')\ P\left(\frac{1}{k^2-k_{n'}^2}\right) \quad (4.13)$$

where P(1/x) represents the principal value. In writing (4.13), we have used the momentum representation of the free space Green function,

$$\frac{e^{ik_{n'}|\underline{r}-\underline{r}'|}}{4\pi|\underline{r}-\underline{r}'|} = \frac{1}{(2\pi)^3}\int d\underline{k}\ \frac{e^{i\underline{k}.(\underline{r}-\underline{r}')}}{(k^2-k_{n'}^2,-i\epsilon)}$$

For a general interaction potential $V(\underline{r})=\sum_{\sigma} V_\sigma\ (\underline{r}-R_\sigma)$, this expression may be calculated using one phonon approximation for inelastic processes and assuming the crystal to have no isotopes and zero nuclear spin, as in the calculation of Im $C_{hg}(n)$ in Chapter II, we get,

$$\text{Re } C_{hg}(n) = -\frac{m_o}{Mv_c(2\pi)^3}\int\frac{df}{\xi}\left\{\frac{V(\underline{f}+\underline{K}_h)V(\underline{f}+\underline{K}_g)}{(1-e^{-\xi/k_BT})}\ (\underline{f}+\underline{K}_h).(\underline{f}+\underline{K}_g)\right.$$

$$e^{-D\left[(\underline{f}+\underline{K}_h)^2+(\underline{f}+\underline{K}_g)^2\right]}P\left(\frac{1}{f^2-2\underline{f}.\underline{k}_n+2m_o\xi/\hbar^2}\right)+\frac{V(\underline{f}-\underline{K}_h)V(\underline{f}-\underline{K}_g)}{(e^{\xi/k_BT}-1)}$$

$$\left.(\underline{f}-\underline{K}_h).(\underline{f}-\underline{K}_g)e^{-D\left[(\underline{f}-\underline{K}_h)^2+(\underline{f}-\underline{K}_g)^2\right]}\ P\left(\frac{1}{f^2+2\underline{f}.\underline{k}_n-2m_o\xi/\hbar^2}\right)\right\} \quad (4.14)$$

where we have summed over all the phonon wave vectors $\underline{f}$, as in the case of Im $C_{hg}(n)$.

Now using the Debye model for lattice vibrations, we put $\xi = \hbar cf$ in eqn. (4.14). Then, we use the screened Coulomb potential as the interaction between the emitted charged particle and the lattice ions as in Sec. 3.2, to get,

$$\text{Re } C_{hg}(n) = -\frac{2m_o(z_1z_2e^2)^2}{\pi M\hbar cv_c} \int \frac{df}{f}\Bigg\{\frac{(\underline{f}+\underline{K}_h).(\underline{f}+\underline{K}_g)}{(1-e^{-\hbar cf/k_BT})}\, P\left(\frac{1}{f^2-2\underline{f}.\underline{k}_n+2m_o cf/\hbar}\right)$$

$$\frac{\exp(-D[(\underline{f}+\underline{K}_h)^2+(\underline{f}+\underline{K}_g)^2])}{[\Lambda^2+(\underline{f}+\underline{K}_h)^2][\Lambda^2+(\underline{f}+\underline{K}_g)^2]} + \frac{(\underline{f}-\underline{K}_h).(\underline{f}-\underline{K}_g)}{(e^{\hbar cf/k_BT}-1)}$$

$$P\left(\frac{1}{f^2+2\underline{f}.\underline{k}_n-2m_o cf/\hbar}\right) \quad \frac{\exp(-D[(\underline{f}-\underline{K}_h)^2+(\underline{f}-\underline{K}_g)^2])}{[\Lambda^2+(\underline{f}-\underline{K}_h)^2][\Lambda^2+(\underline{f}-\underline{K}_g)^2]}\Bigg\} \qquad (4.15)$$

Since the maximum value of f in Debye model, f_o, is small compared to the reciprocal lattice vector K_h, we neglect f in the Debye-Waller exponent and in the denominators, to get,

$$\text{Re } C_{ho}(n) = -\frac{2m_o\rho'(z_1z_2e^2)^2\, e^{-DK_h^2}}{\pi Mc(\Lambda^2+K_h^2)} \int \frac{df}{f}\Bigg[\frac{\underline{f}.(\underline{f}+\underline{K}_h)}{(1-e^{-\hbar cf/k_BT})}$$

$$P\left(\frac{1}{f^2-2\underline{f}.\underline{k}_n+2m_o cf/\hbar}\right)\frac{1}{(\Lambda^2+f^2)} + \frac{\underline{f}.(\underline{f}-\underline{K}_h)}{(e^{\hbar cf/k_BT}-1)}$$

$$P\left(\frac{1}{f^2+2\underline{f}.\underline{k}_n-2m_o cf/\hbar}\right)\frac{1}{(\Lambda^2+f^2)}\Bigg] \qquad (4.16)$$

where $\rho' = 1/v_c$ is the number density of atoms in the crystal. Evaluating the angular integration, choosing $\underline{k}_n$ as z-axis as in Chapter III, we get,

$$\text{Re } C_{ho}(n) = -\frac{2m_o\rho'(z_1z_2e^2)^2 e^{-DK_h^2}}{M\hbar c\, k_n\,(\Lambda^2+K_h^2)} \int_0^{f_o} \frac{f\,df}{(\Lambda^2+f^2)} \left\{\left[f \coth\frac{\hbar cf}{2k_BT}\right.\right.$$

$$\left.\left.\left(1+\frac{K_h\cos\alpha}{2k_n}\right)+\frac{m_ocK_h\cos\alpha}{\hbar k_n}\right]\ln\frac{2k_n+f}{2k_n-f} - 2K_h\cos\alpha\coth\frac{\hbar cf}{2k_BT}\right\} \quad (4.17)$$

Now for high energy particles, where k_n is large compared to f_o, we can write $\ln(1 + f/2k_n) \simeq f/2k_n$ and then in the low temperature limit $\coth(\hbar cf/2k_BT) \simeq 1+2e^{-\hbar cf/k_BT}$, one gets after integration,

$$\text{Re } C_{ho}(n) = -\frac{2m_o\rho'(z_1z_2e^2)^2\, e^{-D_1K_h^2}}{M\hbar c\, k_n^2(\Lambda^2+K_h^2)} \left\{\frac{1}{2}\left(1+\frac{K_h\cos\alpha}{2k_n}\right)\left[f_o^2 - {}^2\ln(1+f_o^2/\Lambda^2)\right]\right.$$

$$+\frac{m_ocK_h\cos\alpha}{\hbar k_n}\left(f_o-\Lambda\tan^{-1}\frac{f_o}{\Lambda}\right)+2\left(1+\frac{K_h\cos\alpha}{2k_n}\right)f_o^2\left[\left(1-e^{-\theta D/T}\right)\left(\frac{T}{\theta_D}\right)^2\right.$$

$$\left.-\frac{T}{\theta_D}e^{-\theta_D/T}\right]-K_hk_n\cos\alpha\ln\left(1+\frac{f_o^2}{\Lambda^2}\right)+2\left[\left(1+\frac{K_h\cos\alpha}{2k_n}\right)^2\Lambda^2+2K_hk_n\cos\alpha\right]$$

$$\left.x\left[ci\left(\frac{\Lambda\hbar c}{k_BT}\right)\cos\left(\frac{\Lambda\hbar c}{k_BT}\right)+si\left(\frac{\Lambda\hbar c}{k_BT}\right)\sin\left(\frac{\Lambda\hbar c}{k_BT}\right)\right]\right\} \quad (4.18)$$

Now at the Bragg condition where the two wave picture holds, $K_h\cos\alpha/2k_n = -(K_h/2k_n)^2$ so that for high energy particles, we can neglect $K_h\cos\alpha/2k_n$ compared to unity, so that eqn.(4.18) can be written as,

$$\text{Re } C_{ho}(n) = -\frac{\hbar\rho'(z_1z_2e^2)^2 e^{-D_1K_h^2}}{Mc(\Lambda^2+K_h^2)E_p} \left\{\frac{1}{2}f_o^2\left[1-\frac{\Lambda^2}{f_o^2}\ln\left(1+\frac{f_o^2}{\Lambda^2}\right)\right]\right.$$

$$+2f_o^2\left[(T/\theta_D)^2\left(1-e^{-\theta D/T}\right)-\frac{T}{\theta_D}e^{-\theta_D/T}\right]+\frac{1}{2}K_h^2\ln(1+f_o^2/\Lambda^2)$$

$$\left.+2(\Lambda^2-K_h^2)\left[ci\left(\frac{\Lambda\hbar c}{k_BT}\right)\cos\left(\frac{\Lambda\hbar c}{k_BT}\right)+si\left(\frac{\Lambda\hbar c}{k_BT}\right)\sin\left(\frac{\Lambda\hbar c}{k_BT}\right)\right]\right\} \quad (4.19)$$

In the same approximation, eqn. (3.25) for Im $C_{ho}(n)$ can be written as,

$$\text{Im } C_{ho}(n) = -\frac{\pi\rho'(2m_o)^{1/2}(z_1z_2e^2)^2 e^{-D_1Kh^2}}{Mc\, E_p^{1/2}(\Lambda^2+K_h^2)} \left\{ f_o + 2f_o\left(\frac{T}{\theta_D}\right)\left(1-e^{-\theta_D/T}\right) \right.$$

$$\left. -\Lambda\left[\tan^{-1}\frac{f_o}{\Lambda} + ci\left(\frac{\Lambda\hbar c}{k_BT}\right)\sin\left(\frac{\Lambda\hbar c}{k_BT}\right) - si\left(\frac{\Lambda\hbar c}{k_BT}\right)\cos\left(\frac{\Lambda\hbar c}{k_BT}\right)\right]\right\} \qquad (4.20)$$

The Fourier transform of $\langle n|V(r)|n\rangle$, the initial state expectation value of the interaction potential is given by,

$$V_h = (1/V')\int d\underline{r}\ \langle n|V(\underline{r})|n\rangle\ e^{-i\underline{K}_h\cdot\underline{r}}$$

$$= \frac{V(\underline{K}_h)}{V'} \sum_{\underline{\sigma}} \langle n|e^{-i\underline{K}_h\cdot\underline{u}_\sigma}|n\rangle \qquad (4.21)$$

which has been calculated by Kothari and Singwi[53] and one gets,

$$V_h = \frac{4\pi z_1z_2e^2}{(\Lambda^2+K_h^2)}\ \rho'\ e^{-W} \qquad (4.22)$$

$$\text{with} \quad W = \frac{\hbar^2}{4MN} K_h^2 \sum_j \frac{1}{\xi_j} \coth\left(\xi_j/k_BT\right) \qquad (4.23)$$

$$= \frac{3\hbar^2}{8k_B\theta_D M}\left[1+4\left(\frac{T}{\theta_D}\right)^2\right]K_h^2 \quad \text{(in the low temperature limit)}$$

The equations (4.19), (4.20) and (4.22) provide the appropriate values of Re C_{ho}, Im C_{ho} and V_h, to be used in the expression (4.11) for intensity.

4.4 Discussion:

The extinction distance ξ_h', defined in eqn. (4.12), is typically less than 100 Å for electron energies above 100 keV while the absorption length ξ_o'' is quite large (more than 100 times) compared to ξ_h'. This is because Im C_{ho} is quite small compared to V_h (see below). Thus a collection of emitting atoms

spread over several extinction distances from the crystal surface, such as might be achieved by bombarding the crystal with radio-active atoms at a definite energy, will give an intensity which is the average of eqn. (4.11) over thickness. This average will eliminate the cosine term leaving only the exponentials, with the average distance to the emitter replacing t.

For typical values of the parameters $\Lambda = 4.2 \times 10^{8}$ cm^{-1} $k_n = 2\times10^{10}$ cm^{-1} and $|V_h/E_p| = 10^{-4}$, we see on numerical evaluation that the magnitude of Re C_{ho}/V_h is about 10^{-5} and that of Im C_{ho}/V_h is about 10^{-3}. Thus the attenuation is very small compared to what has been generally chosen phenomenologically[36]. In the ideal case, let us study the angular characteristics of the intensity pattern for no attenuation (infinite absorption length). In this case, from eqn. (4.11), the average intensity is given by,

$$\langle|\phi|^2\rangle = \overline{|\phi_n(t)|^2} = x^2 + (1-x)^2$$

$$= 1 - y/(1+y^2) \qquad (4.24)$$

where y is approximately given by (from eqn. (4.12)),

$$y \simeq \frac{\sin 2\theta_B}{W_h'}(\theta_B-\theta) \qquad (4.25)$$

The average intensity $\langle|\phi|^2\rangle$ has been plotted against y in Fig. 1. To include the Bragg reflection on the other side of $\theta = 0$, the curve should be reflected about the value of y, corresponding to $\theta = 0$. For electrons, $\theta = 0$ corresponds to $y = -1.5$ and for positrons, to $y = 1.5$. The corresponding curves thus obtained have been shown in Figs. 2 and 3.

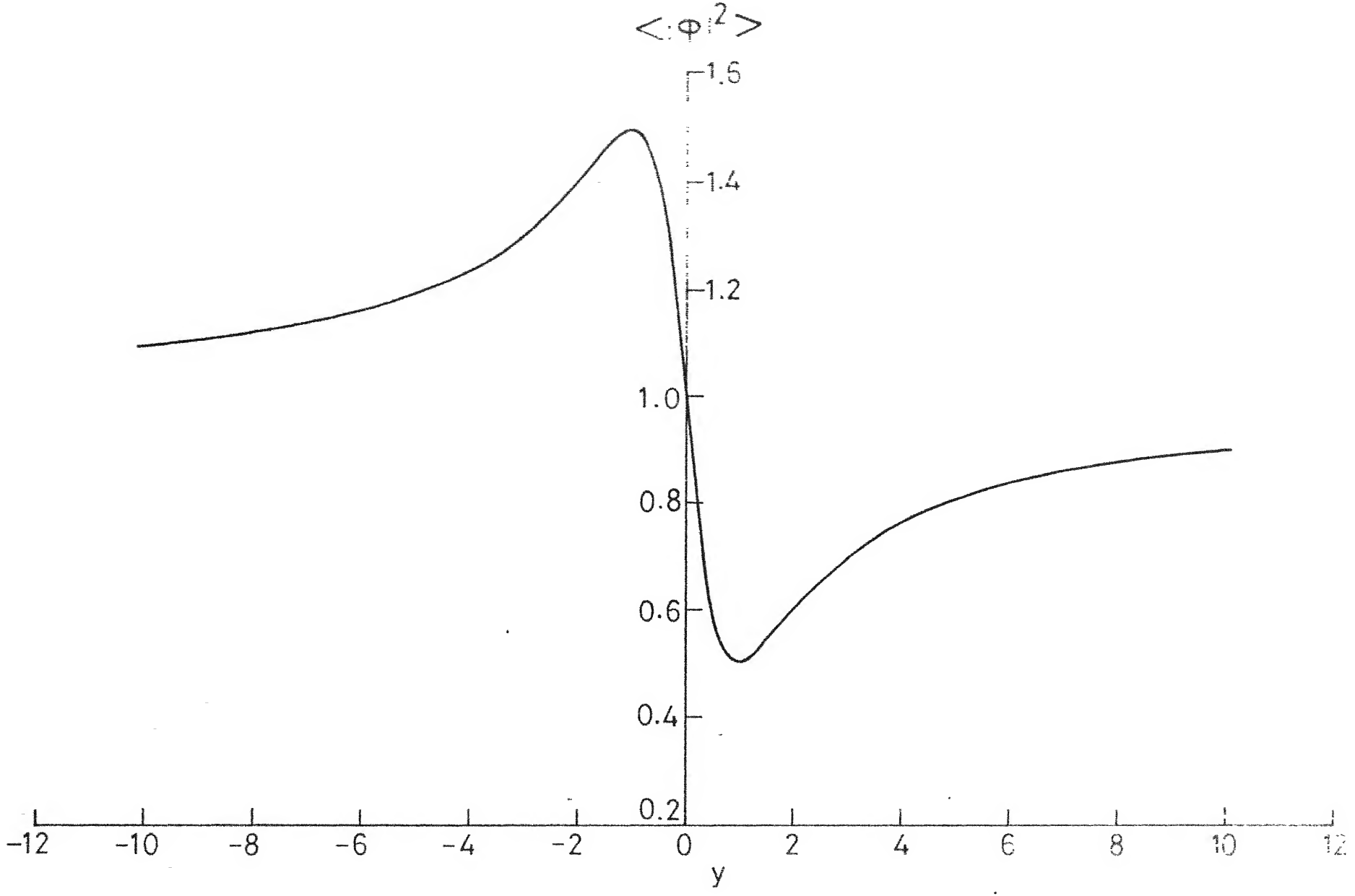

FIG. 1: [illegible] as attenuation.

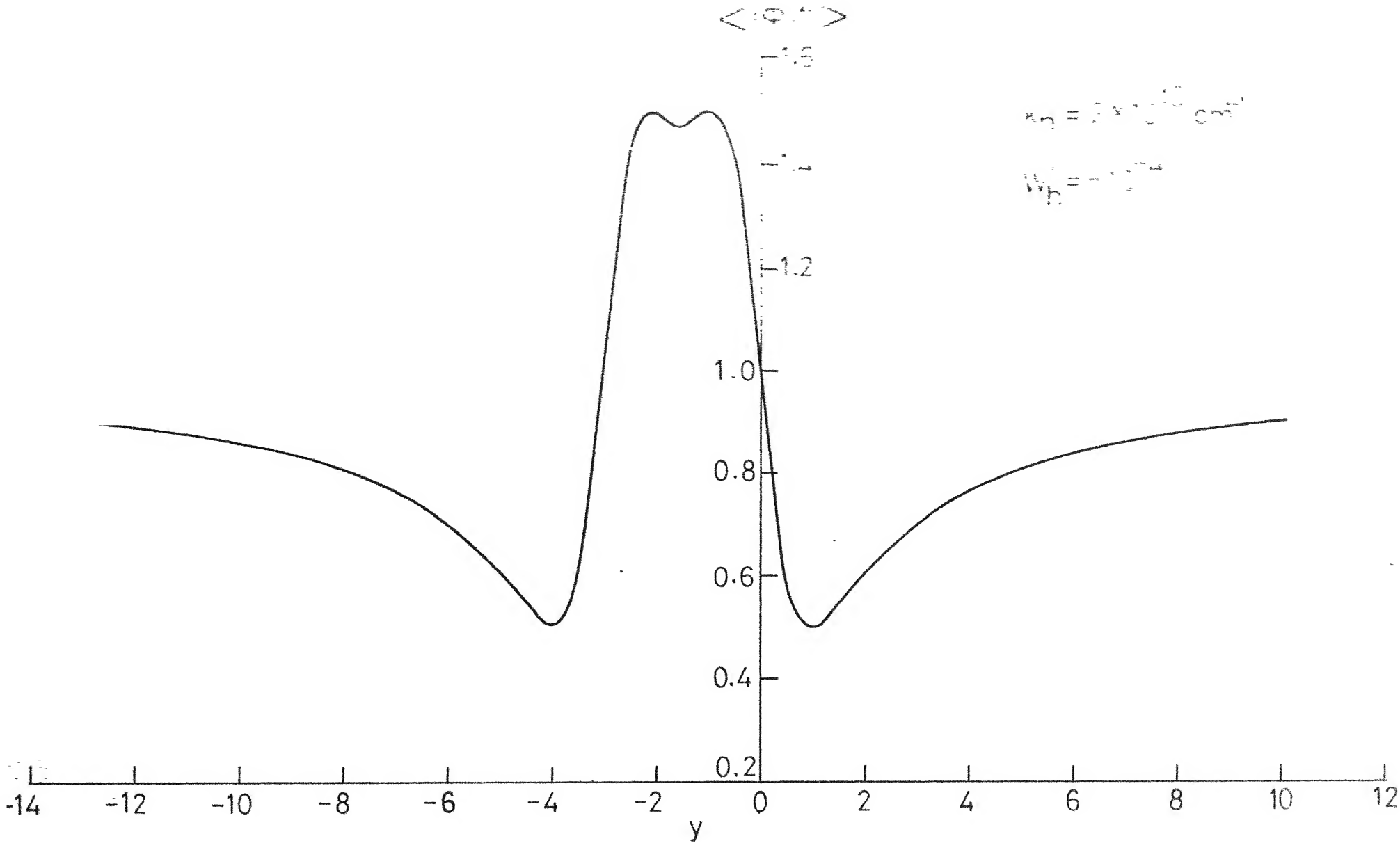

FIG. 2: Angular intensity variation for electrons; two wave solution, no attenuation

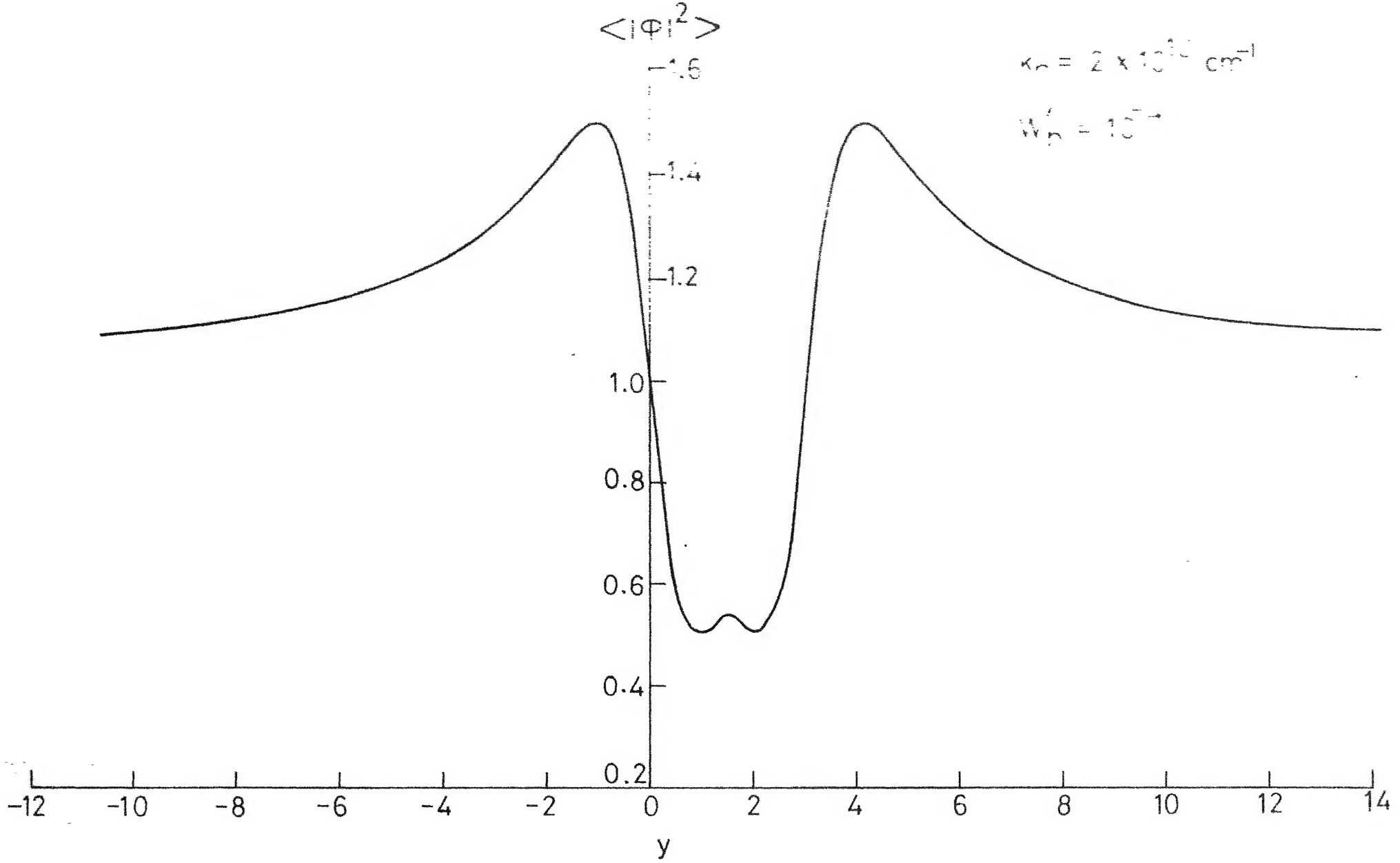

FIG. 3: Angular intensity variation for positrons two wave solution, no attenuation.

It should be noted that the since Re C_{ho} is very small compared to V_h, these curves are essentially identical to those of DeWames et al.[36] without attenuation. Consequently, the angular widths of intensity patterns are also equal to the widths of their curves corresponding to no attenuation case. However, their curves with attenuation correspond to an over estimation of the attenuation ($W_h''/W_h' \sim 0.1$) in view of the fact that Im $C_{ho}/V_h \sim 10^{-3}$ for typical values chosen by DeWames et al.[36], implying thereby very little attenuation. In fact, W_h'' in our calculation is determined once the parameters for W_h' are fixed and need not be chosen phenomenologically. The mass and energy dependence of the attenuation $(m_o/E_p)^{1/2}$ shows that for low energy heavy particles, the attenuation becomes significant. For keV electrons and positrons Re $C_{ho}/V_h \sim 10^{-3}$ and the patterns start getting modified due to this correction.

From eqn.(4.25) we note that the thickness averaged intensity of the two beam solution has the outer wing in the intensity pattern at ($y = \pm 1$),

$$\theta_W = \theta_B + \Delta\theta_B$$

$$= \frac{1}{2}\left[\frac{\hbar K_h}{(2m_o E_p)^{1/2}}\right] + \frac{|V_h| + |\mathrm{Re}C_{ho}|}{\hbar K_h}\left(\frac{2m_o}{E_p}\right)^{1/2} \qquad (4.26)$$

(for electrons, at $y = 1$)

$$= \frac{1}{2}\left[\frac{\hbar K_h}{(2m_o E_p)^{1/2}}\right] + \frac{|V_h| - |\mathrm{Re}C_{ho}|}{\hbar k_h}\left(\frac{2m_o}{E_p}\right)^{1/2} \qquad (4.27)$$

(for positrons, at $y = -1$)

This shows that the condition $\Delta\theta_B/\theta_B << 1$ for validity of the two beam theory depends upon the mass m_o of the incident particle and the strength of the interaction potential V_h.

It also depends upon the particle energy E_p through the term Re C_{ho} which is inversely proportional to E_p. The mass dependence shows that for heavier particles, as soon as $\Delta\theta_B$ becomes comparable to θ_B, the two beam theory is not useful. Similarly for strong interaction potentials (V_h large) the condition $\Delta\theta_B/\theta_B << 1$ is violated. Actually the particle mass and strength of interaction potential, simultaneously govern the validity of the two wave picture. Thus, inspite of the large mass, (comparable to that of proton) neutrons are describable by the two wave picture, since their interaction potential is weak compared to that for proton case (Coulomb or screened Coulomb). Similarly, the electrons and positrons, because of their small mass, may be described by the two beam theory (although marginally, because of strong interaction potential). But for protons, the two beam theory is certainly not applicable.

The energy dependence appears only when Re C_{ho} becomes significant at low energies and under those circumstances, the condition $\Delta\theta_B/\theta_B << 1$ is more favourably satisfied for positions than for electrons. Another interesting consequence of the present theory, in this situation, is an indication of the difference between widths of electron and positron emission patterns. From

eqn. (4.25) we see that since $W_h' = (V_h + \text{Re } C_{ho})/E_p$, it follows that the magnitude of y for $\theta = 0$ is slightly increased for positrons and slightly decreased for electrons (since Re C_{ho} is always negative). This shows that whenever Re C_{ho} becomes significant (at low energies), the angular width of electron emission pattern is small compared to that of positrons. Although this difference is only qualitative and does not quantitatively explain the observed difference[38,39], the difference is qualitatively correct and in the right direction. This feature is usually absent in the two beam theories[36,37].

CHAPTER V

ENERGY LOSS OF CHARGED PARTICLES

5.1 Introduction:

In the preceeding Chapters II, III and IV, we have considered some of the features of the quantum theory of channeling. In particular, we examined the conditions for channeling; energy, temperature and potential dependence of the phenomena and the widths of the emission patterns. One of the most important problem that needs attention in the theory of channeling, is the problem of energy loss of channeled particles. The quantities like the actual penetration depth, the range of the channeled particles and the energy spectra of the emitted (or transmitted) particles, are essentially determined by the rate of the energy loss of the channeled particles.

For neutral particles, such as neutrons, the only mechanism by which the channeled particles lose energy, is through phonon excitations. For charged particles, the total contribution to energy loss may be divided into three parts: (1) Energy loss to phonons (2) Energy loss due to core electrons and (3) Energy loss due to conduction electrons.

The phonon contribution to the rate of energy loss has been considered by Lidiard[69]. He calculated the rate of energy loss due to elastic processes by treating the crystal in

harmonic approximation. By regarding the fast particle coming into the crystal as a perturbation, it has been shown that during the propagation of particle, phonon shock waves are generated which carry away the energy from the particle. For particle velocities V, much greater than the velocity of sound, the rate of energy loss - dE/dt was found to be inversely proportional to V confirming the earlier results of Lehman and Leibfried[68]. Moreover, the phonon contribution to energy loss is found to be strongly directional effect, as expected.

The energy loss due to core electrons is also expected to show directional effects, as was pointed out in Chapter III. The energy transferred to core electrons depends upon impact parameter and must be calculated separately for various core electrons. However, a comprehensive theory of this loss has not yet been worked out. It is expected that this loss should be small compared to that due to conduction electrons, because under channeling conditions, the particles do not come very close to the ions and hence to the various core electrons. In fact Erginsoy[93] has shown that it is a good approximation to neglect this and that the energy loss to valence electrons is the most important contribution to energy loss of charged particles moving under channeling conditions.

Thus the stopping power (dE/dx) of charged particles is mainly governed by the rate of energy loss due to conduction

electrons. In the first approximation these constitute a uniformly distributed degenerate electron gas and their contribution to the total stopping power is not expected to show any dependence on the direction of motion of the particle in the lattice. This approximation is probably better justified in the case of metals, than in semiconductors. In the semiconductors, the valence electron density may be nonuniform so that the energy loss does depend upon the position of the particle. Actually, this nonuniformity of electron density may account for a part of the observed channeling effects.

A general formulation of the response of an electron gas to a longitudinal disturbance is possible in terms of the complex dielectric constant $\epsilon(k, \omega)$. Such a formulation has been given by Lindhard[94] and later by Nozieres and Pines[95] by using first order perturbation theory. The essential steps of the treatment given by Nozieres and Pines are as follows.

Consider the unperturbed electron gas, described by the Hamiltonian,

$$H_o = \sum_i \frac{p_i^2}{2m} + \sum_k \frac{2\pi e^2}{k^2} (\rho_k \rho_{-k} - n) \qquad (5.1)$$

where n is the electron density and ρ_k is the density fluctuations given by,

$$\rho_k = \sum_i e^{-i\underline{k}.\underline{x}_i} \qquad (5.2)$$

In the equations (5.1) and (5.2), summation over i runs over all the electrons, whose positions are denoted by x_i. If the Fourier

components of the external test charge (incoming particle) are written as, $e\{r_k \exp[-i(\omega t + \underline{k}.\underline{r})] + c.c.\}$, then the perturbed Hamiltonian is given by,

$$H_1 = \frac{4\pi e^2}{k^2} (\rho_{-k} r_k e^{-i\omega t} + c.c.) e^{\eta t} \quad (5.3)$$

where η is an infinitesimal quantity. Now expanding the perturbed wave function as,

$$\psi(t) = \sum_n \psi_n e^{-iE_n t/\hbar} a_n(t)$$

and calculating the coefficients in first order perturbation theory,

$$a_n(t) = -\frac{4\pi e^2}{\hbar k^2} \frac{r_k(\rho_{-k})_{no} \exp[i(-\omega+\omega_{no})t + \eta t]}{-\omega+\omega_{no}-i\eta} + \frac{r_{-k}(\rho_k)_{no} \exp[i(\omega_{no}+\omega)t + \eta t]}{\omega+\omega_{no}-i\eta} \quad (5.4)$$

where $(\rho_k)_{no}$ is the matrix element of ρ_k between the crystal eigen states $|n\rangle$ and $|0\rangle$ and $\omega_{no} = (E_n - E_o)/h$. Using the translational invariance, which implies $(\rho_{-k})_{no} = 0$ if $(\rho_k)_{no} \neq 0$, the perturbed expectation value of ρ_k can be calculated from eqn. (5.4), to be (assuming that system is invariant under reflection)

$$\langle\rho_k\rangle = -\frac{4\pi e^2}{\hbar k^2} r_k e^{-i\omega t + \eta t} \sum_n |(\rho_k)_{no}|^2 \left\{\frac{1}{-\omega+\omega_{no}-i\eta} + \frac{1}{\omega+\omega_{no}-i\eta}\right\} \quad (5.5)$$

Now using the Fourier expansions of Macroscopic Poisson eqns.

$$\underline{k}.\epsilon\underline{E}_k = 4\pi e r_k e^{i\omega t}$$

$$\underline{k}.\underline{E}_k = 4\pi e[r_k e^{-i\omega t} + \langle\rho_k\rangle]$$

One can write,

$$\frac{\langle \rho_k \rangle}{r_k\, e^{-i\omega t}} = \frac{1}{\epsilon(k,\omega)} - 1 \qquad (5.6)$$

Then from eqns. (5.5) and (5.6), we get,

$$\mathrm{Im}\,\frac{1}{\epsilon(k,\omega)} = \frac{4\pi^2 e^2}{\hbar k^2} \sum_n |(\rho_k)_{no}|^2 \{\delta(\omega_{no}+\omega)-\delta(\omega_{no}-\omega)\} \qquad (5.7)$$

Therefore, using the lowest order time dependent perturbation theory result for energy loss[105]

$$\frac{dW}{dt} = \frac{2\pi}{\hbar}\left(\frac{4\pi e^2}{k^2}\right)^2 \sum_n |r_k|^2 |(\rho_k)_{no}|^2 \hbar\omega[\delta(\omega_{no}-\omega)-\delta(\omega_{no}+\omega)] \qquad (5.8)$$

one can write from eqns. (5.7) and (5.8),

$$\frac{dW}{dt} = -\frac{8\pi e^2}{k^2} |r_k|^2 \,\mathrm{Im}\,\frac{1}{\epsilon(k,\omega)} \qquad (5.9)$$

For high velocities, where Born approximation is satisfactory each Fourier component of incoming particle density behaves like a test charge of density fluctuation $r_k = 1$ with a frequency $\omega = \underline{k}.\underline{V}$ where V is the particle velocity. Therefore the energy loss suffered by the fast electron is,

$$\frac{dE}{dt} = -\frac{1}{2} \sum_k \frac{8\pi e^2}{k^2} (\underline{k}.\underline{V})\ \mathrm{Im}\,\frac{1}{\epsilon(k,\underline{k}.\underline{V})}$$

Replacing summation by integration $\sum_{\underline{k}} = \frac{1}{(2\pi)^3} \int d\underline{k}$, and performing angular integration we get,

$$\frac{dE}{dt} = -\frac{2e^2}{\pi V} \int_0^\infty \frac{dk}{k} \int_0^{kV} \omega\, \mathrm{Im}\,\frac{1}{\epsilon(k,\omega)}\, d\omega \qquad (5.10)$$

Thus the final expression for stopping power is given by,

$$-\frac{dE}{dx} = \frac{2e^2}{\pi V^2}\int_0^{\infty}\frac{dk}{k}\int_0^{kV}\omega\ \mathrm{Im}\left(\frac{1}{\epsilon(k,\omega)}\right)d\omega \qquad (5.11).$$

If the incident particle has charge $z_1 e$, the factor multiplying the integration becomes $2z_1^2e^2/\pi V^2$.

For high particle velocity, the upper limit of ω - integration may be replaced by ∞ and one gets $-\frac{dE}{dx} \propto \frac{1}{V^2}$. But when the particle velocity cannot be chosen as large, the velocity dependence of the stopping power is modified depending on the form of dielectric function. For low particle velocities $V << V_F$, the Fermi velocity, the problem of stopping power is similar to that of the residual resistivity in a dilute metal alloy where electrons are scattered by stationary charged impurities. The Mott[96] solution of this problem is based on the Born approximation. According to Lindhard[94] the same perturbation treatment is valid for the stopping power problem because the important parameter in the collisions is the relative velocity. For small V, the relative velocity is simply the Fermi velocity V_F, since only the top most electrons can be scattered.

The first treatment of the stopping power on this basis, for particle velocities small compared to the Fermi velocity, is due to Fermi and Teller[97]. They obtained the expression for stopping power of particle with charge $z_1 e$, as,

$$-\frac{dE}{dx} = \frac{2z_1^2\, e^4\, m^2 V}{3\pi\hbar^3}\ln\left(\frac{\hbar V_F}{e^2}\right) \qquad (5.12)$$

which shows the proportionality of the stopping power to the particle

velocity. Here m is the electron mass. Lindhard[94], Lindhard and Winther[98] and Trubnikov and Yavlinskii[99] have used the dielectric response formulation (5.1) and derived an expression which differs only slightly from that of Fermi and Teller, eqn. (5.12). For high density electron gas they obtain,

$$-\frac{dE}{dx} = \frac{2z_1^2 e^4 m^2 V}{3\pi\hbar^3}\left[\ln\left(\frac{\pi\hbar V_F}{e^2}\right) - 1\right] \qquad (5.13)$$

Transmission experiments[100] in which the energy loss of protons and α-particles of 4-30 keV energy has been measured in thin films of various matrials, confirm that the stopping power is proportional to the particle velocity.

In the case of heavy ions, nuclear energy losses are larger than the inelastic losses to electron gas, upto energy in the MeV range. However, under channeling conditions, the cross section of hard nuclear collisions is greatly reduced and it becomes possible to study the electronic stopping power down to relatively low energies (10-50 keV) where normally inelastic losses would be completely masked by nuclear stopping. There is increasing evidence that electronic excitation is appreciable even for low particle velocities. Channeling experiments[101,102] with xenon ions, over a wide range of energies (1-1000 keV) in tungsten single crystals, show that the range of channeled ions changes from the $R \propto E_p^{1.5-2.0}$ behaviour, characteristic of low velocities, where nuclear stopping power dominates, to the $R \propto E_p^{0.5}$ behaviour, consistent with an electronic stopping power proportional to velocity. A discussion on the velocity dependence of

stopping power for various ranges of particle velocity, has been recently given by Lindhard[103].

Here we present the results of a calculation made for stopping power using formula (5.11) and different models for dielectric function which will give us an insight, as to what extent, the stopping power is sensitive to the form of the dielectric function. It is seen that for electron velocity upto about ten times the Fermi velocity, stopping power is very nearly inversely proportional to V and is not very much sensitive to the form of dielectric function. It is also seen that for particle velocities small compared to Fermi velocity, even the use of expression (5.11) leads to the result $-dE/dx$ very nearly proportional to velocity as we see from eqn. (5.13).

5.2 Calculation Using Different Approximations for Dielectric Function:

For convenience of numerical computation, we write eqn.(5.11) in terms of dimensionless variables. Thus expressing k in units of k_F, the Fermi momentum and ω in units of $\hbar k_F^2/2m$, we get,

$$-\frac{dE}{dx} = \frac{e^2 k_F^2}{2\pi K_o^2} \int_o^\infty \frac{dk}{k} \int_o^{2kK_o} \omega \, \mathrm{Im}\left(\frac{1}{\epsilon(k,\omega)}\right) d\omega \qquad (5.14)$$

with $K_o = mV/\hbar k_F = V/V_F$, being the ratio of particle velocity to the Fermi velocity and $\mathrm{Im}\,[1/\epsilon(k,\omega)]$ is to be written in the dimensionless units mentioned above. If $\epsilon(k,\omega) = \epsilon_1(k,\omega) + i\epsilon_2(k,\omega)$, $\epsilon_1(k,\omega)$ and $\epsilon_2(k,\omega)$ being real, $\mathrm{Im}\left(\frac{1}{\epsilon(k,\omega)}\right) = -\frac{\epsilon_2(k,\omega)}{\epsilon_1^2(k,\omega) + \epsilon_2^2(k,\omega)}$

and since $C_2(k,\omega)$ vanishes for $\omega \geq 2k + k^2$, the integral in eqn. (5.14) may be written as,

$$-\frac{dE}{dx} = \frac{e^2 k_F^2}{2\pi K_o^2}\Big[\int_0^{2(K_o-1)} \frac{dk}{k}\int_0^{2k+k^2} \omega\,\mathrm{Im}\left(\frac{1}{\epsilon(k,\omega)}\right) d\omega + \int_{2(K_o-1)}^{\infty} \frac{dk}{k}\int_0^{2kK_o} \omega\,\mathrm{Im}\left(\frac{1}{\epsilon(k,\omega)}\right) d\omega\Big] \qquad (5.15)$$

Now the numerical calculation of the stopping power requires the knowledge of dielectric function. We first give different approximations in which dielectric function has been calculated.

(A) Random Phase Approximation (RPA):

The RPA was developed in the course of studies of screening and collective behaviour of an electron liquid. In the early work[104], primary emphasis was placed on the explicit introduction of collective coordinates (which describe the plasmons) for this purpose. The approximation acquired its name on the basis of the physical argument that under suitable circumstances, a sum of exponential terms with randomly varying phases could be neglected compared to N. Thus the approximation,

$$\rho_{k-q} = \sum_i e^{i(\underline{q}-\underline{k})\cdot\underline{x}_i} \simeq N\,\delta_{k,q}$$

was frequently made when ρ_{k-q} appeared as a multiplicative factor in the basic equations of the theory. This approximation amounts to neglecting the exchange diagrams in the Goldstone diagram analysis. Thus the RPA neglects all the exchange correlations and represents a good approximation for high density electron gas ($r_s < 1$).

The expression for dielectric function in RPA was first calculated by Lindhard[94], using a self consistent field method. This is given by,

$$\epsilon(k,\omega) = 1 + Q_o(k,\omega) \tag{5.16}$$

with, $$Q_o^R(k,\omega) = \frac{k_{FT}^2}{k^2}\left\{\frac{1}{2} + \frac{1}{4k}\left[1-\left(\frac{\omega+k^2}{2k}\right)^2\right] \ln\left|\frac{\omega+2k+k^2}{\omega-2k+k^2}\right| + \frac{1}{4k}\left[1-\left(\frac{\omega-k^2}{2k}\right)^2\right] \ln\left|\frac{\omega-2k-k^2}{\omega+2k-k^2}\right|\right\} \tag{5.17}$$

and $$Q_o^I(k,\omega) = \frac{\pi k_{FT}^2}{4k^3}\,\omega \qquad \text{for } \omega \leq 2k-k^2$$

$$= \frac{\pi k_{FT}^2}{4k^3}\left[1-\left(\frac{\omega-k^2}{2k}\right)^2\right] \quad \text{for } |2k-k^2| \leq \omega \leq 2k+k^2 \tag{5.18}$$

$$= 0 \qquad \text{for } \omega \geq 2k+k^2,$$

$Q_o^R(k,\omega)$ and $Q_o^I(k,\omega)$ representing the real and imaginary parts of $Q_o(k,\omega)$. Here k_{FT} is the Thomas-Fermi wave number in units of k_F and is given by[105,106]

$$k_{FT}^2 = \frac{3\omega_p^2}{k_F^2 V_F^2} = \frac{4}{\pi a_o k_F}$$

where $\omega_p^2 = (4\pi ne^2/m)$ is plasma frequency. The Fermi wave number is given by[106] $k_F = (9\pi/4)^{1/3}\frac{1}{r_o}$, r_o being defined as $4\pi r_o^3/3 = \frac{1}{n}$. r_o is generally expressed in Bohr units as $r_o = r_s a_o$, $a_o = \hbar^2/me^2$ and for metallic density region r_s lies between 1.8 and 5.6. Thus in RPA we have,

$$\mathrm{Im}\left(\frac{1}{\epsilon(k,\omega)}\right) = -\frac{Q_o^I(k,\omega)}{(1+Q_o^R(k,\omega))^2+(Q_o^I(k,\omega))^2} \tag{5.19}$$

(B) Hubbard Approximation:

Hubbard[107] improved upon the results of RPA by taking into account the short range correlations due to exchange effects. He used the diagrammatic technique to include these effects by summing the exchange diagrams in an approximate way. In this approximation, the expression for dielectric function is obtained to be,

$$\epsilon(k,\omega) = 1 + \frac{Q_o(k,\omega)}{1-f(k)\ Q_o(k,\omega)} \qquad (5.20)$$

with,

$$f(k) = \frac{1}{2}\ \frac{k^2}{1+k^2+K_s^2} \qquad (5.21)$$

where K_s is the screening parameter in units of k_F. This screening parameter did not appear in the original formula but it was added later by Hubbard himself, in private communication to several authors[108]. Although, usually the screening parameter K_s is replaced by the Thomas—Fermi wave number k_{FT}, but it has been emphasized[108,109] that to reproduce the compressibility limit properly, K_s should be chosen as given by Nozieres-Pines interpolation formula,

$$K_s^2 = (4 - 0.158\ k_{FT}^2)/(4 + 0.158\ k_{FT}^2) \qquad (5.22)$$

For high density metals, this formula yields values of K_s^2 close to but somewhat less than k_{FT}^2. Thus in this approximation we get,

$$\mathrm{Im}\left(\frac{1}{\epsilon(k,\omega)}\right) = -\frac{Q_o^{\,I}(k,\omega)}{[1+(1-f(k))Q_o^{\,R}(k,\omega)]^2+[(1-f(k))Q_o^{\,I}(k,\omega)]^2} \qquad (5.23)$$

(C) Kleinman Approximation:

Kleinman has used self consistent field[110] method and later the diagrammatic technique[111], to calculate the dielectric functions taking both exchange and Coulomb correlations into account. It has been shown that Hubbards formula (5.20) has correct form only in the static limit ($\omega \to 0$) and that even then Hubbard's f(k) is completely incorrect for large k. Actually the static formula obtained from Kleinman's results which has been confirmed by variational calculations of Langreth[109], is found to give correct results for screening density[112] around a fixed charged impurity which agree with those obtained by Singwi et al.[113] making self constent calculations.

According to Kleinman's formulation,

$$\frac{1}{\epsilon(k,\omega)} - \frac{1}{\epsilon^*(k,-\omega)} = 1 - \frac{1}{2}\left(\frac{\chi(k,\omega)}{\epsilon_{el}(k,\omega)} + \frac{\chi^*(k,-\omega)}{\epsilon^*_{el}(k,-\omega)}\right) \quad (5.24)$$

with $$\epsilon_{el}(k,\omega) = 1 + \frac{\alpha_1\chi(k,\omega)+\alpha_2\chi^*(k,-\omega)+(\alpha_1^2-\alpha_2^2)\chi(k,\omega)\chi^*(k,-\omega)}{1+(\alpha_1-\alpha_2)\chi^*(k,-\omega)} \quad (5.25)$$

where $$\alpha_1 = \frac{1}{2}\left[1 - \frac{1}{2}\frac{k^2}{1+K_s^2}\right];\ \alpha_2 = \frac{1}{2}\left[1 - \frac{1}{2}\frac{k^2}{1+k^2+K_s^2}\right] \quad (5.26)$$

and $\chi(k, \pm\omega) = \chi_1(\pm\omega) + i\chi_2(\pm\omega)$ where k dependence of the real quantities $\chi_1(k, \pm\omega)$ and $\chi_2(k, \pm\omega)$ has been omitted for simplicity. These functions are given by,

$$\chi_1(\pm\omega) = \frac{k^2}{2k^3}\,FT\left\{\left[1-\left(\frac{\omega\pm k^2}{2k}\right)^2\right]\ln\left|\frac{\omega\pm 2k\pm k^2}{\omega\mp 2k\pm k^2}\right| + \frac{k^2\pm\omega}{k}\right\} \quad (5.27)$$

$$\chi_2(\omega) = \frac{\pi k^2}{2k^3}\,\mathrm{FT}\left[1-\left(\frac{\omega+k^2}{2k}\right)^2\right] \qquad \text{if } \omega < 2k-k^2;\ 0 \text{ otherwise}$$

$$\chi_2(-\omega) = \frac{\pi k^2}{2k^3}\,\mathrm{FT}\left[1-\left(\frac{\omega-k^2}{2k}\right)^2\right] \qquad \text{if } k^2-2k<\omega<k^2+2k;\ 0 \text{ otherwise} \tag{5.28}$$

Here $\epsilon_{el}(k,\omega)$ given by eqn. (5.25) has significance of being dielectric function for an electron. This differs from the dielectric function for a test charge $\epsilon(k,\omega)$, given by eqn. (5.24), since the latter has no exchange interaction with the responding electron gas. Now using eqns. (5.24) and (5.25), we get,

$$\begin{aligned}\mathrm{Im}\,(1/\epsilon(k,\omega)) = -(1/2)\Big[\{\chi_2(\omega)-\chi_2(-\omega)+(\alpha_1-\alpha_2)[\chi_1(-\omega)\chi_2(\omega) \\ -\chi_1(\omega)\chi_2(-\omega)]\}+(\alpha_1-\alpha_2)^2[\chi_2(\omega)|\chi(-\omega)|^2-\chi_2(-\omega)|\chi(\omega)|^2]\Big]/\Big[\{1+\alpha \\ \times[\chi_1(\omega)+\chi_1(-\omega)]+(\alpha_1^2-\alpha_2^2)[\chi_1(\omega)\chi_1(-\omega)+\chi_2(\omega)\chi_2(-\omega)]\}^2+\{\alpha_1[\chi_2(\omega) \\ -\chi_2(-\omega)]+(\alpha_1^2-\alpha_2^2)[\chi_1(-\omega)\chi_2(\omega)-\chi_1(\omega)\chi_2(-\omega)]\}^2\Big]\end{aligned} \tag{5.29}$$

$$\begin{aligned}\text{and } \mathrm{Im}(1/\epsilon_{el}(k,\omega)) = -\Big[\alpha_1\chi_2(\omega)-\alpha_2\chi_2(-\omega)+\alpha_2(\alpha_2-\alpha_1)\chi_1(\omega)\chi_2(-\omega)+(\alpha_1+\alpha_2) \\ (\alpha_1-\alpha_2)^2\chi_2(\omega)|\chi(-\omega)|^2+(2\alpha_1^2-\alpha_1\alpha_2-\alpha_2^2)\chi_1(-\omega)\chi_2(\omega)\Big]/\Big[\{1+\alpha \\ \times[\chi_1(\omega)+\chi_1(-\omega)]+(\alpha_1^2-\alpha_2^2)[\chi_1(\omega)\chi_1(-\omega)+\chi_2(\omega)\chi_2(-\omega)]\}^2+\{\alpha_1[\chi_2(\omega) \\ -\chi_2(-\omega)]+(\alpha_1^2-\alpha_2^2)[\chi_1(-\omega)\chi_2(\omega)-\chi_1(\omega)\chi_2(-\omega)]\}^2\Big]\end{aligned} \tag{5.30}$$

(D) Langreth Approximation:

Recently[109], Langreth has used a variational method to calculate the dielectric function. It is shown that Kleinman's theory does not use the Hermitian property of interaction potential. Consequently his results are correct only in the static case ($\omega=0$). For finite frequencies, Langreth gets,

$$\epsilon(k,\omega) = 1 + \frac{\varrho_o(k,\omega)}{1+f(k,\omega)\ \varrho_o(k,\omega)} \tag{5.31}$$

with $$f(k,\omega) = \frac{c_1\left[\chi_L^2(\omega)+\chi_L^{*2}(-\omega)\right]+2c_2\chi_L(\omega)\,\chi_L^*(-\omega)}{\left[\chi_L(\omega)+\chi_L^*(-\omega)\right]^2} \tag{5.32}$$

where $$c_1 = \frac{1}{2}\ \frac{k^2}{1+K_s^2}\ ;\quad c_2 = \frac{1}{2}\ \frac{k^2}{1+k^2+K_s^2} \tag{5.33}$$

and $\chi_L(k,\omega)$, which has been written as $\chi_L(\omega)$ for simplicity, is given by,

$$\chi_L(k,\omega) = -\sum_p \frac{f_p(1-f_{p+k})}{\omega+\epsilon_p-\epsilon_{p+k}+i\eta} \tag{5.34}$$

where f_p is Fermi-function. Langreth did not calculate $\chi_L(k,\omega)$ because he did not use it in any numerical calculation. This may be calculated in a similar way as Lindhard's RPA calculation for dielectric function. The detailed steps to calculate the real and imaginary parts, $\chi_{L1}(\omega)$ and $\chi_{L2}(\omega)$, have been given in the Appendix. The result is,

$$\chi_{L1}(\pm\omega) = -\frac{k_F}{4\pi^2}\left\{\pm\frac{1}{8k}\left[\omega+2\omega\ln\omega\right] - \frac{1}{4} + \frac{1}{4k}\left[1-\left(\frac{\omega\pm k^2}{2k}\right)^2\right]\right.$$
$$\left.\ln|\omega\mp 2k\pm k^2| - \frac{1}{4k}\left[1-\left(\frac{\omega\mp k^2}{2k}\right)^2\right]\ln|\omega\mp 2k\mp k^2|\right\} \text{ for } k < 2 \tag{5.35}$$

$$= -\frac{k_F}{4\pi^2}\left\{\frac{\pm\omega-k^2}{4k^2} + \frac{1}{4k}\left[1-\left(\frac{\omega\mp k^2}{2k}\right)^2\right]\ln\left|\frac{\omega\pm 2k\mp k^2}{\omega\mp 2k\mp k^2}\right|\right\} \text{for } k > 2 \tag{5.36}$$

$$\chi_{L2}(\omega) = \omega k_F/16\pi k \qquad \text{for } \omega \le 2k-k^2$$
$$= \frac{k_F}{16\pi k}\left[1-\left(\frac{\omega-k^2}{2k}\right)^2\right] \text{ for } |2k-k^2| \le \omega \le 2k+k^2 \tag{5.37}$$
$$= 0 \qquad \text{for } \omega \ge 2k+k^2$$

$$\chi_{L2}(-\omega) = 0 \tag{5.38}$$

Now from eqn. (5.31), we can write,

$$\mathrm{Im}(1/\epsilon(k,\omega)) = \Big[(F^R Q_o^I + F^I Q_o^I)\big[1+Q_o^R(1+F^R)-Q_o^I F^I\big]-(1+F^R Q_o^R - F^I Q_o^I)\big[Q_o^R F^I + Q_o^I(1+F^R)\big]\Big] \Big/ \Big[\big[1+Q_o^R(1+F^R)-Q_o^I F^I\big]^2+\big[Q_o^I(1+F^R)+Q_o^R F^I\big]^2\Big] \quad (5.39)$$

where F^R and F^I, the real and imaginary parts of $f(k,\omega)$ in eqn. (5.32), are given by,

$$F^R = \Big[\{c_1[\chi_{L1}^2(\omega)-\chi_{L2}^2(\omega)+\chi_{L1}^2(-\omega)]+2c_2\chi_{L1}(\omega)\chi_{L1}(-\omega)\}\{[\chi_{L1}(\omega)+\chi_{L1}(-\omega)]^2-\chi_{L2}^2(\omega)\}+4\chi_{L2}(\omega)[\chi_{L1}(\omega)+\chi_{L1}(-\omega)][c_1\chi_{L1}(\omega)\chi_{L2}(\omega)+c_2\chi_{L2}(\omega)\chi_{L1}(-\omega)]\Big]/DN \quad (5.40)$$

$$F^I = 2\Big[[c_1\chi_{L1}(\omega)+\chi_{L2}(\omega)+c_2\chi_{L2}(\omega)\chi_{L1}(-\omega)]\{[\chi_{L1}(\omega)+\chi_{L1}(-\omega)]^2-\chi_{L2}^2(\omega)\}-\chi_{L2}(\omega)[\chi_{L1}(\omega)+\chi_{L1}(-\omega)]\{c_1[\chi_{L1}^2(\omega)-\chi_{L2}^2(\omega)+\chi_{L1}^2(-\omega)]+2c_2\chi_{L1}(\omega)\chi_{L1}(-\omega)\}\Big]/DN \quad (5.41)$$

where $DN = ([\chi_{L1}(\omega)+\chi_{L1}(-\omega)]^2-\chi_{L2}^2(\omega))^2+4(\chi_{L1}(\omega)+\chi_{L1}(-\omega))^2\chi_{L2}^2(\omega)$

5.3 Results and Discussion:

Various approximations mentioned above, have been used to calculate the stopping power -dE/dx of electrons, using eqn.(5.15). The double integration involved in the expression has been done numerically, using Simpson's rule. A satisfactory convergence was obtained with 20 as upper limit of k-integration and interval 0.2 for both, k and ω, integrations. The results for electron velocities $2V_F$ and more upto those corresponding to electron energy about 1.5 keV, have been given in Tables IV, V, VI, VII and VIII, for various densities of conduction electrons (in

Table IV: Variation of stopping power (-dE/dx) with particle energy E_p, ($r_s = 2$).

$K_o = \frac{V}{V_F}$	Energy (eV)	Velocity (10^8cm. sec^{-1})	(-dE/dx) in units of 10^{-4} ergs cm^{-1}					
			RPA	Hubbard screened	Hubbard unscreened	Kleinman (electron)	Kleinman (Test charge)	Langreth
2	50.12	4.19	14.161	13.676	13.604	9.442	12.989	14.606
3	112.77	7.97	7.969	7.747	7.714	5.087	7.395	8.226
4	200.47	8.39	5.114	4.988	4.970	3.187	4.782	5.269
5	313.24	10.49	3.581	3.500	3.488	2.196	3.365	3.682
6	451.06	12.59	2.659	2.603	2.595	1.612	2.508	2.731
7	613.95	14.68	2.060	2.019	2.013	1.238	1.949	2.113
8	801.89	16.78	1.648	1.616	1.612	0.984	1.563	1.689
9	1014.9	18.88	1.351	1.326	1.323	0.802	1.284	1.384
10	1253.0	20.98	1.125	1.105	1.102	0.665	1.070	1.151
11	1516.1	23.08	0.936	0.920	0.917	0.553	0.891	0.958
12	1804.3	25.17	0.787	0.773	0.771	0.464	0.749	0.805
13	2117.5	27.27	0.671	0.659	0.657	0.396	0.638	0.686
14	2455.8	29.37	0.578	0.568	0.566	0.341	0.550	0.592
15	2819.1	31.47	0.504	0.495	0.493	0.297	0.479	0.515
16	3207.6	33.57	0.443	0.435	0.434	0.261	0.421	0.453
17	3621.0	35.66	0.392	0.385	0.384	0.231	0.373	0.401
18	4059.6	37.76	0.350	0.343	0.343	0.206	0.332	0.358

Table V: Variation of stopping power (-dE/dx) with particle energy E_p, ($r_s = 3$).

$K_o = \frac{V}{V_F}$	Energy (eV)	Velocity (10^8cm. sec.$^{-1}$)	(-dE/dx) in units of 10^{-4} ergs cm^{-1}					
			RPA	Hubbard screened	Hubbard unscreened	Kleinman (electron)	Kleinman (Test charge)	Langreth
2	22.28	2.79	8.249	8.806	9.474	6.895	9.247	7.861
3	50.12	4.19	4.789	5.029	5.326	3.651	5.178	4.680
4	89.10	5.59	3.115	3.250	3.416	2.269	3.324	3.065
5	139.22	6.99	2.198	2.285	2.391	1.551	2.330	2.169
6	200.47	8.39	1.642	1.702	1.776	1.139	1.732	1.623
7	272.87	9.79	1.277	1.321	1.376	0.872	1.343	1.264
8	356.39	11.19	1.025	1.059	1.100	0.691	1.075	1.015
9	451.06	12.59	0.843	0.869	0.902	0.563	0.882	0.835
10	556.87	13.99	0.703	0.725	0.751	0.466	0.735	0.697
11	556.87	13.99	0.585	0.603	0.625	0.387	0.612	0.580
12	801.89	16.78	0.492	0.507	0.525	0.325	0.514	0.488
13	941.11	18.18	0.419	0.432	0.448	0.277	0.438	0.415
14	1091.5	19.58	0.361	0.372	0.386	0.239	0.378	0.358
15	1253.0	20.98	0.314	0.324	0.336	0.208	0.329	0.312
16	1425.6	22.38	0.277	0.285	0.296	0.183	0.289	0.274
17	1609.3	23.78	0.245	0.253	0.262	0.162	0.256	0.243
18	1804.3	25.17	0.219	0.225	0.233	0.145	0.229	0.217

Table VI: Variation of stopping power (-dE/dx) with particle energy E_p, (r_s = 4).

$K_o = \frac{V}{V_F}$	Energy (eV)	Velocity (10^8cm. sec^{-1})	(-dE/dx) in units of 10^{-4} ergs cm^{-1}					
			RPA	Hubbard screened	Hubbard unscreened	Kleinman (electron)	Kleinman (Test charge)	Langreth
2	12.53	2.10	5.647	5.984	6.110	4.242	5.849	5.500
3	28.19	3.15	3.356	3.499	3.554	2.320	3.390	3.361
4	50.12	4.19	2.204	2.284	2.315	1.465	2.214	2.218
5	78.31	5.24	1.565	1.615	1.635	1.015	1.568	1.576
6	112.77	6.29	1.172	1.208	1.222	0.748	1.174	1.182
7	153.49	7.34	0.915	0.941	0.951	0.577	0.915	0.922
8	200.47	8.39	0.736	0.756	0.763	0.459	0.736	0.742
9	253.72	9.44	0.606	0.622	0.628	0.375	0.606	0.611
10	313.24	10.49	0.506	0.519	0.524	0.311	0.506	0.510
11	379.02	11.54	0.422	0.432	0.436	0.259	0.421	0.425
12	451.06	12.58	0.354	0.363	0.367	0.218	0.354	0.357
13	529.37	13.64	0.302	0.309	0.312	0.185	0.302	0.304
14	613.95	14.68	0.260	0.267	0.269	0.160	0.260	0.262
15	704.79	15.73	0.227	0.232	0.235	0.139	0.227	0.229
16	801.89	16.78	0.199	0.204	0.206	0.122	0.199	0.201
17	905.26	17.83	0.177	0.181	0.183	0.108	0.176	0.178
18	1014.9	18.88	0.157	0.161	0.163	0.097	0.157	0.159
19	1130.8	19.93	0.141	0.145	0.146	0.087	0.141	0.142
20.	1252.9	20.98	0.128	0.131	0.132	0.078	0.127	0.129
21	1381.4	22.03	0.116	0.119	0.120	0.071	0.116	0.117
22	1516.1	23.08	0.105	0.108	0.109	0.065	0.105	0.106
23	1657.0	24.13	0.096	0.099	0.100	0.059	0.096	0.097
24	1804.2	25.17	0.089	0.091	0.092	0.054	0.088	0.089

Table VII: Variation of stopping power (-dE/dx) with particle energy E_p (r_s=5).

$K_o=\frac{V}{V_F}$	Energy (eV)	Velocity (10^8cm. sec^{-1})	(-dE/dx) in units of 10^{-6} ergs cm^{-1} RPA	Hubbard screened	Hubbard unscreened	Kleinman (electron)	Kleinman (Test charge)	Langreth
2	8.019	1.68	4.229	4.479	4.600	3.147	4.361	4.219
3	18.04	2.52	2.560	2.664	2.718	1.742	2.562	2.632
4	32.08	3.36	1.694	1.751	1.781	1.107	1.685	1.745
5	50.12	4.19	1.207	1.244	1.268	0.770	1.198	1.243
6	72.17	5.03	0.907	0.933	0.946	0.570	0.900	0.933
7	98.23	5.87	0.709	0.728	0.738	0.440	0.704	0.729
8	128.30	6.71	0.571	0.586	0.593	0.351	0.567	0.587
9	162.38	7.55	0.471	0.482	0.488	0.287	0.467	0.483
10	200.47	8.39	0.394	0.403	0.408	0.239	0.391	0.404
11	242.57	9.23	0.328	0.336	0.340	0.198	0.325	0.336
12	288.68	10.07	0.276	0.282	0.285	0.167	0.273	0.283
13	338.80	10.91	0.235	0.240	0.243	0.142	0.233	0.241
14	392.93	11.75	0.203	0.207	0.210	0.123	0.201	0.208
15	451.06	12.59	0.176	0.181	0.183	0.107	0,175	0.181
16	513.21	13.43	0.155	0.159	0.161	0.094	0.154	0.159
17	579.37	14.27	0.138	0.141	0.142	0.083	0.136	0.141
18	649.53	15.11	0.123	0.125	0.127	0.074	0.121	0.126
19	723.71	15.94	0.110	0.112	0.114	0.067	0.109	0.113
20	801.89	16.78	0.099	0.102	0.103	0.060	0.098	0.102
21	884.08	17.62	0.090	0.092	0.093	0.054	0.089	0.092
22	970.29	18.46	0.082	0.084	0.085	0.050	0.081	0.084
23	1060.5	19.30	0.075	0.077	0.078	0.045	0.074	0.077
24	1154.7	20.14	0.067	0.071	0.071	0.042	0.068	0.071

tTable VIII: Variation of stopping power (-dE/dx) with particle energy E_p (r_s = 6).

$K_o=\frac{V}{V_F}$	Energy (eV)	Velocity (10^8cm. sec^{-1})	(-dE/dx) in units of 10^{-4} ergs cm^{-1}					
			RPA	Hubbard screened	Hubbard unscreened	Kleinman (electron)	Kleinman (Test charge)	Langreth
2	5.569	1.39	3.422	3.548	3.625	2.490	3.449	3.103
3	12.53	2.10	2.091	2.140	2.173	1.389	2.045	2.033
4	22.28	2.79	1.388	1.414	1.433	0.887	1.352	1.367
5	34.80	3.49	0.991	1.008	1.020	0.619	0.965	0.980
6	50.12	4.19	0.746	0.757	0.766	0.458	0.726	0.740
7	68.22	4.89	0.583	0.592	0.598	0.355	0.569	0.579
8	89.10	5.59	0.470	0.477	0.481	0.283	0.459	0.467
9	112.77	6.29	0.388	0.393	0.397	0.232	0.379	0.386
10	139.22	6.99	0.324	0.329	0.332	0.193	0.317	0.323
11	168.45	7.69	0.270	0.274	0.276	0.160	0.264	0.269
12	200.47	8.39	0.227	0.230	0.232	0.135	0.222	0.226
13	235.28	9.09	0.194	0.196	0.198	0.115	0.189	0.193
14	272.87	9.79	0.167	0.169	0.171	0.099	0.163	0.166
15	313.24	10.49	0.145	0.147	0.149	0.086	0.142	0.145
16	356.40	11.19	0.128	0.129	0.131	0.076	0.125	0.127
17	402.34	11.89	0.113	0.115	0.116	0.067	0.111	0.113
18	451.06	12.59	0.101	0.102	0.103	0.060	0.099	0.100
19	502.58	13.29	0.091	0.092	0.093	0.054	0.088	0.090
20	556.87	13.99	0.082	0.083	0.084	0.049	0.080	0.081
21	613.95	14.68	0.075	0.075	0.076	0.044	0.072	0.074
22	673.81	15.38	0.068	0.068	0.069	0.040	0.066	0.067
23	736.46	16.08	0.062	0.063	0.063	0.037	0.060	0.062
24	801.89	16.78	0.057	0.058	0.058	0.034	0.055	0.057

metallic density range) i.e. for $r_s = 2$ to $r_s = 6$. A comparison between the results of different approximations has been made for a particular electron density ($r_s = 3$) in Fig. 4 where $-dE/dx$ has been plotted against V^{-1}. The graph shows that results of all the approximations for dielectric function show essentially the same behaviour i.e. the stopping power to be very nearly inversely proportional to the particle velocity in the velocity range of $2V_F$ to about 10 V_F. For higher velocities, the velocity dependence tends to become $1/V^2$, as expected. [In Fig. 4, curve 6 corresponds to use of eqn. (5.30) in eqn. (5.14)]. These results establish that the velocity dependence of the energy loss due to conduction electrons is rather independent of the model chosen for dielectric function. The magnitudes of stopping power also do not differ appreciably when different dielectric functions are used. This result is to be contrasted with the fact that static impurity screening is highly sensitive to the particular model used for dielectric function[112-114] where only static dielectric constant ($\omega = 0$) is required.

Finally, we have given few results of stopping power of keV xenon ions in tungsten targets in Table IX. The velocity of the xenon ions is very small compared to the Fermi velocity. Accordingly, $-dE/dx$ is found to be very nearly proportional to the particle velocity (shown in Fig. 5) as also expected from the formula (3.12) or (3.13).

Table IX: Variation of stopping power (-dE/dx) of Xe^{133} in tungsten crystal.

$K_o = \frac{V}{V_F}$	Energy (keV)	Velocity (10^8cm. sec^{-1})	(-dE/dx) in units of 10^{-4} ergs cm^{-1}	
			RPA	Hubbard (screened)
0.010	0.467	0.026	0.198	0.226
0.012	0.673	0.031	0.255	0.293
0.014	0.916	0.036	0.288	0.331
0.016	1.196	0.041	0.325	0.375
0.018	1.514	0.047	0.355	0.408
0.020	1.869	0.052	0.365	0.421
0.022	2.262	0.057	0.423	0.488
0.024	2.691	0.062	0.463	0.534

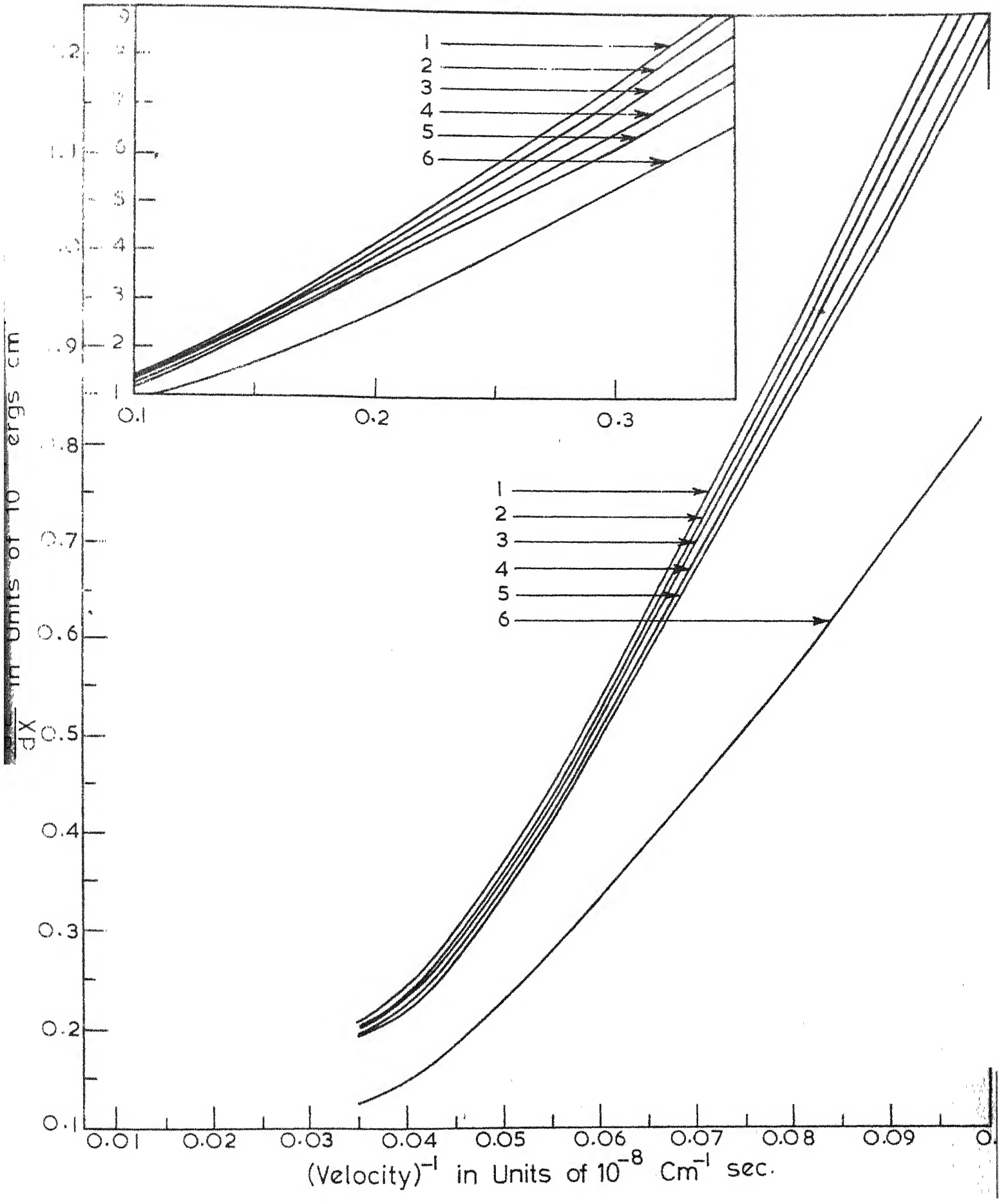
1
2
3
4
5
6
0.1
0.2
0.3
1
2
3
4
5
6
0.1
0.2
0.3
0.4
0.5
0.6
0.7
0.8
0.9
1.1
1.2
0.01
0.02
0.03
0.04
0.05
0.06
0.07
0.08
0.09
$\frac{dP}{dX}$ in Units of 10 ergs cm
(Velocity)$^{-1}$ in Units of 10^{-8} Cm^{-1} sec.

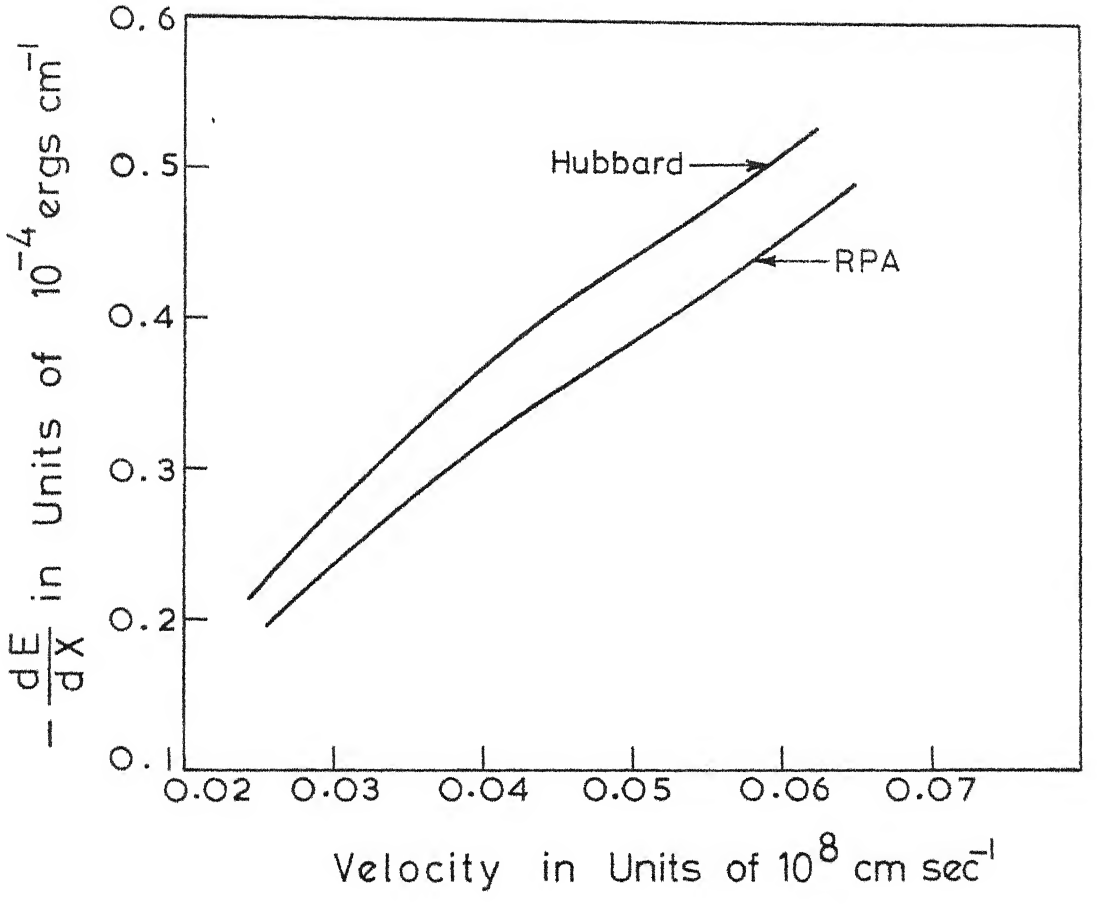
0.6
0.5
0.4
0.3
0.2
0.1
Hubbard
RPA
$-\frac{dE}{dX}$ in Units of 10^{-4} ergs cm^{-1}
0.02
0.03
0.04
0.05
0.06
0.07
Velocity in Units of 10^{8} cm sec^{-1}

CHAPTER VI

CONCLUSION

Several interesting conclusions regarding the phenomena of channeling of particles in perfect crystals, emerge from the results of the investigations presented in this work. The fact that the present quantum-mechanical theory confirms some of the results expected classically, is in itself interesting and is in the usual spirit of quantum mechanics. Thus the validity of the condition for anomalous transmission, requires that the magnitude of the reciprocal lattice vector $\underline{K}_h$, corresponding to the plane (or axis) with which the incident particles are being diffracted under the Bragg condition $|\underline{K}_h+\underline{k}_n|=|\underline{k}_n|$, should be smallest possible. For energetic particle (in which case $\underline{k}_n$ is large compared to $\underline{K}_h$) this means that the incident particles should enter into the crystal very nearly parallel to the principal (or low index) crystallographic directions or planes. This is what was expected classically in view of the fact that low index planes and strings are separated by maximum distance between consecutive planes or strings and hence give rise to open channels through which particles may propagate with minimum attenuation. This aspect is implicit in the Lindhard's classical treatment. The effects of lattice vibrations are found to decrease the channeling effects and the temperature dependence appears as Debye-Waller factor, as one should have expected.

There are several significant results obtained in the present formalism which change many of the classical notions, altogether. It is usually argued that for high energy particles, since the deBroglie wavelength of the particle is small compared to the lattice spacing, there should not be any significant interference effects. On the other hand it is well known that the phenomena observed in the electron microscope must be described in terms of wave interference: Bragg angles and resonance widths dominate the intensity patterns even when the electron wavelength is very small compared to the lattice spacing of the target crystal. To this end, the present quantum-mechanical treatment shows that the existence of anomalous effect has nothing to do with the wavelength of the incident particle, but rather is determined by two criteria, namely that the interaction potential must be sufficiently weak compared to the particle energy and that the interaction be localized in the vicinity of the lattice sites. If the range of the interaction is small compared to the mean square displacement, as is expected to be case for neutrons, the attenuation of both the waves ϕ_n^+ and ϕ_n^- in the two beam theory, is independent of the potential width and is determined only by the mean square displacement. On the other hand, for long range interaction potentials, the condition for anomalous transmission cannot be satisfied. Comparison between the results of two potential models used for charged particles, the screened Coulomb and the Born-Mayer, shows that the former is more favourable for

channeling. Even for equal range, the penetration depth is larger for screened Coulomb potential than for the Born-Mayer potential. It is also seen that the channeling condition has some energy dependent terms. Although these terms are small at high particle energies, they become significant to reduce the channeling effect, at low particle energies. Similarly, in addition to the usual Debye-Waller factor, a small temperature dependence comes in the channeling-parameter $(1-\epsilon)$ which does not show any significant effect at low temperatures.

It is interesting to note that energy dependence $(1/E_p)$ of the exponents in the equations (3.17), (3.29) and (3.43), for $|\phi_n^+|^2$. When the channeling parameter $(1-\epsilon)$ is not exactly zero but a small quantity i.e. channeling condition is approximately satisfied, the wave ϕ_n^+ will channel the particles but there will be some attenuation. The attenuation upto a given distance traversed will be governed by E_p^{-1}. Thus the distance at which a given fraction of the initially channeled particles is present in the channel, is proportional to E_p. This conclusion is in confirmation with the experimentally established fact that $X_{1/2}$, the thickness into the crystal at which one half of the initially channeled particles have escaped from the channel is proportional to the particle energy E_p.

The quantum theory of the directional effects in the charged particle emission in the crystals, presented in the Chapter IV, also leads to very important conclusions. The

mass and the potential dependence of the angles θ_B and $\Delta\theta_B$ in equations (4.26) and (4.27) shows that whenever the particle mass or the strength of potential becomes small, the interference and Bragg diffraction effects modify the emitted intensity pattern significantly (since $\Delta\theta_B/\theta_B$ becomes small and the classical orbital picture is no more applicable.) This completely modifies the classical notion of particle trajectory being independent of mass for given energy and potential. The classical limit is regained only when the particle mass becomes very large compared to the electron mass (more than 200 to 300 times electron mass) because in this limit $\Delta\theta_B$ becomes comparable to θ_B and two beam theory loses its validity. Moreover, in this formulation, the attenuation of the emitted particle emerges automatically as a manifestation of inelastic processes in terms of imaginary part of renormalization matrix and need not be chosen phenomenologically. The actual attenuation is found to be small compared to what is usually chosen phenomenologically and is proportional to $(m_o/E_p)^{1/2}$. The temperature dependence of the attenuation appears as Debye-Waller factor. Another interesting feature of the present formalism is an indication of the difference in the widths of electron and positron emission patterns even in the two beam theory. The magnitude of this difference is determined by the magnitude of Re C_{ho} which is relatively small but has an energy dependence E_p^{-1}. Thus at low particle energies, one can see that the positron emission pattern has more width as compared to that of electron emission

pattern, as has been experimentally observed[38,39]. Although, the present results do not quantitavely explain the experimentally observed difference, they are certainly in the right direction and give a qualitative explanation which is usually absent in the earlier two beam theories[36,37].

The calculation of energy loss of charged particles presented in Chapter V shows that the contribution of conduction electrons to the stopping power is inversely proportional to the particle velocity for velocities greater than the Fermi velocity upto about 10 times the Fermi velocity. For higher particle velocities, the dependence goes over to $1/V^2$. From Fig.4, it is also clear that the velocity dependence of the stopping power is rather insensitive to the particular approximation used for the dielectric function. The actual magnitude is also not very sensitive to the form of dielectric function.

Thus we see that the present quantum mechanical treatment of channeling phenomena in crystals leads to many new interesting features, not expected classically. It is expected that a more detailed analysis using many beam theory may yield few more fine structures, with the same basic characteristics obtained here in the two beam theory. More realistic models for lattice vibrations may also be examined using formulation of Chapter II. The problem of energy loss of channeled particles requires a little more attention. Firstly an elegant formulation for the

contribution of core electrons to energy loss is very much desirable because it is expected to show directional effects, in addition to giving a correction to energy loss due to conduction electrons. Secondly, as has been pointed out recently[115], that even the conduction electron contribution is also expected to show some directional effects and stopping power may be slightly different under channeling conditions than in normal conditions. This is significant in semiconductors where the density of conduction electrons is not uniform. Therefore, it is desirable to improve upon the dielectric formulation of energy loss due to conduction electrons and to develop a unified formulation for the energy loss of charged particles due to conduction and core electrons.

REFERENCES

1. J. Stark and G. Wendt, Ann. Phys. 38, 921 (1912); J. Stark, Z. Phys. 13, 973 (1912).

2. M.T. Robinson and O.S. Den, Appl. Phys. Letters 2, 30 (1963); Phys. Rev. 132, 2385 (1963).

3. G.R. Piercy, F. Brown, J.A. Davies and M.Mc Cargo, Phys. Rev. Letters 10, 399 (1963).

4. H. Lutz and R. Sizemann, Phys. Letters 5, 113 (1963).

5. R.S. Nelson and M.W. Thompson, Phil. Mag. 8, 1677 (1963). ibid. 9, 1069 (1964).

6. G. Dearnaley, I.E.E.E. Trans. Nucl. Sci, NS 11 (1964), C. Erginsoy, H.E. Wegner and M.W. Gibson, Phys. Rev. Letters 13, 530 (1964); A.R. Sattler and G. Dearnaley, Phys. Rev. Letters, 15, 59 (1965).

7. S. Datz, T.S. Noggle and C.D. Moak, Nucl. Instr.Methods 38, 221 (1963).

8. E.V. Kornelson, F. Brown, J.A. Davies, B. Domeij and G.R. Piercy, Phys. Rev. 136, 849 (1964) and the references given therein.

9. J. Lindhard, Phys. Letters 12, 126 (1964); Kgl. Danske Videnskab. Selskab, Mat. Fys. Medd. 34, No. 14(1965).

10. L. Eriksson, J.A. Davies and P. Jespersgaard, Phys. Rev. 161 , 219 (1967); L. Eriksson, Phys. Rev. 161, 235 (1967); J.A. Davies, L. Eriksson and J.L. Whitton, Can. J. Phys. 46, 1573 (1968).

11. J.A. Davies, J. Denhartog and J.L. Whitton, Phys. Rev. 165, 345 (1968); J.A. Davies, L. Eriksson, N.G.E. Johansson and I.V. Mitchell, Phys. Rev. 181, 548 (1969).

12. S.T. Picraux, J.A. Davies, L. Eriksson, N.G.E.Johansson and J.W. Mayer, Phys. Rev. 180, 873 (1969).

13. W. Brandt, J.M. Khan, D.L. Potter and R.D. Worley, Phys. Rev. Letters, 14, 42 (1965); J.M. Khan, D.L. Potter, R.D. Worley and H.P. Smith, Phys. Rev. 148, 413 (1966), ibid, 163, 81 (1967).

14. M.W. Thompson, Phys. Rev. Letters 13, 756 (1964).

15(a). Nucl. Instr. Methods 38, 153-276 (1965).
(b). Can. J. Phys. 46, 449-782 (1968).

16. E. Bogh, in Interaction of Radiation with Solids, edited by A. Bishay (Plenum Press, Inc.New York 1967), p. 361.

17. L. Eriksson, J.A. Davies, J. Denhartog, Hj Matzke and J.L. Whitton, Can. Nucl. Tech. 5, 40 (1966).

18. J.W. Mayer, L. Eriksson, S.T. Picraux and J.A. Davies, Can. J. Phys. 46, 663 (1968).

19. E. Bogh, Can. J. Phys. 46, 653 (1968).

20. F. Brown, D.A. Marsden and R.D. Werner, Phys. Rev. Letters, 20, 1449 (1968).

21. L. Eriksson, J.A. Davies, N.G.E. Johansson and J.W. Mayer, J. Appl. Phys. 40, 842 (1964).

22. L. Eriksson, J.A. Davies and J.W. Mayer, Science 163, 627 (1969); Radiation effects in Semiconductors (Plenum Press 1968) p. 398.

23. L. Eriksson, G.R. Bellavance and J.A. Davies, Radiation Effects 1, 71 (1969); J.W. Mayer, J.A. Davies and L. Eriksson, Appl. Phys. Letters 11, 365 (1967); J.A. Davies, L.Eriksson and J.W. Mayer, Appl. Phys. Letters 12, 255 (1968).

24. Hj Matzke and J.A. Davies, J. Appl. Phys. 38, 805 (1967).

25. G.K. Werner, J. Appl. Phys. 26, 1056 (1955); Phys. Rev. 102, 690 (1956).

26. P.K. Rol, J.M. Fuit, F.P. Viehbock and M. de Jong, Proc. 4-th Int. Conf. on Ionization Phen. in Gases, Uppsala (ed. N.R. Misson, North Holland Pub. Co., Amsterdam 1959), p. 257.

27. A.L. Southern, W.R. Willis and M.T. Robinson, J.Appl.Phys. 34, 153 (1963); M.W. Thompson, Proc. 5-th Int. Conf. on Ionization Phen. in Gases, Munich (ed. H.Maeker, North Holland, Pub. Co., Amsterdam 1961) p. 85.

28. C. Lehman, Nucl. Instr. Methods 38, 263 (1965).

29. S. Datz, C.Erginsoy, G.Leibfried and H.O. Lutz, Ann.Rev. Nucl. Science 17, 129 (1967).

30. J.A. Davies, Physics in Canada 23, 13 (1967); C. Erginsoy in Interaction of Radiation with Solids edited by A.Bishay (Plenum Press, Inc. New York 1967) p. 341.

31. N. Bohr, Mat. Fys. Medd., Dan. Vid. Selskab. 18, No. 8 (1948).

32. J. Lindhard, M. Scharff and H.E. Schiott, Mat. Fys. Medd., Dan. Vid. Selskab 33, No. 14 (1963).

33. J. Lindhard, V. Nielsen and M. Scharff, Mat. Fys. Medd., Dan. Vid. Selskab. 36, No. 10 (1968), Notes on Atomic Collisions I and IV.

34. E. Bogh, Proc. Int. Conf. Solid State Phys. Research with Accelerators 1967 (edited by A.N. Golland) BNL 50083, p. 76.

35. P. Lervig, J. Lindhard and V. Nielsen, Nucl. Phys. A 96, 481 (1967).

36. R.E. DeWames and W.F. Hall, Acta. Cryst. A24, 206 (1968).

37. R.E. DeWames, W.F. Hall and G.W. Lehman, Phys. Rev. 174, 392 (1968).

38. E. Uggerhoj, Phys. Letters 22, 382 (1966).

39. E. Uggerhoj and J.U. Andersen, Can. J. Phys. 46, 543 (1968).

40. J.M. Cowley, Phys. Letters 26A, 623 (1968).

41. W.B. Gibbson, C. Erginsoy, E. Wigner and B.R. Appleton, Phys. Rev. Letters 15, 357 (1965).

42. W.B. Gibbson, C. Erginsoy and H.E. Wagner, Bull. Am. Phys. Soc. 10, 43 (1965).

43. L.T. Chadderton, Phys. Letters 23, 303 (1966).

44. H. Yoshioka, J. Phys. Soc. (Japan) 12, 618 (1957).

45. H. Yoshioka and Y. Kainuma, J. Phys. Soc. (Japan) 17, Suppl. B-II, 134 (1962).

46. N. Kato, J. Phys. Soc. (Japan) 7, 397 (1952).

47. H.A. Bethe, Ann. d. Phys. Lpz 87, 55 (1928).

48. A. Howie, Proc. Int. Conf. Solid State Phys. Research with Accelerators 1967 (edited by A.N. Golland) BNL 50083, p. 15.

49. R.E. DeWames, W.F. Hall and G.W. Lehman, Phys. Rev. 148,181 (1966).

50. A.P. Pathak and M. Yussouff, Phys. Rev. B2, 4723 (1970).

51. G. Borrman, Trends in Atomic Physics, ed. by O.R. Frisch et. al. (John Wiley and Sons, Inc. New York 1959).

52. B.W. Batterman and H. Cole, Rev. Mod. Phys. 36, 681 (1964).

53. M. Yussouff, Ph.D. Thesis, Department of Phys. Indian Institute of Technology, Kanpur 1966.

54. M. Sachdev, Ph.D. Thesis, Department of Phys. Indian Institute of Technology, Kanpur 1970.

55. P.B. Hirsch et al., Electron Microscopy of Thin Crystals (Butler Worths Scientific Publications Ltd., London 1965) Chap. 12, p. 276.

56. A.P. Pathak and M. Yussouff, Proc. Nucl. Phys. Solid State Phys. Symposium 1968 (Bombay) p. 370.

57. L.S. Kothari and K.S. Singwi, Solid State Physics (edited by F. Seitz and D. Turbbull) 8, 110 (1959), Academic Press, New York.

58. R.J. Glauber, Phys. Rev. 98, 1692 (1955).

59. L.S. Kothari and K.S. Singwi, Solid State Physics (edited by F. Seitz and D. Turnbull) 8 125 (1959), Academic Press, New York.

60. See for instance C. Kittel, Quantum Theory of Solids, (John Wiley and Sons Inc. New York,1963).

61. P. Debye, Ann. Phys. 39, 789 (1912).

62. M. Blackmann, Handbuch d. Physik 7, 1 (1955).

63. J. W. Knowles, Acta Cryst. 9, 61 (1956).

64. J. Blatt and V. Weiskopf, Theoretical Nuclear Physics (John Wiley and Sons Inc., New York, 1952), p.74.

65. E. Fermi, Ricerca Sci. 7, 13 (1936), English Translation available as USAEC Rept. N.P. 2385.

66. G. Placzek, Phys. Rev. 86, 377 (1952).

67. Tables of Integrals, Series and Products by I.S.Gradshteyn and I.M. Ryzhik (Academic Press, New York 1965).

68. C. Lehman and G. Leibfried, J. Appl. Phys. 34, 2821(1963).

69. A.B. Lidiard, Proc. Winter School on Physics of Imperfect Crystalline Solids, Trieste 1970 (IAEA Viena).

70. J.B. Gibbson, A.N. Golland, M. Milgram and G.H.Vineyard, Phys. Rev. 120, 1229 (1960); M. Born and J.E. Mayer, Z. Physik 75, 1 (1932).

71. A.P. Pathak and M. Yussouff, Tech. Rept. No. 46/70, Department of Physics, Indian Institute of Technology Kanpur, (Submitted to Phys. Stat. Sol.).

72. J.A. Brinkman, Radiation damage in solids, (Academic Press, New York 1962), p. 830.

73. L.C.Feldman, B.R. Appleton and W.L. Brown, Proc. Int. Conf. Solid State Phys. Research with Accelerators 1967 (Edited by A.N. Golland),BNL 50083, p. 58.

74. E.D. Wolf and T.E. Everhart, Appl. Phys. Letters 14, 299 (1969).

75. D.C. Joy, E.M. Schulson, J.P. Jakubovies and C.G. Van Essen, Phil. Mag. 20, 843 (1969).

76. J.W. Steeds and U. Valdre, Fourth European Regional Conference on Electron Microscopy, Rome (1968) p. 43

77. J.U.Andersen, Y.M. Augustyniak and E.Uggerhoj, Phys. Rev. (To be published); E. Uggerhoj and F. Frandsen, Phys. Rev. B2, 582 (1970).

78. A. Howie, Int. Conf. on electron diffraction and nature of defects in crystals, Melbourne, 1965 (N.Y. Pergamon Press, Inc. 1966) paper No. IA-4, 2 pp.

79. A. Howie, Phil. Mag. 14, 223 (1966).

80. M.S. Spring, Phys. Letters 31A, 421 (1970).

81. B. Domeij, Ark. Fys. (Sweden) Swedish Phys. Conf. Upsala 30, pages 32, 569 (1965), ibid., 32, 179 (1966).

82. B. Domeij, Nucl. Instr. Methods, 38, 207 (1965).

83. B. Domeij and K. Bjorkqvist, Phys. Lett. 14, 127 (1965).

84. D.S. Gammell and R.E. Holland, Phys. Rev. Letters 14, 945 (1965).

85. R.L. Walker, B.L. Berman, R.C. Der, T.M. Kavanogh and J.M. Khan, Phys. Rev. Letters 25, 5 (1970).

86. M. Von Laue, Materiewellen und Ihre Interferenzen, Leipzig, Akademische Verlagsgesellscheft, Geest and Portig A.G. (1948).

87. C.J. Humphreys and P.B. Hirsch, Phil. Mag. 18, 115 (1968).

88. C.R.Hall and R.B. Hirsch, Proc. Roy. Soc. (London), A286, 158 (1965).

89. A.P. Pathak and M. Yussouff, Phys. Rev. (to be published).

90. J.U. Andersen and E. Uggerhoj, Can. J. Phys. 46, 518 (1968).

91. E. Bogh and J.L. Whitton, Phys. Rev. Letters 19, 553 (1967).

92. W.H. Zachariasen, Theory of X-ray diffraction in crystals, New York, John Wiley, London, Chapman and Hall.

93. C. Erginsoy in Interaction of Radiation with Solids, (edited by A. Bishay, Plenum Press, Inc. New York 1967), p. 353.

94. J. Lindhard, Mat. Fys. Medd. Dan. Vid. Selskab 28, No. 8(1954).

95. P. Nozieres and D. Pines, Nuovo Cimento 9, 470 (1958).

96. F. Seitz, Modern Theory of Solids (Mc Graw Hill, New York 1940).

97. E. Fermi and E. Teller, Phys. Rev. 72, 399 (1947).

98. J. Lindhard and A. Winther, Mat. Fys. Medd. Dan. Vid. Selskab. 34, No. 4 (1964).

99. B.A. Trubnikov and Yu. N. Yavlinskii, Soviet Phys. J.E.T.P. 21, 167 (1965).

100. A. Van Wijangaarden and H.E. Duck Worth, Can. J. Phys. 40, 1749 (1962).

101. G.R. Piercy, M. Mc Cargo, F. Brown and J.A. Davies, Can.J. Phys. 42, 1116 (1964).

102. J.A. Davies, L. Eriksson and P. Jespersgaard, Nucl.Instr. Methods. 38, 245 (1965).

103. J. Lindhard, Proc. Roy. Soc. (London), A311, 11 (1969).

104. D. Pines and D. Bohm,Phys. Rev. 85, 338 (1952); ibid. 92, 609 (1953).

105. D. Pines and P. Nozieres, The Theory of Quantum Liquids, Vol. I (Benjamin 1966).

106. S. Raims, Wave Mechanics of Metals (Amsterdam, North Holland 1961).

107. J. Hubbard, Proc. Roy. Soc. (London) A243, 336 (1957).

108. L.J. Sham, Proc. Roy. Soc. (London) A 283, 33 (1965); S.H. Vosko, R. Taylor and G.H. Keech, Can. J. Phys. 43, 1187 (1965); V. Heine and I. Abarenkov, Phil. Mag. 9, 451 (1964); L.M. Falicov and V. Heine, Advan. Phys. 10, 57(1961).

109. D.C. Langreth, Phys. Rev. 181, 753 (1969).

110. L. Kleinman, Phys. Rev. 160, 585 (1967).

111. L. Kleinman, Phys. Rev. 172, 383 (1968).

112. A.P. Pathak, Phys. Rev. B2, 3021 (1970).

113. K.S. Singwi, A. Sjolander, M.P. Tosi and R.H. Land, Phys. Rev. B1, 1044 (1970).

114. A.P. Pathak, Phys. Stat. Solidi 43, 551 (1971).

115. F. Bonsignori and A. Desalvo,Nuovo Cim. Letters 1, 589 (1969); J. Phys. Chem. Solids 31, 2191 (1970).

APPENDIX

If we write ω, p and k in energy units (i.e. $\epsilon_p = p^2$ etc.), the function $\chi_L(k,\omega)$ may be written as

$$\chi_L(k,\omega) = \chi_{L1}(\omega) + i\chi_{L2}(\omega) = -\sum_{\underline{p}} \frac{f_p(1-f_{p+k})}{\omega+\epsilon_p-\epsilon_{p+k}+i\eta} \qquad (A.1)$$

$$= -\sum_{\underline{p}} \frac{f_p(1-f_{p+k})}{\omega-k^2-2\underline{p}.\underline{k}+i\eta}$$

$$= -\frac{1}{(2\pi)^3}\int d\underline{p}\ \frac{f_p(1-f_{p+k})}{\omega-k^2-2\underline{p}.\underline{k}+i\eta} \qquad (A.2)$$

Now using the property of Fermi-function f_p at zero temperature, where $f_p = 1$ for $p < k_F$ and 0 otherwise, we can write from (A.2), the real and imaginary parts as,

$$\chi_{L1}(\omega) = -\frac{1}{4\pi^2}\int_{k_F-k}^{k_F} p^2\,dp \int_{x_o}^{1} \frac{dx}{\omega-k^2-2pkx} \quad \text{for } k<k_F \qquad (A.3)^*$$

$$= -\frac{1}{4\pi^2}\left[\int_0^{k-k_F} p^2dp \int_{-1}^{+1} \frac{dx}{\omega-k^2-2pkx}\right.$$

$$\left. + \int_{k-k_F}^{k_F} p^2dp \int_{x_o}^{1} \frac{dx}{\omega-k^2-2pkx}\right] \text{for } k_F<k<2k_F \qquad (A.4)$$

$$= -\frac{1}{4\pi^2}\int_0^{k_F} p^2dp \int_{-1}^{+1} \frac{dx}{\omega-k^2-2pkx} \quad \text{for } k>2k_F \qquad (A.5)$$

and $$\chi_{L2}(\omega) = \frac{1}{4\pi}\int_{\sqrt{k_F^2-\omega}}^{k_F} p^2dp \int_{-1}^{+1} dx\ \delta(\omega-k^2-2pkx) \quad \text{for } \omega \leq 2kk_F-k^2 \qquad (A.6\,a)$$

---

* Here $-x_o = (k_F^2 - p^2 - k^2)/2pk$.

$$= \frac{1}{4\pi} \int_{\frac{\omega-k^2}{2k}}^{k_F} p^2 dp \int_{-1}^{+1} dx\ \delta(\omega - k^2 - 2pkx)$$

$$\text{for } 2kk_F - k^2 < \omega < 2kk_F + k^2 \qquad \text{(A.6b)}$$

$$= 0 \qquad \text{for } \omega > 2kk_F + k^2$$

$\chi_{L1}(-\omega)$ is obtained by replacing ω by $-\omega$ in the expressions (A.3), (A.4) and (A.5) while $\chi_{L2}(-\omega)$ becomes zero because of the product of Fermi functions $f_p(1-f_{p+k})$ when used in angular integration with $\delta(\omega+k^2+2\underline{p}.\underline{k})$, gives zero.

Now performing the angular integrations in eqns. (A.3) to (A.6), one gets,

$$\chi_{L1}(\omega) = -\frac{1}{32\pi^2 k^3}\left[\int_{\omega+k^2-2kk_F}^{\omega-k^2-2kk_F} (\omega-k^2-p)\ln p\, dp + 2k^2 \int_{\omega+k^2+2kk_F}^{\omega} \ln p\, dp\right] \text{ for } k<2k_F \qquad \text{(A.7)}$$

$$= -\frac{1}{32\pi^2 k^3}\left[\int_{\omega-k^2-2kk_F}^{\omega-k^2+2kk_F} (p-\omega+k^2)\ln p\, dp\right]$$

$$\text{for } k > 2k_F \qquad \text{(A.8)}$$

The p-integrations may also be done easily and finally we get,

$$\chi_{L1}(\omega) = -\frac{k_F}{4\pi^2}\left\{\frac{1}{8kk_F}\left[\omega + 2\omega \ln|\omega|\right] - 1/4 + \frac{k_F}{4k}\left[1-\left(\frac{\omega+k^2}{2kk_F}\right)^2\right]\right.$$

$$\left.\ln|\omega+k^2-2kk_F| - \frac{k_F}{4k}\left[1-\left(\frac{\omega-k^2}{2kk_F}\right)^2\right]\ln|\omega-k^2-2kk_F|\right\}$$

$$\text{for } k < 2k_F \qquad \text{(A.9)}$$

$$= -\frac{k_F}{4\pi^2}\left\{\frac{\omega-k^2}{4k^2}+\frac{k_F}{4k}\left[1-\left(\frac{\omega-k^2}{2kk_F}\right)^2\right]\ln\left|\frac{\omega-k^2+2kk_F}{\omega-k^2-2kk_F}\right|\right\}$$

$$\text{for } k > 2k_F \qquad \text{(A.10)}$$

$$\text{and } \chi_{L2}(\omega) = \frac{\omega}{16\pi k} \qquad \text{for } \omega < 2kk_F-k^2 \qquad \text{(A.11)}$$

$$= \frac{1}{16\pi k}\left[k_F^2-\left(\frac{\omega-k^2}{2kk_F}\right)^2\right] \text{ for } 2kk_F-k^2 \leq \omega \leq 2kk_F+k^2$$

If we write these equations in the dimensionless units used in the text, we get eqns. (5.35) to (5.38).